hco := Nuc*k air(Tc)/od;

```
:= 0.5*od*(((od+2*fh)/od)-1)*(1+0.35*ln((od+2*fh)/od));
         effe := (tanh(sqrt(2*heo/(ft*k))*w)/(sqrt(2*heo/(ft*k))*w));
         effc := \frac{(\tanh(\operatorname{sgrt}(2*\operatorname{hco}/(\operatorname{ft}*k))*w)}{(\operatorname{sgrt}(2*\operatorname{hco}/(\operatorname{ft}*k))*w))}
      End:
    If fintype = 3 then
      Begin
         Afe := ((nc+0.5)*St*Sl-nc*3.14159*od*od*0.25)*2*
                  (\text{Le*fn}/0.0254);
         Abe := ((nc*Le*3.14159)/(fs+ft))*od*fs;
         Afc := ((nc+0.5)*St*Sl-nc*3.14159*od*od*0.25)*2*
                  (Lc*10/0.0254);
         Abc := ((nc*Lc*3.14159)/(fs+ft))*od*fs;
         mfae := 2*nc*Le*(Sd-od-(2*ft*fh)/(fs+ft));
         mfac := 2*nc*Lc*(Sd-od-(2*ft*fh)/(fs+ft));
         V_{maxe} := mh/(den air(Th)*mfae);
         Vmaxc := mc/(den air(Tc)*mfac);
         Ree := Vmaxe*od*den_air(Th)/vis_air(Th);
         Rec := Vmaxc*od*den air(Tc)/vis air(Tc);
         Pre := Cp air(Th)*vis air(Th)/k air(Th);
         Prc := Cp air(Tc)*vis air(Tc)/k air(Tc);
         heo := 0.14*exp(-0.328*ln(Ree))*exp(-0.502*ln(St/Sl))
                  *exp(0.031*ln(fs/od))*den air(Th)*Vmaxe*Cp air(Th)
                  *exp((-2/3)*ln(Pre));
         hco := 0.14*exp(-0.328*ln(Rec))*exp(-0.502*ln(St/Sl))
                  *exp(0.031*ln(fs/od))*den air(Tc)*Vmaxc*Cp air(Tc)
                  *exp((-2/3)*ln(Prc));
             := 1.27*((St/2)/(0.5*od))*sqrt((sqrt((St/2)*(St/2)+Sl*Sl)/2)
         fp
                  /(St/2)-0.3);
              := (fp-1)*(1+0.35*ln(fp));
         effe := (tanh(sqrt(2*heo/(ft*k))*w*(od/2))/(sqrt(2*heo/(ft*k))*w
                  *(od/2)));
         effc := (tanh(sqrt(2*hco/(ft*k))*w*(od/2))/(sqrt(2*hco/(ft*k))*w
                 *(od/2));
      End;
  End:
Aeo := effe*Afe+Abe:
Aco := effe*Afc+Abc;
Aei := 3.14159*id*Le*nc;
Aci := 3.14159*id*Lc*nc;
    := (Th+Tc)/2;
T
If T \le 55 then
Begin
Re := ((Q/Aei)/(Vwl(T)*Lw(T)))*(sqrt(Sw(T)/(9.81*(dwl(T)-dwg(T)))));
```

```
Pr := Cpw(T)*Vwl(T)/kw(T);
         hei := \exp(\ln(41.27)+0.37*\ln(Re)+0.4*\ln(Pr))*kw(T)/
                  (\operatorname{sqrt}(\operatorname{Sw}(T)/(9.81*(\operatorname{dwl}(T)-\operatorname{dwg}(T)))));
         hci := \exp(1.324*\ln(0.94*(\exp(0.245*\ln(\text{dwl}(T)*(\text{dwl}(T)-\text{dwg}(T))*9.81
                  *kw(T)*kw(T)*kw(T)*Lw(T)/(Vwl(T)*Lc*(Q/Aci))))));
         End:
         If T > 55 then
         Begin
         x := (1/(Vwl(T)*Lw(T)))*sqrt(Sw(T)/(9.81*(dwl(T)-dwg(T))));
             := Lw(T)*Vwl(T)/kw(T);
         hei := \exp(0.9332*(\ln(18.688)-\ln(x)-1.0716*\ln(y)+0.0716*\ln(O/Aei)));
         hci := \exp(1.30378*(\ln(0.943)+0.233*\ln(\operatorname{sqr}(\operatorname{dwl}(T))*9.81*\operatorname{Lw}(T)*
                 kw(T)*kw(T)*kw(T)*Aci/(Vwl(T)*Lc*Q)));
         End:
         UA001 := \frac{1}{(1/(heo*Aeo)+1/(hco*Aco)+1/(hei*Aei)+1/(hci*Aci)}
                     +\ln(\text{od/id})/(2*3.14159*k*\text{Le*nc})+\ln(\text{od/id})/(2*3.14159*k*\text{Lc*nc});
 End;
Function UA002(Th,Tc,mh,mc,Q,nc:real):real;{calculate UA of ethanol}
           k = 14.9; {thermal conductivity of metal}
 Const
 Var
         Aeo, Aei, Aco, Aci, Afe, Afc, Abe, Abc, heo, hei,
         hco,hci,mfac,mfae,Vmaxe,Vmaxc,Ree,
         Rec, Pre, Prc, Nuc, Nuc, w, effe, effc, Zc, Zef, Zep, phe2, phe3, T, Z, Re, a: real;
         del Tsat, x, y, heif, heip, Pr, fp: real;
         Ve, Vc, Vmaxe1, Vmaxe2, Vmaxc1, Vmaxc2: real;
 Begin
        If arrangement = 1 then
           Begin
             If fintype = 1 then
               Begin
                   Abe := nc*Le*3.14159*od:
                   Abc := nc*Lc*3.14159*od;
                   Afe := 0;
                   Afc := 0;
                   Ve := mh/(den air(Th)*cross section area);
                  Vc := mc/(den air(Tc)*cross section area);
                   Vmaxe := St*Ve/(St-od);
                  Vmaxc := St*Vc/(St-od);
                  Ree := den air(Th)*Vmaxe*od/vis air(Th);
                  Rec := den air(Tc)*Vmaxc*od/vis air(Tc);
                  Pre := Cp air(Th)*vis air(Th)/k air(Th);
                  Prc := Cp \operatorname{air}(Tc)*\operatorname{vis} \operatorname{air}(Tc)/k \operatorname{air}(Tc);
                  Nue := C_{aligned(Ree)*exp(m_aligned(Ree)*ln(Ree))}
                            *exp(0.36*ln(Pre));
                  Nuc := C aligned(Rec)*exp(m aligned(Rec)*ln(Rec))
```

```
*exp(0.36*ln(Prc));
         heo := Nue*k air(Th)/od;
         hco := Nuc*k air(Tc)/od;
         effe := 0:
         effc := 0:
      End:
    If fintype = 2 then
      Begin
         Afe := ((nc*Le*3.14159)/(fs+ft))*(0.5*(sqr(od+2*fh)-sqr(od))
                  +(od+2*fh)*ft);
         Abe := ((nc*Le*3.14159)/(fs+ft))*od*fs;
         Afc := ((nc*Lc*3.14159)/(fs+ft))*(0.5*(sqr(od+2*fh)-sqr(od))
                  +(od+2*fh)*ft);
         Abc := ((nc*Lc*3.14159)/(fs+ft))*od*fs;
         mfae := nc*Le*(St-od-(2*ft*fh)/(fs+ft));
         mfac := nc*Lc*(St-od-(2*ft*fh)/(fs+ft));
         Vmaxe := mh/(den air(Th)*mfae);
         Vmaxc := mc/(den air(Tc)*mfac);
         Ree := Vmaxe*od*den air(Th)/vis air(Th);
         Rec := Vmaxc*od*den_air(Tc)/vis_air(Tc);
         Pre := Cp air(Th)*vis air(Th)/k air(Th);
         Prc := Cp air(Tc)*vis air(Tc)/k air(Tc);
         Nue := 0.30*\exp(0.625*\ln(\text{Ree}))*\exp(-0.375*
                  ln((nc*Le*3.14159*od)/(Afe+Abe)))
                  *exp(0.333*ln(Pre));
         Nuc := 0.30*\exp(0.625*\ln(\text{Rec}))*\exp(-0.375*
                  ln((nc*Lc*3.14159*od)/(Afc+Abc)))
                  *exp(0.333*ln(Prc));
         heo := Nue*k air(Th)/od;
         hco := Nuc*k air(Tc)/od;
         w := 0.5*od*(((od+2*fh)/od)-1)*(1+0.35*ln((od+2*fh)/od));
         effe := (tanh(sqrt(2*heo/(ft*k))*w)/(sqrt(2*heo/(ft*k))*w));
         effc := (\tanh(\operatorname{sqrt}(2*\operatorname{hco}/(\operatorname{ft}*k))*w)/(\operatorname{sqrt}(2*\operatorname{hco}/(\operatorname{ft}*k))*w));
      End:
 End:
If arrangement = 2 then
 Begin
    If fintype = 1 then
      Begin
         Abe := nc*Le*3.14159*od;
         Abc := nc*Lc*3.14159*od;
         Afe := 0;
         Afc := 0:
         Ve := mh/(den air(Th)*cross section area);
```

```
Vc := mc/(den air(Tc)*cross section area);
     Vmaxe1:= St*Ve/(St-od);
     Vmaxc1:= St*Vc/(St-od);
     Vmaxe2:= St*Ve/(2*(Sd-od));
     Vmaxc2:= St*Vc/(2*(Sd-od));
    If Vmaxe1 > Vmaxe2 then Vmaxe := Vmaxe1
     else Vmaxe := Vmaxe2:
     If Vmaxc1 > Vmaxc2 then Vmaxc := Vmaxc1
     else Vmaxc := Vmaxc2:
     Ree := den air(Th)*Vmaxe*od/vis air(Th);
     Rec := den air(Tc)*Vmaxc*od/vis air(Tc);
     Pre := Cp \operatorname{air}(Th)*\operatorname{vis} \operatorname{air}(Th)/k \operatorname{air}(Th);
     Prc := Cp air(Tc)*vis air(Tc)/k air(Tc);
     Nue := C staggered(Ree,St,Sl)*exp(m_staggered(Ree)*ln(Ree))
              *exp(0.36*ln(Pre));
    Nuc := C \text{ staggered(Rec,St,Sl)*exp(m staggered(Rec)*ln(Rec))}
              *exp(0.36*ln(Prc));
    heo := Nue*k air(Th)/od;
    hco := Nuc*k air(Tc)/od:
     effe := 0:
     effc := 0:
  End;
If fintype = 2 then
  Begin
     Afe := ((nc*Le*3.14159)/(fs+ft))*(0.5*(sqr(od+2*fh)-sqr(od))
              +(od+2*fh)*ft);
     Abe := ((nc*Le*3.14159)/(fs+ft))*od*fs;
     Afc := ((nc*Lc*3.14159)/(fs+ft))*(0.5*(sqr(od+2*fh)-sqr(od))
              +(od+2*fh)*ft);
     Abc := ((nc*Lc*3.14159)/(fs+ft))*od*fs;
     mfae := 2*nc*Le*(Sd-od-(2*ft*fh)/(fs+ft));
    mfac := 2*nc*Lc*(Sd-od-(2*ft*fh)/(fs+ft));
     Vmaxe := mh/(den air(Th)*mfae);
     Vmaxc := mc/(den air(Tc)*mfac);
    Ree := Vmaxe*od*den air(Th)/vis air(Th);
    Rec := Vmaxc*od*den air(Tc)/vis air(Tc);
    Pre := Cp air(Th)*vis air(Th)/k air(Th);
    Prc := Cp air(Tc)*vis air(Tc)/k air(Tc);
    Nue := 0.242*\exp(0.658*\ln(\text{Ree}))*\exp(0.297*\ln(\text{fs/fh}))
              \exp(-0.091 * \ln(St/S1)) * \exp(0.33333 * \ln(Pre));
    Nuc := 0.242*\exp(0.658*\ln(\text{Rec}))*\exp(0.297*\ln(\text{fs/fh}))
              \exp(-0.091*\ln(St/S1))*\exp(0.33333*\ln(Prc));
    heo := Nue*k air(Th)/od;
    hco := Nuc*k air(Tc)/od;
```

```
= 0.5*od*(((od+2*fh)/od)-1)*(1+0.35*ln((od+2*fh)/od));
          effe := \frac{(\tanh(\operatorname{sgrt}(2*\operatorname{heo}/(\operatorname{ft}*k))*w)}{(\operatorname{sgrt}(2*\operatorname{heo}/(\operatorname{ft}*k))*w))};
          effc := \frac{(\tanh(\operatorname{sgrt}(2*\operatorname{hco}/(\operatorname{ft}*k))*w)}{(\operatorname{sgrt}(2*\operatorname{hco}/(\operatorname{ft}*k))*w))};
       End:
     If fintype = 3 then
       Begin
          Afe := ((nc+0.5)*St*Sl-nc*3.14159*od*od*0.25)*2*
                    (Le*fn/0.0254);
          Abe := ((nc*Le*3.14159)/(fs+ft))*od*fs;
          Afc := ((nc+0.5)*St*Sl-nc*3.14159*od*od*0.25)*2*
                    (Lc*10/0.0254);
          Abc := ((nc*Lc*3.14159)/(fs+ft))*od*fs;
          mfae := 2*nc*Le*(Sd-od-(2*ft*fh)/(fs+ft));
          mfac := 2*nc*Lc*(Sd-od-(2*ft*fh)/(fs+ft));
          Vmaxe := mh/(den air(Th)*mfae);
          Vmaxc := mc/(den air(Tc)*mfac);
          Ree := Vmaxe*od*den air(Th)/vis air(Th);
          Rec := Vmaxc*od*den air(Tc)/vis air(Tc);
          Pre := Cp air(Th)*vis air(Th)/k air(Th);
          Prc := Cp \operatorname{air}(Tc)*\operatorname{vis} \operatorname{air}(Tc)/k \operatorname{air}(Tc);
          heo := 0.14*exp(-0.328*ln(Ree))*exp(-0.502*ln(St/Sl))
                    *exp(0.031*ln(fs/od))*den air(Th)*Vmaxe*Cp_air(Th)
                    *exp((-2/3)*ln(Pre)):
          hco := 0.14*exp(-0.328*ln(Rec))*exp(-0.502*ln(St/Sl))
                    *exp(0.031*ln(fs/od))*den air(Tc)*Vmaxc*Cp air(Tc)
                    *exp((-2/3)*ln(Prc));
              := 1.27*((St/2)/(0.5*od))*sqrt((sqrt((St/2)*(St/2)+S1*S1)/2)
          fp
                    /(St/2)-0.3);
                = (fp-1)*(1+0.35*ln(fp));
          effe := (tanh(sqrt(2*heo/(ft*k))*w*(od/2))/(sqrt(2*heo/(ft*k))*w
                   *(od/2)));
          effc := (tanh(sqrt(2*hco/(ft*k))*w*(od/2))/(sqrt(2*hco/(ft*k))*w
                    *(od/2));
       End;
  End:
Aeo := effe*Afe+Abe;
Aco := effe*Afc+Abc:
Aei := 3.14159*id*Le*nc;
Aci := 3.14159*id*Lc*nc:
T
    = (Th+Tc)/2;
    := (1/(Vel(T)*Lae(T)))*sqrt(Se(T)/(9.81*(del(T)-deg(T))));
X
y := Lae(T)*Vel(T)/ke(T);
hei := \exp(1.01*(\ln(17.625)-\ln(x)-0.99*\ln(y)-0.01*\ln(Q/Aei)));
hci := \exp(1.35135*(\ln(0.93)+0.26*\ln(\operatorname{sqr}(\operatorname{del}(T))*9.81*\operatorname{Lae}(T)*
```

```
ke(T)*ke(T)*ke(T)*Aci/(Vel(T)*Lc*Q)));
        UA002 := 1/(1/(heo*Aeo)+1/(hco*Aco)+1/(hei*Aei)+1/(hci*Aci)
                   +\ln(\text{od/id})/(2*3.14159*k*\text{Le*nc})+\ln(\text{od/id})/(2*3.14159*k*\text{Lc*nc});
 End:
            UAmix(Th,Tc,mh,mc,Q,n,wc:real):real;
Function
 Begin
        UAmix := UA001(Th, Tc, mh, mc, Q, n)*wc+UA002(Th, Tc, mh, mc, Q, n)*(1-wc);
 End:
Begin
        {main program}
     writeln('PROGRAM HEAT PIPE 001
                                                      ');
     writeln:
      Writeln('This program is used for calculating performance of the thermosyphon');
     writeln(' heat exchanger operating at low temperature with 2-kinds of working');
     writeln('fluids (water-ethanol)');
     writeln:
     writeln(' Developed by Atipoang Nuntaphan, Ph.D. student');
     writeln('Thermal Technology Division, School of Energy and Materials,');
     writeln('King Mongkut's',' University of Technology Thonburi');
     writeln:
      writeln:
     writeln(' Please enter informations below ');
     writeln(' 1. Heat exchanger informations');
     write(' 1.1 Input number of rows
                                                                       ');
     readln(nr);
     write(' 1.2 Input number of column
                                                                       ');
     readln(nc);
     write(' 1.3 Input outside diameter of tube (m)
                                                                       ');
     readln(od);
     write(' 1.4 Input inside diameter of tube (m)
                                                                       ');
     readin(id);
     write(' 1.5 Input evaporator length (m)
                                                                       ');
     readln(Le);
     write(' 1.6 Input condenser length (m)
                                                                       ');
     readln(Lc);
     writeln(' 1.7 Input type of fin
                                                                       '):
                  1. bare tube 2. circular finned 3. plain plate finned
     write('
                                                                       `);
     readln(fintype);
     write(' 1.8 Input fin thickness (m) (input 0 for bare tube)
                                                                       ');
     readln(ft);
     write(' 1.9 Input fin gap (m) (input 0 for bare tube)
                                                                       ');
     write(' 1.10 Input fin height (m) (input 0 for bare tube)
                                                                       ');
     readln(fh);
```

```
write(' 1.11 Input number of fins (fin/inch) (input 0 for bare tube) ');
readln(fn);
writeln(' 1.12 Input pipe arrangement
                                                                     ');
             1. aligned
                          2. staggered
                                                                     ');
write('
readln(arrangement);
write(' 1.13 Input transverse pitch (St) (m)
                                                                     ');
readin(St);
write(' 1.14 Input longitudinal pitch (Sl) (m)
                                                                     ");
readln(Sl);
write(' 1.15 Input directional pitch (Sd) (m) (input 0 for aligned)
                                                                     ");
readln(Sd);
write(' 1.16 Input cross section area of duct (m^2)
                                                                     ");
readln(cross_section_area);
writeln:
writeln(' 2. Working conditions ');
write(' 2.1 Input inlet temperature of hot gas (C)
                                                                     ');
readin(Thi);
write(' 2.2 Input inlet temperature of cold gas (C)
                                                                     ');
readin(Tci);
write(' 2.3 Input mass flow rate of hot gas (kg/s)
                                                                     ');
readln(mh);
write(' 2.4 Input mass flow rate of cold gas (kg/s)
                                                                     ');
readin(mc);
writeln(' 2.5 Input flow pattern
             1. parallel flow 2. counter flow
write('
                                                                     ');
read(flowpattern);
writeln;
If flowpattern = 1 then
  Begin
     Th[1] := Thi;
     Tc[1] := Tci;
     For i := 1 to nr do
     Begin
        write(' row = ',i);
        O[i] := 1200;
        Q[i] := UA001(Th[i],Tc[i],mh,mc,Q[i]/nc,nc)*(Th[i]-Tc[i]);
        Th[i+1] := Th[i]-Q[i]/(mh*Cp air(Th[i]));
        Tc[i+1] := Q[i]/(mc*Cp air(Tc[i]))+Tc[i];
        For j := 1 to 200 do
          Begin
             lmtd
                     := ((Th[i]-Tc[i])-(Th[i+1]-Tc[i+1]))/ln((Th[i]-Tc[i])
                       /(Th[i+1]-Tc[i+1]));
                     := UA001((Th[i]+Th[i+1])/2,(Tc[i]+Tc[i+1])/2,mh,mc,
             Q[i]
                        Q[i]/nc,nc)*lmtd;
```

```
Th[i+1] := Th[i]-Q[i]/(mh*Cp air((Th[i]+Th[i+1])/2));
             Tc[i+1] := Tc[i]+Q[i]/(mc*Cp_air((Tc[i]+Tc[i+1])/2));
          End;
        Qw := Q[i]; Thow := Th[i+1]; Tcow := Tc[i+1];
        For j := 1 to 200 do
          Begin
                     := ((Th[i]-Tc[i])-(Th[i+1]-Tc[i+1]))/ln((Th[i]-Tc[i])
             lmtd
                        /(Th[i+1]-Tc[i+1]));
                    := UA002((Th[i]+Th[i+1])/2,(Tc[i]+Tc[i+1])/2,mh,mc,
             Q[i]
                       Q[i]/nc,nc)*lmtd;
             Th[i+1] := Th[i]-Q[i]/(mh*Cp_air((Th[i]+Th[i+1])/2));
             Tc[i+1] := Tc[i]+Q[i]/(mc*Cp_air((Tc[i]+Tc[i+1])/2));
          End;
       Qe := Q[i]; Thoe := Th[i+1]; Tcoe := Tc[i+1];
       If Qw > Qe then
          Begin
            Th[i+1] := Thow;
            Tc[i+1] := Tcow;
            Q[i] := Qw;
            writeln('Th,out = ',Th[i+1]:1:2,'Tc,out = ',Tc[i+1]:1:2,
                     Q = ',Q[i]:1:2,' water');
          End;
       If Qe > Qw then
          Begin
            Th[i+1] := Thoe;
            Tc[i+1] := Tcoe;
            Q[i] := Qe;
            writeln(' Th,out = ',Th[i+1]:1:2,' Tc,out = ',Tc[i+1]:1:2,
                     Q = ',Q[i]:1:2,' ethanol');
          End;
    End;
     Qtotal := 0;
    for i := 1 to nr do
       Begin
           Qtotal := Qtotal + Q[i];
       End;
    writeln('Qtotal = ',Qtotal:1:2);
 End;
If flowpattern = 2 then
 Begin
    for i := 1 to nr do
       Begin
          Q[i] := 1200;
          wc[i] := 1;
```

```
End;
for i := 1 to nr+1 do
       Begin
                Th[i] := Thi-2*(i-1);
                Tc[i] := Tci+2*(nr+1-i);
       End:
for j := 1 to nr do {start row j}
       Begin
                wc[i] := 1;
                for a := 1 to 200 do
                       Begin
                                for i := 1 to nr do
                                       Begin
                                                Q[i]
                                                                := UAmix((Th[i]+Th[i+1])/2,(Tc[i]+
                                                                            Tc[i+1]/2,mh,mc,Q[i]/nc,nc,wc[i])*
                                                                            abs((Th[i]+Th[i+1]-Tc[i]-Tc[i+1])/2);
                                                Tc[i] := Q[i]/(mc*Cp air((Tc[i]+Tc[i+1])/2))+Tc[i+1];
                                               Th[i+1] := Th[i]-Q[i]/(mh*Cp_air((Th[i]+Th[i+1])/2));
                                      End:
                      End;
               for a := 1 to 200 do
                      Begin
                               for i := 1 to nr do
                                       Begin
                                                                 := UAmix((Th[i]+Th[i+1])/2,(Tc[i]+
                                               Q[i]
                                                                            Tc[i+1]/2,mh,mc,Q[i]/nc,nc,wc[i])*
                                                                           ((Th[i]-Tc[i])-(Th[i+1]-Tc[i+1]))/ln((Th[i]-Tc[i])/ln((Th[i]-Tc[i])/ln((Th[i]-Tc[i])/ln((Th[i]-Tc[i])/ln((Th[i]-Tc[i])/ln((Th[i]-Tc[i])/ln((Th[i]-Tc[i])/ln((Th[i]-Tc[i])/ln((Th[i]-Tc[i])/ln((Th[i]-Tc[i])/ln((Th[i]-Tc[i])/ln((Th[i]-Tc[i])/ln((Th[i]-Tc[i])/ln((Th[i]-Tc[i])/ln((Th[i]-Tc[i])/ln((Th[i]-Tc[i])/ln((Th[i]-Tc[i])/ln((Th[i]-Tc[i])/ln((Th[i]-Tc[i])/ln((Th[i]-Tc[i])/ln((Th[i]-Tc[i])/ln((Th[i]-Tc[i])/ln((Th[i]-Tc[i])/ln((Th[i]-Tc[i])/ln((Th[i]-Tc[i])/ln((Th[i]-Tc[i])/ln((Th[i]-Tc[i])/ln((Th[i]-Tc[i])/ln((Th[i]-Tc[i])/ln((Th[i]-Tc[i])/ln((Th[i]-Tc[i])/ln((Th[i]-Tc[i])/ln((Th[i]-Tc[i]-Tc[i])/ln((Th[i]-Tc[i]-Tc[i])/ln((Th[i]-Tc[i]-Tc[i])/ln((Th[i]-Tc[i]-Tc[i]-Tc[i])/ln((Th[i]-Tc[i]-Tc[i]-Tc[i]-Tc[i]-Tc[i]-Tc[i]-Tc[i]-Tc[i]-Tc[i]-Tc[i]-Tc[i]-Tc[i]-Tc[i]-Tc[i]-Tc[i]-Tc[i]-Tc[i]-Tc[i]-Tc[i]-Tc[i]-Tc[i]-Tc[i]-Tc[i]-Tc[i]-Tc[i]-Tc[i]-Tc[i]-Tc[i]-Tc[i]-Tc[i]-Tc[i]-Tc[i]-Tc[i]-Tc[i]-Tc[i]-Tc[i]-Tc[i]-Tc[i]-Tc[i]-Tc[i]-Tc[i]-Tc[i]-Tc[i]-Tc[i]-Tc[i]-Tc[i]-Tc[i]-Tc[i]-Tc[i]-Tc[i]-Tc[i]-Tc[i]-Tc[i]-Tc[i]-Tc[i]-Tc[i]-Tc[i]-Tc[i]-Tc[i]-Tc[i]-Tc[i]-Tc[i]-Tc[i]-Tc[i]-Tc[i]-Tc[i]-Tc[i]-Tc[i]-Tc[i]-Tc[i]-Tc[i]-Tc[i]-Tc[i]-Tc[i]-Tc[i]-Tc[i]-Tc[i]-Tc[i]-Tc[i]-Tc[i]-Tc[i]-Tc[i]-Tc[i]-Tc[i]-Tc[i]-Tc[i]-Tc[i]-Tc[i]-Tc[i]-Tc[i]-Tc[i]-Tc[i]-Tc[i]-Tc[i]-Tc[i]-Tc[i]-Tc[i]-Tc[i]-Tc[i]-Tc[i]-Tc[i]-Tc[i]-Tc[i]-Tc[i]-Tc[i]-Tc[i]-Tc[i]-Tc[i]-Tc[i]-Tc[i]-Tc[i]-Tc[i]-Tc[i]-Tc[i]-Tc[i]-Tc[i]-Tc[i]-Tc[i]-Tc[i]-Tc[i]-Tc[i]-Tc[i]-Tc[i]-Tc[i]-Tc[i]-Tc[i]-Tc[i]-Tc[i]-Tc[i]-Tc[i]-Tc[i]-Tc[i]-Tc[i]-Tc[i]-Tc[i]-Tc[i]-Tc[i]-Tc[i]-Tc[i]-Tc[i]-Tc[i]-Tc[i]-Tc[i]-Tc[i]-Tc[i]-Tc[i]-Tc[i]-Tc[i]-Tc[i]-Tc[i]-Tc[i]-Tc[i]-Tc[i]-Tc[i]-Tc[i]-Tc[i]-Tc[i]-Tc[i]-Tc[i]-Tc[i]-Tc[i]-Tc[i]-Tc[i]-Tc[i]-Tc[i]-Tc[i]-Tc[i]-Tc[i]-Tc[i]-Tc[i]-Tc[i]-Tc[i]-Tc[i]-Tc[i]-Tc[i]-Tc[i]-Tc[i]-Tc[i]-Tc[i]-Tc[i]-Tc[i]-Tc[i]-Tc[i]-Tc[i]-Tc[i]-Tc[i]-Tc[i]-Tc[i]-Tc[i]-Tc[i]-Tc[i]-Tc[i]-Tc[i]-Tc[i]-Tc[i]-Tc[i]-Tc[i]-Tc[i]-Tc[i]-Tc[i]-Tc[i]-Tc[i]-Tc[i]-Tc[i]-Tc[i]-Tc[i]-Tc[i]-Tc[i]-Tc[i]-Tc[i]-Tc[i]-Tc[i]-Tc[i]-Tc[i]-Tc[i]-Tc[i]-Tc[i]-Tc[i]-Tc[i]-Tc[i]-Tc[i]-Tc[i]-Tc[i]-Tc[i]-Tc[i]-Tc[i]-Tc
                                                                            (Th[i+1]-Tc[i+1]);
                                               Tc[i] := Q[i]/(mc*Cp\_air((Tc[i]+Tc[i+1])/2))+Tc[i+1];
                                               Th[i+1] := Th[i]-Q[i]/(mh*Cp_air((Th[i]+Th[i+1])/2));
                                      End;
                      End;
               Qw := Q[i];
               wc[j] := 0;
               for a := 1 to 200 do
                      Begin
                               for i := 1 to nr do
                                      Begin
                                               Q[i] := UAmix((Th[i]+Th[i+1])/2,(Tc[i]+
                                                                           Tc[i+1]/2,mh,mc,Q[i]/nc,nc,wc[i])*
                                                                           abs((Th[i]+Th[i+1]-Tc[i]-Tc[i+1])/2);
                                              Tc[i] := Q[i]/(mc*Cp\_air((Tc[i]+Tc[i+1])/2))+Tc[i+1];
                                              Th[i+1] := Th[i]-Q[i]/(mh*Cp_air((Th[i]+Th[i+1])/2));
                                     End;
```

```
End;
                         for a := 1 to 200 do
                                    Begin
                                                   for i := 1 to nr do
                                                               Begin
                                                                                                      := UAmix((Th[i]+Th[i+1])/2,(Tc[i]+
                                                                             Q[i]
                                                                                                                           Tc[i+1]/2,mh,mc,Q[i]/nc,nc,wc[i])*
                                                                                                                           ((Th[i]-Tc[i])-(Th[i+1]-Tc[i+1]))/ln((Th[i]-Tc[i])/ln((Th[i]-Tc[i])/ln((Th[i]-Tc[i])/ln((Th[i]-Tc[i])/ln((Th[i]-Tc[i])/ln((Th[i]-Tc[i])/ln((Th[i]-Tc[i])/ln((Th[i]-Tc[i])/ln((Th[i]-Tc[i])/ln((Th[i]-Tc[i])/ln((Th[i]-Tc[i])/ln((Th[i]-Tc[i])/ln((Th[i]-Tc[i])/ln((Th[i]-Tc[i])/ln((Th[i]-Tc[i])/ln((Th[i]-Tc[i])/ln((Th[i]-Tc[i])/ln((Th[i]-Tc[i])/ln((Th[i]-Tc[i])/ln((Th[i]-Tc[i])/ln((Th[i]-Tc[i])/ln((Th[i]-Tc[i])/ln((Th[i]-Tc[i])/ln((Th[i]-Tc[i])/ln((Th[i]-Tc[i])/ln((Th[i]-Tc[i])/ln((Th[i]-Tc[i])/ln((Th[i]-Tc[i])/ln((Th[i]-Tc[i])/ln((Th[i]-Tc[i])/ln((Th[i]-Tc[i])/ln((Th[i]-Tc[i])/ln((Th[i]-Tc[i])/ln((Th[i]-Tc[i])/ln((Th[i]-Tc[i])/ln((Th[i]-Tc[i])/ln((Th[i]-Tc[i])/ln((Th[i]-Tc[i])/ln((Th[i]-Tc[i])/ln((Th[i]-Tc[i])/ln((Th[i]-Tc[i])/ln((Th[i]-Tc[i])/ln((Th[i]-Tc[i])/ln((Th[i]-Tc[i])/ln((Th[i]-Tc[i])/ln((Th[i]-Tc[i])/ln((Th[i]-Tc[i])/ln((Th[i]-Tc[i]-Tc[i])/ln((Th[i]-Tc[i]-Tc[i]-Tc[i]-Tc[i]-Tc[i]-Tc[i]-Tc[i]-Tc[i]-Tc[i]-Tc[i]-Tc[i]-Tc[i]-Tc[i]-Tc[i]-Tc[i]-Tc[i]-Tc[i]-Tc[i]-Tc[i]-Tc[i]-Tc[i]-Tc[i]-Tc[i]-Tc[i]-Tc[i]-Tc[i]-Tc[i]-Tc[i]-Tc[i]-Tc[i]-Tc[i]-Tc[i]-Tc[i]-Tc[i]-Tc[i]-Tc[i]-Tc[i]-Tc[i]-Tc[i]-Tc[i]-Tc[i]-Tc[i]-Tc[i]-Tc[i]-Tc[i]-Tc[i]-Tc[i]-Tc[i]-Tc[i]-Tc[i]-Tc[i]-Tc[i]-Tc[i]-Tc[i]-Tc[i]-Tc[i]-Tc[i]-Tc[i]-Tc[i]-Tc[i]-Tc[i]-Tc[i]-Tc[i]-Tc[i]-Tc[i]-Tc[i]-Tc[i]-Tc[i]-Tc[i]-Tc[i]-Tc[i]-Tc[i]-Tc[i]-Tc[i]-Tc[i]-Tc[i]-Tc[i]-Tc[i]-Tc[i]-Tc[i]-Tc[i]-Tc[i]-Tc[i]-Tc[i]-Tc[i]-Tc[i]-Tc[i]-Tc[i]-Tc[i]-Tc[i]-Tc[i]-Tc[i]-Tc[i]-Tc[i]-Tc[i]-Tc[i]-Tc[i]-Tc[i]-Tc[i]-Tc[i]-Tc[i]-Tc[i]-Tc[i]-Tc[i]-Tc[i]-Tc[i]-Tc[i]-Tc[i]-Tc[i]-Tc[i]-Tc[i]-Tc[i]-Tc[i]-Tc[i]-Tc[i]-Tc[i]-Tc[i]-Tc[i]-Tc[i]-Tc[i]-Tc[i]-Tc[i]-Tc[i]-Tc[i]-Tc[i]-Tc[i]-Tc[i]-Tc[i]-Tc[i]-Tc[i]-Tc[i]-Tc[i]-Tc[i]-Tc[i]-Tc[i]-Tc[i]-Tc[i]-Tc[i]-Tc[i]-Tc[i]-Tc[i]-Tc[i]-Tc[i]-Tc[i]-Tc[i]-Tc[i]-Tc[i]-Tc[i]-Tc[i]-Tc[i]-Tc[i]-Tc[i]-Tc[i]-Tc[i]-Tc[i]-Tc[i]-Tc[i]-Tc[i]-Tc[i]-Tc[i]-Tc[i]-Tc[i]-Tc[i]-Tc[i]-Tc[i]-Tc[i]-Tc[i]-Tc[i]-Tc[i]-Tc[i]-Tc[i]-Tc[i]-Tc[i]-Tc[i]-Tc[i]-Tc[i]-Tc[i]-Tc[i]-Tc[i]-Tc[i]-Tc[i]-Tc[i]-Tc[i]-Tc[i]-Tc[i]-Tc[i]-Tc[i]-Tc[i]-Tc[i]-Tc[i]-Tc[i]-Tc[i]-Tc[i]-Tc[i]-Tc[i]-Tc[i]-Tc
                                                                                                                           (Th[i+1]-Tc[i+1]);
                                                                             Tc[i] := Q[i]/(mc*Cp\_air((Tc[i]+Tc[i+1])/2))+Tc[i+1];
                                                                             Th[i+1] := Th[i]-Q[i]/(mh*Cp air((Th[i]+Th[i+1])/2));
                                     End;
                         Qe := Q[i];
                         If Qw > Qe then wc[j] := 1 else wc[j] := 0;
                         for a := 1 to 200 do
                                     Begin
                                                   for i := 1 to nr do
                                                               Begin
                                                                             Q[i] := UAmix((Th[i]+Th[i+1])/2,(Tc[i]+
                                                                                                                          Tc[i+1]/2,mh,mc,Q[i]/nc,nc,wc[i])*
                                                                                                                           abs((Th[i]+Th[i+1]-Tc[i]-Tc[i+1])/2);
                                                                             Tc[i] := Q[i]/(mc*Cp\_air((Tc[i]+Tc[i+1])/2))+Tc[i+1];
                                                                             Th[i+1] := Th[i]-Q[i]/(mh*Cp_air((Th[i]+Th[i+1])/2));
                                                               End:
                                     End;
                         for a := 1 to 200 do
                                     Begin
                                                   for i := 1 to nr do
                                                               Begin
                                                                             Q[i] := UAmix((Th[i]+Th[i+1])/2,(Tc[i]+
                                                                                                                          Te[i+1]/2,mh,mc,Q[i]/nc,nc,wc[i])*
                                                                                                                          ((Th[i]-Tc[i])-(Th[i+1]-Tc[i+1]))/ln((Th[i]-Tc[i])/ln((Th[i]-Tc[i])/ln((Th[i]-Tc[i])/ln((Th[i]-Tc[i])/ln((Th[i]-Tc[i])/ln((Th[i]-Tc[i])/ln((Th[i]-Tc[i])/ln((Th[i]-Tc[i])/ln((Th[i]-Tc[i])/ln((Th[i]-Tc[i])/ln((Th[i]-Tc[i])/ln((Th[i]-Tc[i])/ln((Th[i]-Tc[i])/ln((Th[i]-Tc[i])/ln((Th[i]-Tc[i])/ln((Th[i]-Tc[i])/ln((Th[i]-Tc[i])/ln((Th[i]-Tc[i])/ln((Th[i]-Tc[i])/ln((Th[i]-Tc[i])/ln((Th[i]-Tc[i])/ln((Th[i]-Tc[i])/ln((Th[i]-Tc[i])/ln((Th[i]-Tc[i])/ln((Th[i]-Tc[i])/ln((Th[i]-Tc[i])/ln((Th[i]-Tc[i])/ln((Th[i]-Tc[i])/ln((Th[i]-Tc[i])/ln((Th[i]-Tc[i])/ln((Th[i]-Tc[i])/ln((Th[i]-Tc[i])/ln((Th[i]-Tc[i])/ln((Th[i]-Tc[i]-Tc[i])/ln((Th[i]-Tc[i]-Tc[i])/ln((Th[i]-Tc[i]-Tc[i]-Tc[i])/ln((Th[i]-Tc[i]-Tc[i]-Tc[i]-Tc[i]-Tc[i]-Tc[i]-Tc[i]-Tc[i]-Tc[i]-Tc[i]-Tc[i]-Tc[i]-Tc[i]-Tc[i]-Tc[i]-Tc[i]-Tc[i]-Tc[i]-Tc[i]-Tc[i]-Tc[i]-Tc[i]-Tc[i]-Tc[i]-Tc[i]-Tc[i]-Tc[i]-Tc[i]-Tc[i]-Tc[i]-Tc[i]-Tc[i]-Tc[i]-Tc[i]-Tc[i]-Tc[i]-Tc[i]-Tc[i]-Tc[i]-Tc[i]-Tc[i]-Tc[i]-Tc[i]-Tc[i]-Tc[i]-Tc[i]-Tc[i]-Tc[i]-Tc[i]-Tc[i]-Tc[i]-Tc[i]-Tc[i]-Tc[i]-Tc[i]-Tc[i]-Tc[i]-Tc[i]-Tc[i]-Tc[i]-Tc[i]-Tc[i]-Tc[i]-Tc[i]-Tc[i]-Tc[i]-Tc[i]-Tc[i]-Tc[i]-Tc[i]-Tc[i]-Tc[i]-Tc[i]-Tc[i]-Tc[i]-Tc[i]-Tc[i]-Tc[i]-Tc[i]-Tc[i]-Tc[i]-Tc[i]-Tc[i]-Tc[i]-Tc[i]-Tc[i]-Tc[i]-Tc[i]-Tc[i]-Tc[i]-Tc[i]-Tc[i]-Tc[i]-Tc[i]-Tc[i]-Tc[i]-Tc[i]-Tc[i]-Tc[i]-Tc[i]-Tc[i]-Tc[i]-Tc[i]-Tc[i]-Tc[i]-Tc[i]-Tc[i]-Tc[i]-Tc[i]-Tc[i]-Tc[i]-Tc[i]-Tc[i]-Tc[i]-Tc[i]-Tc[i]-Tc[i]-Tc[i]-Tc[i]-Tc[i]-Tc[i]-Tc[i]-Tc[i]-Tc[i]-Tc[i]-Tc[i]-Tc[i]-Tc[i]-Tc[i]-Tc[i]-Tc[i]-Tc[i]-Tc[i]-Tc[i]-Tc[i]-Tc[i]-Tc[i]-Tc[i]-Tc[i]-Tc[i]-Tc[i]-Tc[i]-Tc[i]-Tc[i]-Tc[i]-Tc[i]-Tc[i]-Tc[i]-Tc[i]-Tc[i]-Tc[i]-Tc[i]-Tc[i]-Tc[i]-Tc[i]-Tc[i]-Tc[i]-Tc[i]-Tc[i]-Tc[i]-Tc[i]-Tc[i]-Tc[i]-Tc[i]-Tc[i]-Tc[i]-Tc[i]-Tc[i]-Tc[i]-Tc[i]-Tc[i]-Tc[i]-Tc[i]-Tc[i]-Tc[i]-Tc[i]-Tc[i]-Tc[i]-Tc[i]-Tc[i]-Tc[i]-Tc[i]-Tc[i]-Tc[i]-Tc[i]-Tc[i]-Tc[i]-Tc[i]-Tc[i]-Tc[i]-Tc[i]-Tc[i]-Tc[i]-Tc[i]-Tc[i]-Tc[i]-Tc[i]-Tc[i]-Tc[i]-Tc[i]-Tc[i]-Tc[i]-Tc[i]-Tc[i]-Tc[i]-Tc[i]-Tc[i]-Tc[i]-Tc[i]-Tc[i]-Tc[i]-Tc[i]-Tc[i]-Tc[i]-Tc[i]-Tc[i]-Tc[i]-Tc[i]-Tc[i]-Tc[i]-Tc[i]-Tc[i]-Tc[i]-Tc[i]-Tc[i]-Tc[i]-Tc[i]-Tc
                                                                                                                          (Th[i+1]-Tc[i+1]);
                                                                            Tc[i] := Q[i]/(mc*Cp\_air((Tc[i]+Tc[i+1])/2))+Tc[i+1];
                                                                            Th[i+1] := Th[i]-Q[i]/(mh*Cp_air((Th[i]+Th[i+1])/2));
                                                              End;
                                    End;
           End; {end row j}
for j := 1 to nr do
           Begin
                         writeln(' row ',j,' Q = ',Q[j]:1:2);
                         If wc[j] = 1 then
                                 Begin
```

```
writeln(' working fluid = water');
                   End;
                 If wc[j] = 0 then
                   Begin
                      writeln('working fluid = ethanol');
                 writeln(' Thi = ',Th[j]:1:2,' Tho = ',Th[j+1]:1:2,' Tci = ',Tc[j+1]:1:2,
                        Tco = ',Tc[j]:1:2);
              End;
           Qtotal := 0;
           for j := 1 to nr do
              Begin
                 Qtotal := Qtotal+Q[j];
              End;
           writeln(' Qtotal = ',Qtotal:1:2);
        End;
End.
```

A.2 <u>Simulation Program for Selecting the Suitable Mixture Content of TEG-Water for</u> <u>High Operating Temperature Thermosyphon Heat Exchanger</u>

1. Method for Using Program

This program is used to calculate the suitable mixture content of TEG-water in each row of the thermosyphon heat exchanger for reducing the flooding phenomenon of the working fluid inside the thermosyphon. The method for input primary data is similar to that of previous program. The outputs of this program are the suitable mixture content, the heat transfer rate and the inlet and the outlet temperature of the hot and the cold streams in each row.

2. Detail of the Program

```
Program Heat Pipe 002; {heat transfer rate at high operating temperature}
Uses
       Wincrt:
Var
       Thi, Tci, Qtotal, factor, Bo, Xvteg, T: real;
       mh,mc,Le,Lc,fs,fh,ft,St,Sd,Sl,od,fn,id,Qc: real;
       Q : array[1..100] of real;
       Th : array[1..100] of real;
       Tc : array[1..100] of real;
       Occ : array[1..100] of real;
       Xvtegc: array[1..100] of real;
       Imtd,Thow,Tcow,Thoe,Tcoe : real;
       fintype,arrangement,flowpattern,cross_section_area: real;
       a,nr,nc,i,j,k: integer;
       wc: array[1..100] of real;
       mixture: string[10];
  Function den air(T:real):real; {calculate density of air}
  Begin
      den air := 0.000005*sqr(T+273.15)-0.0063*(T+273.15)+2.6043;
Function vis air(T:real):real; {calculate viscosity of air}
  Begin
      vis air := (-0.0003*sqr(T+273.15)+0.6361*(T+273.15)+17.349)/10000000;
  End:
Function Cp air(T:real):real; {calculate Cp of air}
 Begin
      Cp\_air := (0.0000004*sqr(T+273.15)-0.0002*(T+273.15)+1.0324)*1000;
 End:
```

```
Function k air(T:real):real; {calculate thermal conductivity of air}
 Begin
     k air := (-0.00003*sqr(T+273.15)+0.0955*(T+273.15)+0.24)/1000;
 End;
Function Pw(T:real):real; {vapor pressure of water}
 Var Pc,Tc,b1,b2,b3,b4,Tr: real;
 Begin
     Pc := 22.093*1000000; Tc := 647.25;
     b1 := -7.78747:
                           b2 := 1.50255:
     b3 := -2.81152:
                           b4 := -1.22268:
     T_r := (T+273.15)/T_c;
     Pw := \exp(\ln(Pc) + (1/Tr) + (b1 + (1-Tr) + b2 + \exp((3/2) + \ln(1-Tr)))
         +b3*exp(3*ln(1-Tr))+b4*exp(6*ln(1-Tr)));
 End:
Function Dwl(T:real):real; {density of liquid water}
 Var dc, Tc, b1, b2, b3, b4, Tr: real;
 Begin
     dc := 315.5; Tc := 647.25;
     b1 := 2.24670; b2 := -2.09405;
     b3 := 2.73700; b4 := -1.74750;
     Tr := (T+273.15)/Tc;
     Dwl := dc * exp(b1 * exp((1/3) * ln(1-Tr)) + b2 * exp((2/3) * ln(1-Tr))
          +b3*(1-Tr)+b4*exp((4/3)*ln(1-Tr)));
 End:
Function Dwg(T:real):real; {density of vapor water}
 Var dc, Tc, b1, b2, b3, b4, Tr: real;
 Begin
     dc := 315.5; Tc := 647.25;
     b1 := -1.38200; b2 := -6.06253;
     b3 := 5.91090;
                     b4 := -6.68477;
     Tr := (T+273.15)/Tc;
     Dwg := dc*exp(b1*exp((1/3)*ln(1/Tr-1))+b2*exp((2/3)*ln(1/Tr-1))
          +b3*(1/Tr-1)+b4*exp((4/3)*ln(1/Tr-1)));
 End;
Function Lw(T:real):real; {latent heat of water}
 Var Tc,b1,b2,b3,b4,Tr : real;
 Begin
     Tc := 647.25;
     b1 := 1.7035*100000;
                                b2 := 1.12332*100000000;
     b3 := -1.47041*10000000; b4 := 6.35750*1000000;
     Tr := (T+273.15)/Tc;
     Lw := b1*exp((1/3)*ln(1-Tr))+b2*exp((2/3)*ln(1-Tr))
         +b3*(1-Tr)+b4*exp((4/3)*ln(1-Tr));
 End;
```

```
Function Cpw(T:real):real; {density of liquid water}
 Var Tc,b1,b2,b3,b4,Tr: real;
 Begin
      Tc := 647.25;
      b1 := -1.4995*10000; b2 := 8.8*0.01;
                        b4 := -7.05*0.1;
      b3 := -6.82*0.1;
      Tr := (T+273.15)/Te;
      Cpw := b1*(1+b2*exp((-2/3)*ln(1-Tr))+b3*exp((-1/3)*ln(1-Tr))
          +b4*exp((1/3)*ln(1-Tr)));
 End:
Function Vwl(T:real):real; {dynamic viscosity ofliquid water}
  Var Tc,b1,b2,b3,b4,Tr: real;
 Begin
     Tc := 647.25;
     b1 := -1.01083*10; b2 := 1.39621;
     b3 := 4.8431*0.1; b4 := 7.1019*0.1;
      Tr := (T+273.15)/Tc;
      Vwl := \exp(b1+b2*\exp((1/3)*\ln(1/Tr-1))+b3*\exp((4/3)*\ln(1/Tr-1))
          +b4*exp((7/3)*ln(1/Tr-1));
 End:
Function Vwg(T:real):real; {dynamic viscosity of vapor water}
 Var Tc,b1,b2,b3,b4,Tr: real;
 Begin
     Tc := 647.25;
     b1 := -1.0373*10; b2 := -8.6737*0.1;
     b3 := -2.9699*0.1; b4 := 9.051*0.01;
      Tr := (T+273.15)/Tc;
      Vwg := \exp(b1+b2*\exp((1/3)*\ln(1/Tr-1))+b3*\exp((4/3)*\ln(1/Tr-1))
          +b4*exp((7/3)*ln(1/Tr-1));
 End;
Function kw(T:real):real; {thermal conductivity water}
 Var Tc,b1,b2,b3,b4,b5,Tr: real;
 Begin
     Tc := 647.25;
     b1 := -1.63975;
                       b2 := 1.11421*10;
     b3 := -2.00805*10; b4 := 1.67447*10;
     b5 := -5.78763;
     Tr := (T+273.15)/Tc;
     kw := b1+b2*Tr+b3*Tr*Tr+b4*Tr*Tr*Tr+b5*Tr*Tr*Tr*Tr;
Function tanh(x:real):real; {calculate hyperbolic tangent}
 Begin
     tanh := (exp(x)-exp(-x))/(exp(x)+exp(-x));
 End;
```

```
Function Sw(T:real):real; {surface tension water}
 Var Tc,b1,b2,b3,b4,Tr: real;
 Begin
     Tc := 647.25;
     b1 := 2.358*0.1; b2 := -6.25*0.1;
     b3 := 1.256;
     Tr := (T+273.15)/Tc;
     Sw := b1*exp(b3*ln(1-Tr))*(1+b2*(1-Tr));
 End:
Function Pt(T:real):real; {vapor pressure of TEG}
 Var a,b: real;
 Begin
     a := (T+273.15)/710.15;
     b := -3.2121*(1/\exp(2.3086*\ln(a))-1)+1.1106*(\exp(7*\ln(a))-1);
     Pt := 101325*33.2*exp(b);
 End;
Function Dtl(T:real):real; {density of liquid TEG}
 Begin
     Dtl:= -1.2979*T+1212.3:
Function Dtg(T:real):real; {density of vapor TEG}
 Begin
     Dtg:=-4*0.000001*T*T*T+0.0012*T*T-0.0712*T+1.5854;
 End:
Function Lt(T:real):real; {latent heat of TEG}
 Var x,Tr,Tbr: real;
 Begin
     Tr := (T+273.15)/710.15;
     Tbr := 0.7857;
     x := (Tbr/Tr)*(1-Tr)/(1-Tbr);
     Lt := 502046*(Tr/Tbr)*(x+exp(0.35298*ln(x)))/(1+exp(0.13856*ln(x)));
 End:
Function Cpt(T:real):real; {density of liquid TEG}
 Begin
     Cpt := 4.5756*T+2037.2;
Function Vtl(T:real):real; {dynamic viscosity of liquid TEG}
 Begin
     Vtl:= 1.3994*exp(-1.159*ln(T));
Function kt(T:real):real; {thermal conductivity TEG}
 Begin
     kt := -0.00004*T+0.1975;
 End:
```

```
Function Ste(T:real):real; {surface tension TEG}
 Begin
     Ste := 0.001*(126.314+exp((11/9)*ln(1-(T+273.15)/710.15)));
 End:
Function Dml(T, Xvteg:real):real; {density of liquid water-TEG mixture}
 Var x:real;
 Begin
     x := dtl(T)*Xvteg/(dtl(T)*Xvteg+dwl(T)*(1-Xvteg));
     Dml:=dtl(T)*x+dwl(T)*(1-x);
 End;
Function Dmg(T.Xvteg:real):real; {density of vapor water-TEG mixture}
 Begin
     If Xvteg = 0.25 then
       Begin
          Dmg := 0.0071*\exp(1.3375*\ln(T));
       End;
     If Xvteg = 0.5 then
       Begin
          Dmg := 0.0004*exp(1.9077*ln(T));
     If Xvteg = 0.75 then
       Begin
          Dmg := 0.00006*exp(2.3188*ln(T));
       End:
 End:
Function Lm(T,Xvteg:real):real; {latent heat of water-TEG mixture}
 Var x:real;
 Begin
     x := Dtl(T)*Xvteg/(Dtl(T)*Xvteg+Dwl(T)*(1-Xvteg));
     Lm := Lt(T)*x+Lw(T)*(1-x);
 End;
Function Sm(T,Xvteg:real):real; {surface tension of water-TEG mixture}
 Var Ww,Wt,B,W,Ww1,Ww2,xm,x:real;
 Begin
     xm := (1-Xvteg)*Dwl(T)/(Xvteg*Dtl(T)+(1-Xvteg)*Dwl(T));
     x := (xm/18)/((xm/18)+((1-xm)/150));
     Ww := x*(150/Dtl(T))/(x*(150/Dtl(T))+(1-x)*(18/Dwl(T)));
     Wt := (1-x)*(150/Dtl(T))/(x*(150/Dtl(T))+(1-x)*(18/Dwl(T)));
     B := \ln(\exp(6*\ln(Ww))/Wt)/\ln(10);
     W := (0.441*6/(T+273.15))*((Ste(T)*exp(0.667*ln(150/Dtl(T)))/6)
          -Sw(T)*exp(0.667*ln(18/Dwl(T))));
     Ww1 := 0.1;
     For i := 1 to 100 do
       Begin
```

```
Ww2 := 1-\exp(6*\ln(Ww1))/(\exp((B+W)*\ln(10)));
          Ww1 := Ww2;
       End:
     Sm := \exp(4*\ln(Ww1*sqrt(sqrt(Sw(T)))+(1-Ww1)*sqrt(sqrt(Ste(T)))));
 End;
Function C staggered(Re,St,Sl:real):real; {Zhukauskas factor}
 Var s: real;
 Begin
     If Re<100 then C_staggered := 0.9
     Else
        Begin
           If Re<1000 then C staggered := 0.51
           Else
             Begin
                s := St/Sl;
                If Re<200000 then
                  Begin
                     If s < 2 then C_staggered := 0.35*exp(0.2*ln(s))
                     else C_staggered := 0.4;
                  End
                Else
                  Begin
                     If Re<1000000 then C_staggered := 0.022;
                  End;
             End;
        End;
 End;
Function m staggered(Re:real):real; {Zhukauskas factor}
 Begin
     If Re<100 then m staggered := 0.4
     Else
           If Re<1000 then m_staggered := 0.5
           Else
             Begin
                If Re<200000 then m staggered := 0.6
                Else
                  Begin
                     If Re < 1000000 then m staggered := 0.84;
                   End;
             End;
        End;
Function C_aligned(Re:real):real; {Zhukauskas factor}
```

```
Begin
      If Re<100 then C_aligned := 0.8
      Else
        Begin
           If Re < 1000 then C aligned := 0.51
           Else
              Begin
                 If Re < 200000 then C aligned := 0.27
                 Else
                   Begin
                      If Re < 1000000 then C_aligned := 0.21;
                   End:
              End;
        End:
 End:
Function m aligned(Re:real):real; {Zhukauskas factor}
 Begin
      If Re < 100 then m aligned := 0.4
      Else
        Begin
           If Re < 1000 then m aligned := 0.5
           Else
              Begin
                 If Re < 200000 then m aligned := 0.63
                 Else
                   Begin
                      If Re < 1000000 then m aligned := 0.84;
                   End;
              End;
        End;
 End;
Function UA003(Th,Tc,mh,mc,Q,nc,Xvteg:real):real;{calculate UA of water-TEG}
           k = 14.9; {thermal conductivity of metal}
 Const
 Var
Aeo, Aei, Aco, Aci, Afe, Afc, Abe, Abc, heo, hei, hco, hci, mfac, mfae, Vmaxe, Vmaxc, Ree,
        Rec, Pre, Prc, Nue, Nuc, w, effe, effc, Zc, Zef, Zep, phe2, phe3, T, Z, Re, a: real;
        del Tsat,x,y,heif,heip,Pr,fp,P,xw,xt,yw,yt:real;
        Ve, Vc, Vmaxe1, Vmaxe2, Vmaxc1, Vmaxc2, heiw, heit, heiw, heit : real;
 Begin
        If arrangement = 1 then
          Begin
            If fintype = 1 then
              Begin
                 Abe := nc*Le*3.14159*od;
```

```
Abc := nc*Lc*3.14159*od;
     Afe := 0:
     Afc := 0;
     Ve := mh/(den air(Th)*cross section area);
     Vc := mc/(den air(Tc)*cross section area);
     Vmaxe := St*Ve/(St-od);
     Vmaxc := St*Vc/(St-od);
     Ree := den air(Th)*Vmaxe*od/vis air(Th);
     Rec := den air(Tc)*Vmaxc*od/vis air(Tc);
    Pre := Cp air(Th)*vis air(Th)/k air(Th);
    Prc := Cp \operatorname{air}(Tc)*\operatorname{vis} \operatorname{air}(Tc)/k \operatorname{air}(Tc);
    Nue := C \text{ aligned(Ree)*exp(m aligned(Ree)*ln(Ree))}
           *exp(0.36*ln(Pre));
    Nuc := C aligned(Rec)*exp(m aligned(Rec)*ln(Rec))
           *exp(0.36*ln(Prc));
    heo := Nue*k air(Th)/od;
    heo := Nuc*k air(Tc)/od;
    effe := 0:
    effc := 0;
 End:
If fintype = 2 then
 Begin
     Afe := ((nc*Le*3.14159)/(fs+ft))*(0.5*(sqr(od+2*fh)-sqr(od))
           +(od+2*fh)*ft);
     Abe := ((nc*Le*3.14159)/(fs+ft))*od*fs;
     Afc := ((nc*Lc*3.14159)/(fs+ft))*(0.5*(sqr(od+2*fh)-sqr(od))
           +(od+2*fh)*ft);
    Abc := ((nc*Lc*3.14159)/(fs+ft))*od*fs;
    mfae := nc*Le*(St-od-(2*ft*fh)/(fs+ft));
    mfac := nc*Lc*(St-od-(2*ft*fh)/(fs+ft));
    Vmaxe := mh/(den_air(Th)*mfae);
    Vmaxc := mc/(den air(Tc)*mfac);
    Ree := Vmaxe*od*den air(Th)/vis air(Th);
    Rec := Vmaxc*od*den air(Tc)/vis air(Tc);
    Pre := Cp_air(Th)*vis_air(Th)/k_air(Th);
    Prc := Cp air(Tc)*vis air(Tc)/k air(Tc);
    Nue := 0.30*\exp(0.625*\ln(\text{Ree}))*\exp(-0.375*
           ln((nc*Le*3.14159*od)/(Afe+Abe)))
           *exp(0.333*ln(Pre)):
    Nuc := 0.30*\exp(0.625*\ln(\text{Rec}))*\exp(-0.375*
          ln((nc*Lc*3.14159*od)/(Afc+Abc)))
           *exp(0.333*ln(Prc));
    heo := Nue*k air(Th)/od;
    hco := Nuc*k_air(Tc)/od;
```

```
:= 0.5*od*(((od+2*fh)/od)-1)*(1+0.35*ln((od+2*fh)/od));
         effe := \frac{(\tanh(\operatorname{sqrt}(2*\operatorname{heo}/(\operatorname{ft}*k))*w)}{(\operatorname{sqrt}(2*\operatorname{heo}/(\operatorname{ft}*k))*w)};
         effc := (tanh(sqrt(2*hco/(ft*k))*w)/(sqrt(2*hco/(ft*k))*w));
      End:
 End:
If arrangement = 2 then
 Begin
    If fintype = 1 then
      Begin
         Abe := nc*Le*3.14159*od;
         Abc := nc*Lc*3.14159*od;
         Afe := 0;
         Afc := 0;
         Ve := mh/(den_air(Th)*cross_section_area);
         Vc := mc/(den air(Tc)*cross section area);
         Vmaxe1:= St*Ve/(St-od);
         Vmaxc1:= St*Vc/(St-od);
         Vmaxe2:= St*Ve/(2*(Sd-od));
         Vmaxc2:= St*Vc/(2*(Sd-od));
         If Vmaxe1 > Vmaxe2 then Vmaxe := Vmaxe1
         else Vmaxe := Vmaxe2;
         If Vmaxc1 > Vmaxc2 then Vmaxc := Vmaxc1
         else Vmaxc := Vmaxc2:
         Ree := den air(Th)*Vmaxe*od/vis air(Th);
         Rec := den air(Tc)*Vmaxc*od/vis_air(Tc);
         Pre := Cp air(Th)*vis air(Th)/k air(Th);
         Prc := Cp air(Tc)*vis air(Tc)/k air(Tc);
         Nue := C staggered(Ree,St,Sl)*exp(m_staggered(Ree)*ln(Ree))
               *\exp(0.36*\ln(\text{Pre}));
         Nuc := C staggered(Rec,St,Sl)*exp(m_staggered(Rec)*ln(Rec))
               *exp(0.36*ln(Prc));
         heo := Nue*k air(Th)/od;
         hco := Nuc*k air(Tc)/od;
         effe := 0;
         effc := 0;
      End:
    If fintype = 2 then
      Begin
         Afe := ((nc*Le*3.14159)/(fs+ft))*(0.5*(sqr(od+2*fh)-sqr(od))
               +(od+2*fh)*ft);
         Abe := ((nc*Le*3.14159)/(fs+ft))*od*fs;
         Afc := ((nc*Lc*3.14159)/(fs+ft))*(0.5*(sqr(od+2*fh)-sqr(od))
               +(od+2*fh)*ft);
         Abc := ((nc*Lc*3.14159)/(fs+ft))*od*fs;
```

```
mfae := 2*nc*Le*(Sd-od-(2*ft*fh)/(fs+ft));
     mfac := 2*nc*Lc*(Sd-od-(2*ft*fh)/(fs+ft));
     Vmaxe := mh/(den air(Th)*mfae);
     Vmaxc := mc/(den air(Tc)*mfac);
     Ree := Vmaxe*od*den air(Th)/vis air(Th);
     Rec := Vmaxc*od*den air(Tc)/vis air(Tc);
     Pre := Cp \operatorname{air}(Th)*\operatorname{vis} \operatorname{air}(Th)/k \operatorname{air}(Th);
     Prc := Cp \operatorname{air}(Tc)*vis \operatorname{air}(Tc)/k \operatorname{air}(Tc);
     Nue := 0.242*\exp(0.658*\ln(\text{Ree}))*\exp(0.297*\ln(\text{fs/fh}))
            *exp(-0.091*ln(St/Sl))*exp(0.33333*ln(Pre));
     Nuc := 0.242*\exp(0.658*\ln(\text{Rec}))*\exp(0.297*\ln(\text{fs/fh}))
            \exp(-0.091*\ln(St/Sl))*\exp(0.33333*\ln(Prc));
     heo := Nue*k air(Th)/od;
     hco := Nuc*k air(Tc)/od;
           := 0.5*od*(((od+2*fh)/od)-1)*(1+0.35*ln((od+2*fh)/od));
     effe := (\tanh(\operatorname{sgrt}(2*\operatorname{heo}/(\operatorname{ft}*k))*w)/(\operatorname{sgrt}(2*\operatorname{heo}/(\operatorname{ft}*k))*w));
     effc := (\tanh(\operatorname{sqrt}(2*\operatorname{hco}/(\operatorname{ft}*k))*w)/(\operatorname{sqrt}(2*\operatorname{hco}/(\operatorname{ft}*k))*w));
  End:
If fintype = 3 then
 Begin
     Afe := ((nc+0.5)*St*Sl-nc*3.14159*od*od*0.25)*2*
               (Le*fn/0.0254);
     Abe := ((nc*Le*3.14159)/(fs+ft))*od*fs;
     Afc := ((nc+0.5)*St*Sl-nc*3.14159*od*od*0.25)*2*
               (Lc*10/0.0254);
     Abc := ((nc*Lc*3.14159)/(fs+ft))*od*fs;
     mfae := 2*nc*Le*(Sd-od-(2*ft*fh)/(fs+ft));
     mfac := 2*nc*Lc*(Sd-od-(2*ft*fh)/(fs+ft));
     Vmaxe := mh/(den air(Th)*mfae);
     V maxc := mc/(den air(Tc)*mfac);
     Ree := Vmaxe*od*den air(Th)/vis_air(Th);
     Rec := Vmaxc*od*den air(Tc)/vis air(Tc);
     Pre := Cp air(Th)*vis air(Th)/k air(Th);
     Prc := Cp air(Tc)*vis air(Tc)/k_air(Tc);
     heo := 0.14*exp(-0.328*ln(Ree))*exp(-0.502*ln(St/Sl))
            *exp(0.031*ln(fs/od))*den air(Th)*Vmaxe*Cp air(Th)
            *exp((-2/3)*ln(Pre));
     hco := 0.14*exp(-0.328*ln(Rec))*exp(-0.502*ln(St/Sl))
            *exp(0.031*ln(fs/od))*den air(Tc)*Vmaxc*Cp air(Tc)
            *exp((-2/3)*ln(Prc));
     fp := 1.27*((St/2)/(0.5*od))*sqrt((sqrt((St/2)*(St/2)+Si*Si)/2)
            /(St/2)-0.3);
     w := (fp-1)*(1+0.35*ln(fp));
     effe := \frac{(\tanh(\sqrt{t^*k}))^*w^*(od/2)}{(\operatorname{sqrt}(2^*heo/(t^*k))^*w}
```

```
*(od/2)));
         effc := (tanh(sqrt(2*hco/(ft*k))*w*(od/2))/(sqrt(2*hco/(ft*k))*w
               *(od/2)));
      End;
 End:
Aeo := effe*Afe+Abe;
Aco := effe*Afc+Abc:
Aei := 3.14159*id*Le*nc;
Aci := 3.14159*id*Lc*nc;
T := (Th+Tc)/2;
If Xvteg > 0 then
  Begin
   If Xvteg < 1 then
    Begin
         := (-8.6856*sqr(Xvteg)+4.3062*Xvteg+10.711)*T*T
           +(1561.8*sqr(Xvteg)-1564.4*Xvteg-101.65)*T
           +(-5337.6*sqr(Xvteg)-7864.8*Xvteg+16019);
    xw := (P-Pt(T))/(Pw(T)-Pt(T));
    xt := 1-xw:
    yw := ((1/P)-(1/Pt(T)))/((1/Pw(T))-(1/Pt(T)));
    vt := 1-vw;
     {calculate heat transfer coefficient of water}
         := (1/(Vwl(T)*Lw(T)))*sqrt(Sw(T)/(9.81*(Dwl(T)-Dwg(T))));
         := Lw(T)*Vwl(T)/kw(T);
    heiw := \exp(0.9332*(\ln(18.688)-\ln(x)-1.0716*\ln(y)+0.0716*\ln(Q/Aei)));
    heiw := \exp(1.30378*(\ln(0.943)+0.233*\ln(\operatorname{sqr}(\operatorname{Dwl}(T))*9.81*\operatorname{Lw}(T)*
           kw(T)*kw(T)*kw(T)*Aci/(Vwl(T)*Lc*Q)));
     {calculate heat transfer coefficient of TEG}
         := (1/(Vtl(T)*Lt(T)))*sqrt(Ste(T)/(9.81*(Dtl(T)-Dtg(T))));
         := Lt(T)*Vtl(T)/kt(T);
    heit := \exp(0.910249*\ln(20.565*\exp(0.0986*\ln(Q/Aei)))
           (x*exp(1.0986*ln(y))));
    hcit := \exp(1.2195*\ln(0.943*\exp(0.18*\ln(\operatorname{sqr}(\mathrm{Dtl}(T))*9.81*\mathrm{Lt}(T)*
           kt(T)*kt(T)*kt(T)*Aci/(Vtl(T)*Lc*Q)))));
     {calculate heat transfer coefficient of mixture}
    hei := xw*(heiw)+xt*(heit);
    hci := yw*(hciw)+yt*(hcit);
    End;
   If Xvteg = 1 then
    Begin
    x := (1/(Vtl(T)*Lt(T)))*sqrt(Ste(T)/(9.81*(Dtl(T)-Dtg(T))));
    y := Lt(T)*Vtl(T)/kt(T);
    hei := \exp(0.910249*\ln(20.565*\exp(0.0986*\ln(Q/Aei))/
          (x*exp(1.0986*ln(y))));
```

```
hci := \exp(1.2195*)\ln(0.943*\exp(0.18*)\ln(\operatorname{sqr}(Dtl(T))*9.81*Lt(T)*)
                   kt(T)*kt(T)*kt(T)*Aci/(Vtl(T)*Lc*Q)))));
            End:
          End:
        If Xvteg = 0 then
          Begin
             {calculate heat transfer coefficient of water}
             x := (1/(Vwl(T)*Lw(T)))*sqrt(Sw(T)/(9.81*(Dwl(T)-Dwg(T))));
                 := Lw(T)*Vwl(T)/kw(T);
             hei := \exp(0.9332*(\ln(18.688)-\ln(x)-1.0716*\ln(y)+0.0716*\ln(Q/Aei)));
             hci := \exp(1.30378*(\ln(0.943)+0.233*\ln(\operatorname{sqr}(Dwl(T))*9.81*Lw(T)*)
                   kw(T)*kw(T)*kw(T)*Aci/(Vwl(T)*Lc*Q)));
          End:
        UA003 := 1/(1/(heo^*Aeo)+1/(hco^*Aco)+1/(hei^*Aei)+1/(hci^*Aci)
              +\ln(\text{od/id})/(2*3.14159*k*\text{Le*nc})+\ln(\text{od/id})/(2*3.14159*k*\text{Lc*nc});
 End:
Begin
        {main program}
     writeln('PROGRAM HEAT PIPE 002
                                                      ');
     writeln:
     Writeln('This program is used for calculating performance of the thermosyphon');
     writeln(' heat exchanger operating at high temperature with binary working');
     writeln(' fluids (water-TEG');
     writeln:
     writeln(' Developed by Atipoang Nuntaphan, Ph.D. student ');
     writeln('Thermal Technology Division, School of Energy and Materials,');
     writeln('King Mongkut"s',' University of Technology Thonburi');
     writeln:
      writeln:
     writeln(' Please enter informations below');
     writeln(' 1. Heat exchanger informations');
     write(' 1.1 Input number of rows
                                                               ');
     readin(nr);
                                                                ');
     write(' 1.2 Input number of column
     readln(nc);
                                                                  ');
     write(' 1.3 Input outside diameter of tube (m)
     readln(od);
     write(' 1.4 Input inside diameter of tube (m)
                                                                  );
     readln(id);
     write(' 1.5 Input evaporator length (m)
                                                                ');
     readln(Le);
     write(' 1.6 Input condenser length (m)
                                                                ");
     readln(Lc);
     writeln(' 1.7 Input type of fin
                                                            ');
```

```
1. bare tube 2. circular finned 3. plain plate finned ');
write('
readln(fintype);
        1.8 Input fin thickness (m) (input 0 for bare tube)
                                                                   ");
write('
readln(ft);
write(' 1.9 Input fin gap (m) (input 0 for bare tube)
                                                                  );
readin(fs):
        1.10 Input fin height (m) (input 0 for bare tube)
                                                                   ');
write('
readln(fh);
write(' 1.11 Input number of fins (fin/inch) (input 0 for bare tube) ');
readln(fn);
writeln(' 1.11 Input pipe arrangement
                                                              ');
             1. aligned
                           2. staggered
                                                          ");
write('
readln(arrangement);
write(' 1.12 Input transverse pitch (St) (m)
                                                               ');
readln(St);
write(' 1.13 Input longitudinal pitch (Sl) (m)
                                                               ");
readln(SI);
write(' 1.14 Input directional pitch (Sd) (m) (input 0 for aligned)
                                                                      1);
readln(Sd);
write(' 1.15 Input cross section area of duct (m^2)
                                                                  ');
readln(cross section area);
writeln;
writeln(' 2. Working conditions ');
write(' 2.1 Input inlet temperature of hot gas (C)
                                                                 ');
readln(Thi);
write(' 2.2 Input inlet temperature of cold gas (C)
                                                                 ');
readln(Tci);
write(' 2.3 Input mass flow rate of hot gas (kg/s)
                                                                 ');
readln(mh);
write(' 2.4 Input mass flow rate of cold gas (kg/s)
                                                                 ');
readln(mc);
                                                          );
');
writeln(' 2.5 Input flow pattern
             1. parallel flow 2. counter flow
write('
read(flowpattern);
writeln;
{PARALLEL FLOW}
If flowpattern = 1 then
  Begin
     Th[1] := Thi;
     Tc[1] := Tci;
     For i := 1 to nr do
     Begin
        write(' row = ',i);
        Q[i] := 1200;
```

```
Xvteg := 0;
Q[i] := UA003(Th[i],Tc[i],mh,mc,Q[i]/nc,nc,Xvteg)*(Th[i]-Tc[i]);
Th[i+1] := Th[i]-Q[i]/(mh*Cp_air(Th[i]));
Te[i+1] := Q[i]/(mc*Cp\_air(Te[i]))+Te[i];
For j := 1 to 200 do
  Begin
     lmtd
             := ((Th[i]-Tc[i])-(Th[i+1]-Tc[i+1]))/ln((Th[i]-Tc[i])
             /(Th[i+1]-Tc[i+1]));
     Q[i]
             := UA003((Th[i]+Th[i+1])/2,(Tc[i]+Tc[i+1])/2,
             mh,mc,Q[i]/nc,nc,Xvteg)*lmtd;
     Th[i+1] := Th[i]-Q[i]/(mh*Cp air((Th[i]+Th[i+1])/2));
     Tc[i+1] := Tc[i]+Q[i]/(mc*Cp_air((Tc[i]+Tc[i+1])/2));
  End:
{calculate critical heat flux of water}
     := 0.5*((Th[i]+Th[i+1])/2+(Tc[i]+Tc[i+1])/2);
      := id*sqrt(9.81*(Dwl(T)-Dwg(T))/Sw(T));
factor := \exp(0.14*\ln(\text{Dwl}(T)/\text{Dwg}(T)))* \operatorname{sqr}(\tanh(\exp(0.25*\ln(\text{Bo}))));
      := 0.69 * factor * Lw(T) * (3.14159 * id * id/4) *
       \exp(0.25*\ln(9.81*Sw(T)*(Dwl(T)-Dwg(T)))*
       \exp(-2*\ln(\exp(-0.25*\ln(Dwg(T)))+\exp(-0.25*\ln(Dwl(T)))));
If Qc > Q[i] then
  Begin
     Q[i]
            := Q[i];
  End;
If Qc < Q[i] then
  Begin
     Repeat
     Xvteg := Xvteg+0.25;
     For j := 1 to 200 do
        Begin
                   := ((Th[i]-Tc[i])-(Th[i+1]-Tc[i+1]))
                   \ln(Th[i]-Tc[i])/(Th[i+1]-Tc[i+1]);
                  := UA003((Th[i]+Th[i+1])/2,(Tc[i]+Tc[i+1])/2,
           Q[i]
                   mh,mc,Q[i]/nc,nc,Xvteg)*lmtd;
           Th[i+1] := Th[i]-Q[i]/(mh*Cp_air((Th[i]+Th[i+1])/2));
           Tc[i+1] := Tc[i]+Q[i]/(mc*Cp\_air((Tc[i]+Tc[i+1])/2));
        End;
     {calculate critical heat flux of mixture}
          := 0.5*((Th[i]+Th[i+1])/2+(Tc[i]+Tc[i+1])/2);
           := id*sqrt(9.81*(Dml(T,Xvteg)-Dmg(T,Xvteg))/
     Bo
               Sm(T,Xvteg));
     factor := \exp(0.14*\ln(\text{Dmi}(T,X\text{vteg})/\text{Dmg}(T,X\text{vteg})))*
            sqr(tanh(exp(0.25*ln(Bo))));
          = 0.69 * factor * Lm(T, Xvteg) * (3.14159 * id * id/4) *
```

```
\exp(0.25*\ln(9.81*Sm(T,Xvteg)*(Dml(T,Xvteg)-
                    Dmg(T,Xvteg))*exp(-2*ln(exp(-0.25*ln(Dmg(T,Xvteg)))+
                    \exp(-0.25*\ln(\mathrm{Dml}(\mathrm{T,Xvteg})))));
             Until Q[i] < Qc;
          End;
        Writeln('row',i,' Q = ',Q[i]:1:2,' Tho = ',Th[i+1]:1:2,' Tco = ',
                 Tc[i+1]:1:2,' Xteg = ', Xvteg:1:2);
    End:
    Qtotal := 0;
    for i := 1 to nr do
        Begin
           Qtotal := Qtotal+Q[i];
        End;
    writeln(' Qtotal = ',Qtotal:1:2);
{COUNTER FLOW}
If flowpattern = 2 then
 Begin
    for i := 1 to nr do
       Begin
          Q[i] := 1200;
       End;
    for i := 1 to nr+1 do
       Begin
          Th[i] := Thi-2*(i-1);
          Tc[i] := Tci+2*(nr+1-i);
       End;
    for a := 1 to 200 do
       Begin
          for i := 1 to nr do
            Begin
               Q[i] := UA003((Th[i]+Th[i+1])/2,(Tc[i]+Tc[i+1])/2
                      ,mh,mc,Q[i]/nc,nc,0)*
                      abs((Th[i]+Th[i+1]-Tc[i]-Tc[i+1])/2);
               Tc[i] := Q[i]/(mc*Cp\_air((Tc[i]+Tc[i+1])/2))+Tc[i+1];
               Th[i+1] := Th[i]-Q[i]/(mh*Cp_air((Th[i]+Th[i+1])/2));
            End;
       End:
    for a := 1 to 200 do
       Begin
          for i := 1 to nr do
            Begin
               Q[i] := UA003((Th[i]+Th[i+1])/2,(Tc[i]+Tc[i+1])/2,
                      mh,mc,Q[i]/nc,nc,0)*
```

```
((Th[i]-Tc[i])-(Th[i+1]-Tc[i+1]))/
                  ln((Th[i]-Tc[i])/(Th[i+1]-Tc[i+1]));
          Tc[i] := Q[i]/(mc*Cp air((Tc[i]+Tc[i+1])/2))+Tc[i+1];
          Th[i+1] := Th[i]-Q[i]/(mh*Cp_air((Th[i]+Th[i+1])/2));
       End:
  End;
{Calculate critical heat flux}
for i := 1 to nr do
  Begin
     Т
          := 0.5*((Th[i]+Th[i+1])/2+(Tc[i]+Tc[i+1])/2);
     {water}
          := id*sqrt(9.81*(Dwl(T)-Dwg(T))/Sw(T));
     factor := \exp(0.14*\ln(\text{Dwl}(T)/\text{Dwg}(T)))* \operatorname{sqr}(\tanh(\exp(0.25*\ln(\text{Bo}))));
     Qcc[1] := 0.69*factor*Lw(T)*(3.14159*id*id/4)*
            \exp(0.25*\ln(9.81*Sw(T)*(Dwl(T)-Dwg(T)))*
            \exp(-2*\ln(\exp(-0.25*\ln(\text{Dwg}(T)))+\exp(-0.25*\ln(\text{Dwl}(T)))));
     {25% TEG}
     Xvteg := 0.25;
           := id*sqrt(9.81*(Dml(T,Xvteg)-Dmg(T,Xvteg))/Sm(T,Xvteg));
     factor := \exp(0.14*\ln(Dml(T,Xvteg)/Dmg(T,Xvteg)))*
            sqr(tanh(exp(0.25*ln(Bo))));
     Qcc[2] := 0.69*factor*Lm(T,Xvteg)*(3.14159*id*id/4)*
            \exp(0.25*\ln(9.81*Sm(T,Xvteg)*(Dml(T,Xvteg)-
            Dmg(T,Xvteg)))*
            \exp(-2*\ln(\exp(-0.25*\ln(\mathrm{Dmg}(T,\mathrm{Xvteg})))+
            \exp(-0.25*\ln(Dml(T,Xvteg)))));
     {50% TEG}
     Xvteg := 0.50;
     Bo := id*sqrt(9.81*(Dml(T,Xvteg)-Dmg(T,Xvteg))/Sm(T,Xvteg));
     factor := \exp(0.14*\ln(Dml(T,Xvteg)/Dmg(T,Xvteg)))*
            sqr(tanh(exp(0.25*ln(Bo))));
     Qcc[3] := 0.69*factor*Lm(T,Xvteg)*(3.14159*id*id/4)*
            \exp(0.25*\ln(9.81*Sm(T,Xvteg)*(Dml(T,Xvteg)-
            Dmg(T,Xvteg)))*
            \exp(-2*\ln(\exp(-0.25*\ln(Dmg(T,Xvteg)))+
            \exp(-0.25*\ln(Dml(T,Xvteg)))));
     {75% TEG}
     Xvteg := 0.75;
           := id*sqrt(9.81*(Dml(T,Xvteg)-Dmg(T,Xvteg))/Sm(T,Xvteg));
     factor := \exp(0.14*\ln(\text{Dml}(T,\text{Xvteg})/\text{Dmg}(T,\text{Xvteg})))*
            sgr(tanh(exp(0.25*ln(Bo))));
     Qcc[4] := 0.69*factor*Lm(T,Xvteg)*(3.14159*id*id/4)*
            \exp(0.25*\ln(9.81*Sm(T,Xvteg)*(Dml(T,Xvteg)-
```

```
Dmg(T,Xvteg)))*
             \exp(-2*\ln(\exp(-0.25*\ln(Dmg(T,Xvteg)))+
             \exp(-0.25*\ln(\mathrm{Dml}(T,\mathrm{Xvteg})))));
      {TEG}
            := id*sqrt(9.81*(Dtl(T)-Dtg(T))/Ste(T));
      Bo
      factor := \exp(0.14*\ln(\text{Dtl}(T)/\text{Dtg}(T)))* \operatorname{sqr}(\tanh(\exp(0.25*\ln(\text{Bo}))));
      Qcc[5] := 0.69*factor*Lt(T)*(3.14159*id*id/4)*
             \exp(0.25*\ln(9.81*Ste(T)*(Dtl(T)-Dtg(T)))*
             \exp(-2*\ln(\exp(-0.25*\ln(Dtg(T)))+\exp(-0.25*\ln(Dtl(T)))));
      If Q[i] < Qcc[1] then Xvtegc[i] := 0
      else
         Begin
         If Q[i] < Qcc[2] then Xvtegc[i] := 0.25
         else
           Begin
           If Q[i] < Qcc[3] then Xvtegc[i] := 0.50
           else
              If Q[i] < Qcc[4] then Xvtegc[i] := 0.75
              else
                 Begin
                If Q[i] < Qcc[5] then Xvtegc[i] := 1.0
                 else writeln(' critical heat flux higher than that of TEG
                 in row ',i);
                 End;
              End;
           End:
         End;
  End;
{Re-calculate heat transfer rate}
for a := 1 to 200 do
  Begin
     for i := 1 to nr do
       Begin
                 := UA003((Th[i]+Th[i+1])/2,(Tc[i]+Tc[i+1])/2,
           Q[i]
                  mh,mc,Q[i]/nc,nc,Xvtegc[i])*
                  ((Th[i]-Tc[i])-(Th[i+1]-Tc[i+1]))/
                  ln((Th[i]-Tc[i])/(Th[i+1]-Tc[i+1]));
          Tc[i] := Q[i]/(mc*Cp\_air((Tc[i]+Tc[i+1])/2))+Tc[i+1];
          Th[i+1] := Th[i]-Q[i]/(mh*Cp air((Th[i]+Th[i+1])/2));
       End;
  End;
{Show data}
for i := 1 to nr do
```

```
Begin
                If Xvtegc[j] = 0 then mixture := 'water 100%';
                If Xvtegc[j] = 0.25 then mixture := 'TEG 25%';
                If Xvtegc[j] = 0.50 then mixture := 'TEG 50%';
                If Xvtegc[j] = 0.75 then mixture := 'TEG 75%';
                If Xvtegc[j] = 1.0 then mixture := 'TEG 100%';
                writeln('row',j,'Q = ',Q[j]:1:2,' %TEG = ',mixture);
                writeln('Thi = ',Th[j]:1:2,'Tho = ',Th[j+1]:1:2,'Tci = ',
                         Tc[j+1]:1:2, Tco = Tc[j]:1:2);
             End;
           Qtotal := 0;
           for j := 1 to nr do
             Begin
                Qtotal := Qtotal + Q[j];
             End;
           writeln(' Qtotal = ',Qtotal:1:2);
       End;
End.
```

.

APPENDIX B
PUBLICATIONS

Kiatsiriroat T., Nuntaphan A. and Tiansuwan J., 2000, Thermal Performance Enhancement of Thermosyphon Heat Pipe with Binary Working Fluids, Experimental Heat Transfer, 13:137-152.

Experimental Heat Transfer, 13:137-152, 2000 Copyright © 2000 Taylor & Francis 0891-6152/00 \$12.00 + .00



THERMAL PERFORMANCE ENHANCEMENT OF THERMOSYPHON HEAT PIPE WITH BINARY WORKING FLUIDS

T. Kiatsiriroat

Department of Mechanical Engineering, Chiang Mai University, Chiang Mai, Thailand

A. Nuntaphan and J. Tiansuwan

School of Energy and Materials, King Mongkut's University of Technology Thonburi, Bangkok, Thailand

Thermal performance of a thermosyphon heat pipe using ethanol-water and TEG-water with variations of parameters such as the mixture content, the pipe diameter, and the working temperature have been studied in this research work. From the experiments, it is found that at low temperature of heat source (less than 80°C), the ethanol-water mixture has a higher heat transfer rate than that of water and close to that of pure ethanol. In the case of TEG-water mixture, the heat transfer rate of the thermosyphon varies with the content of TEG in the mixture, and it is found that TEG in the mixture can increase the critical heat flux due to the flooding limit in a small thermosyphon.

The boiling equation of Rohsenow and the condensation equation of Nusselt are modified to predict the heat transfer coefficients inside the thermosyphon. For the mixtures, the weighted average of the heat transfer coefficient of each component can be used to predict the total heat transfer coefficient. Furthermore, it is found that Faghri's equation can be used to predict the critical heat flux due to the flooding limit of the thermosyphon with the binary mixtures.

At present, development of heat exchangers for energy recovery from industrial waste heat has become an interesting topic for energy conservation programs. The thermosyphon heat pipe, one type of heat exchanger, has been used in many industrial processes because of its advantages, such as high thermal conductivity, low cost, and ease of construction.

The thermosyphon heat pipe shown in Figure 1 can be divided into three parts, evaporator, adiabatic, and condenser. When heat is added at the evaporator section, the working fluid inside the heat pipe vaporizes and carries heat from the heat source to the condenser section where heat is rejected to the heat sink. The working fluid condensate returns to the evaporator section by gravity.

The thermosyphon normally uses a single component, usually water, as a working fluid, because water has a high working temperature range (50-200°C) [1] and high latent heat of vaporization. However, in some working conditions, the

The authors gratefully acknowledge the support provided by the Thailand Research Fund for carrying out this study.

Address correspondence to Prof. T. Kiatsiriroat, Department of Mechanical Engineering, Chiang Mai University, Chiang Mai 50200, Thailand.

T. KIATSIRIROAT ET AL.

NOMENCLATURE			
A Bo	area, m² Bond number	Subscripts	
C _p	heat capacity, J/kg K, J/mol °C	1	high-volatile component
D	diamter of pipe, m	2	low-volatile component
g	gravitational acceleration (= 9.81 m/s ²)	ave	average
h	heat transfer coefficient, W/m ² K	c	condenser
k	thermal conductivity, W/m K	cs	cross section
L	length, m	e	evaporator inlet, inside
ṁ	mass rate of flow, kg/s	i	
Pr	Prandtl number, $(C_p \mu/k)$	iđ	ideal
Q	heat transfer rate, W	I	liquid
T x Z	temperature, °C, K mole fraction thermal resistance, K/W	max o s	maximum outlet surface
λ	latent heat of vaporization, J/kg	U	vapor
μ	viscosity, kg/ms	W	
ρ σ	density, kg/m ³ surface tension, N/m		

temperature of the heat source may be lower or higher than that of the normal range and the heat transfer rate of the thermosyphon heat pipe tends to decrease. Some experiments [2] showed that some binary mixtures could give better performance than that of a single working fluid.

In the case of a lower-temperature heat source (lower than 80°C), ethanol-water is proposed as a working fluid because ethanol has a lower boiling point than water. Consequently, it can be boiled easily and higher performance of the thermosyphon should be obtained. In the case of a higher-temperature heat source (more than 200°C), for water, the transfer of heat may be hindered by a critical limit, particularly the flooding or dryout limit. To extend these limits, triethylene glycol (TEG)-water is proposed as a working fluid. Because TEG has a high

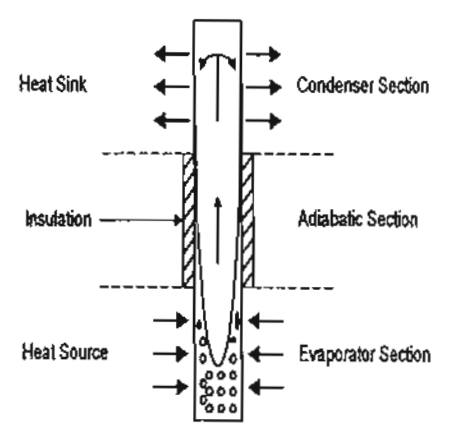


Figure 1. The thermosyphon heat pipe.

boiling point (278°C at normal pressure), TEG in the mixture may retard the limits [3].

The aim of this research work is to study the performance of a thermosyphon using binary working fluids, ethanol-water and TEG-water, and find a heat transfer model which can predict the heat transfer coefficients of the mixtures.

THE EXPERIMENT AND TEST PROCEDURE

Figure 2 shows a schematic diagram of the experimental apparatus. It consists of a thermosyphon heat pipe, a heat source, and a heat sink. In this experiment, three diameter sizes of thermosyphon, 25.40, 19.05, and 12.70 mm with 2-mm wall thickness, have been tested. All of the pipes are made of 304 stainless steel. The total length of each is 100 cm, of which 40 cm is for the evaporator, 40 cm is for the condenser, and 20 cm is for the adiabatic section. There is a pressure gauge at the top of each pipe for measuring the inside pressure. The evaporator section of the thermosyphon is dipped in a hot oil bath and the condenser is cooled by water from a constant-head tank.

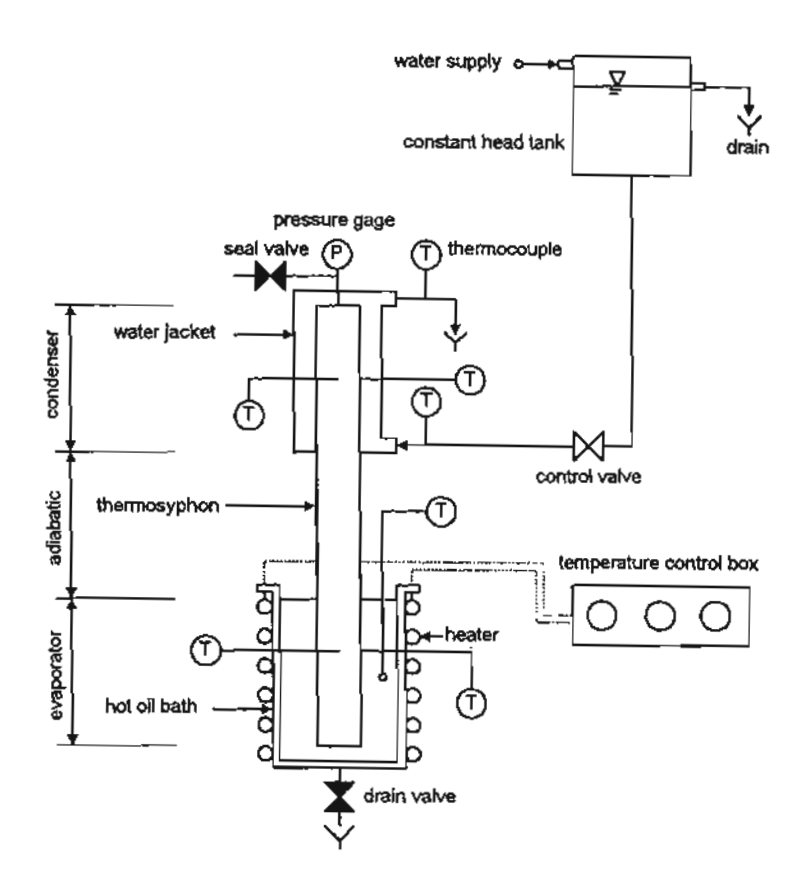


Figure 2. The experiment apparatus.

Seven K-type thermocouples with $\pm 0.5\%$ accuracy are attached to the outer surface of the thermosyphon at 5, 20, 35, 50, 65, 80, and 95 cm from the evaporator end. Moreover, for the biggest tested thermosyphon, seven thermocouples are inserted into the pipe to measure the inside temperatures, and they are located at the same distances as the outer surface measurement.

A hot paraffin oil bath, which is a cylinder of 8.89 cm in diameter and 50 cm in length, is used to generate heat to the thermosyphon. To achieve a uniform oil temperature, air bubbles are supplied to perturb the oil.

The heat sink is a well-insulated water jacket having water flowing in and out to absorb heat at the condenser section. The water jacket is a 5-cm cylindrical tube, 45 cm long. Two thermocouples are inserted into the inlet and outlet ports of the water jacket to measure the water temperature. The flow rate of the cooling water is controlled by a constant-head tank between 6 and 19 g/s.

Ethanol-water and TEG-water at 0, 25, 50, 75, and 100% by volume of higher-volatile component are used as working fluids. The filling ratio for all tests is 50% of the evaporator section's volume. The temperature of the hot oil is controlled within a range of 50 to 225°C. The experiments have been carried out under steady-state conditions.

RESULTS AND DISCUSSION

Temperature Distributions Inside the Thermosyphon

The temperature distributions inside the thermosyphon are shown in Figures 3a and 3b for ethanol-water and TEG-water, respectively.

In Figure 3a it is found that the temperature difference of the evaporator and the condenser sections for the low-temperature heat source (60° C) are dependent on the amount of ethanol in water. At this heat source temperature, a small amount of water could be vaporized, so the transfer of heat is hindered and a high temperature difference between the evaporator and the condenser sections is obtained. At the higher heat source temperature (150° C), both components in the binary mixtures can be boiled and heat transfer rates are high, so the temperature distributions of the fluids inside the thermosyphon are nearly uniform.

The temperature distributions of TEG-water are shown in Figure 3b. Since TEG has a very high boiling point (278°C) so even the heat source temperature is 150°C, a small amount of TEG could be vaporized, which results in low heat transfer rate and high temperature difference between the evaporator and the condenser sections. But when water is mixed with the TEG, better heat transfer is achieved.

Heat Transfer Rate

The heat transfer rate can be calculated by

$$Q = \dot{m}_w C_p (T_{wo} - T_{wi}) \tag{1}$$

where \dot{m}_{w} is the flow rate of the cooling water, and T_{wi} and T_{wo} are the average temperatures at the inlet and the outlet of the cooling water at the water jacket, respectively.

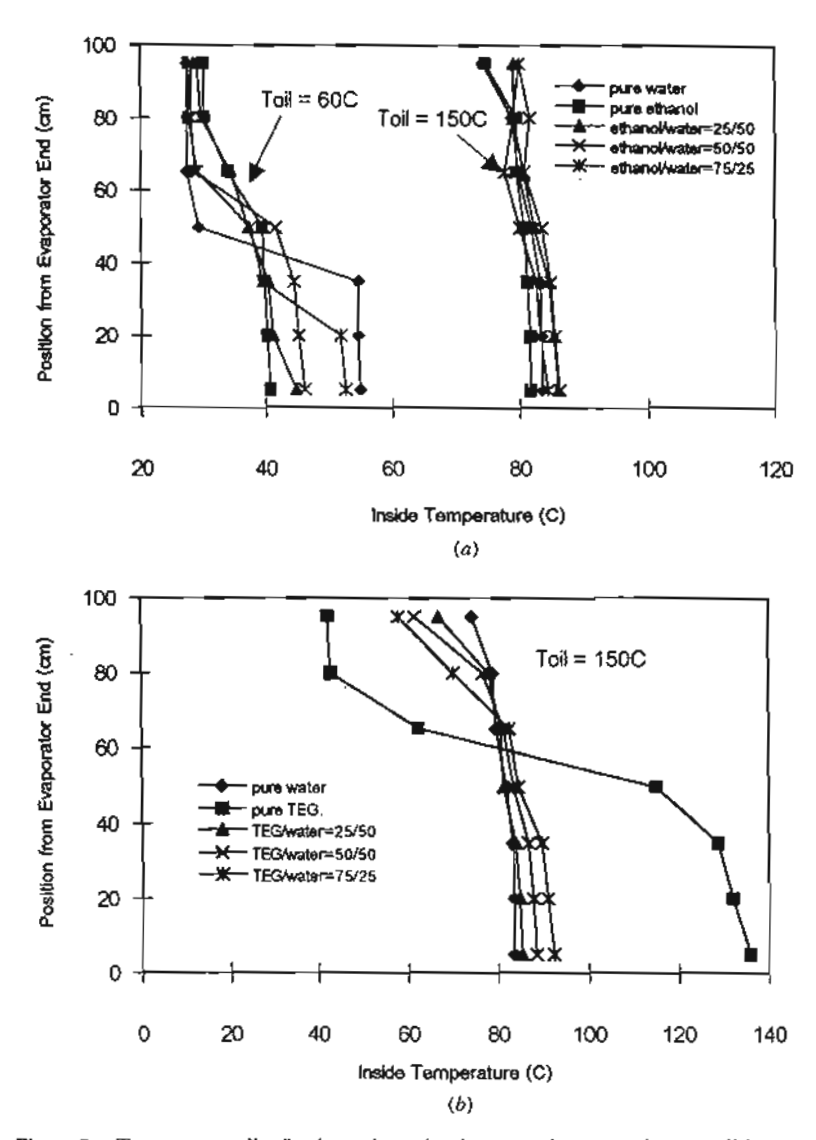


Figure 3. Temperature distributions along the thermosyphon at various conditions: (a) working fluid ethanol-water, tube diameter 25.4 mm; (b) working fluid TEG-water, tube diameter 25.4 mm.

The heat transfer rates at various hot oil temperatures are shown in Figures 4a-4f. In the case of ethanol-water mixtures (Figures 4a-4c), it is found that, at low hot-oil temperature, the heat transfer rates of ethanol-water mixtures are higher than for pure water and close to that of pure ethanol. But when the hot-oil temperature is increased, the heat transfer rate for pure water increases more rapidly than those of the mixtures and overcomes the mixtures at high temperature. This phenomenon occurs because at low temperature, ethanol can be boiled more easily than water and a better heat transfer rate is obtained. At high

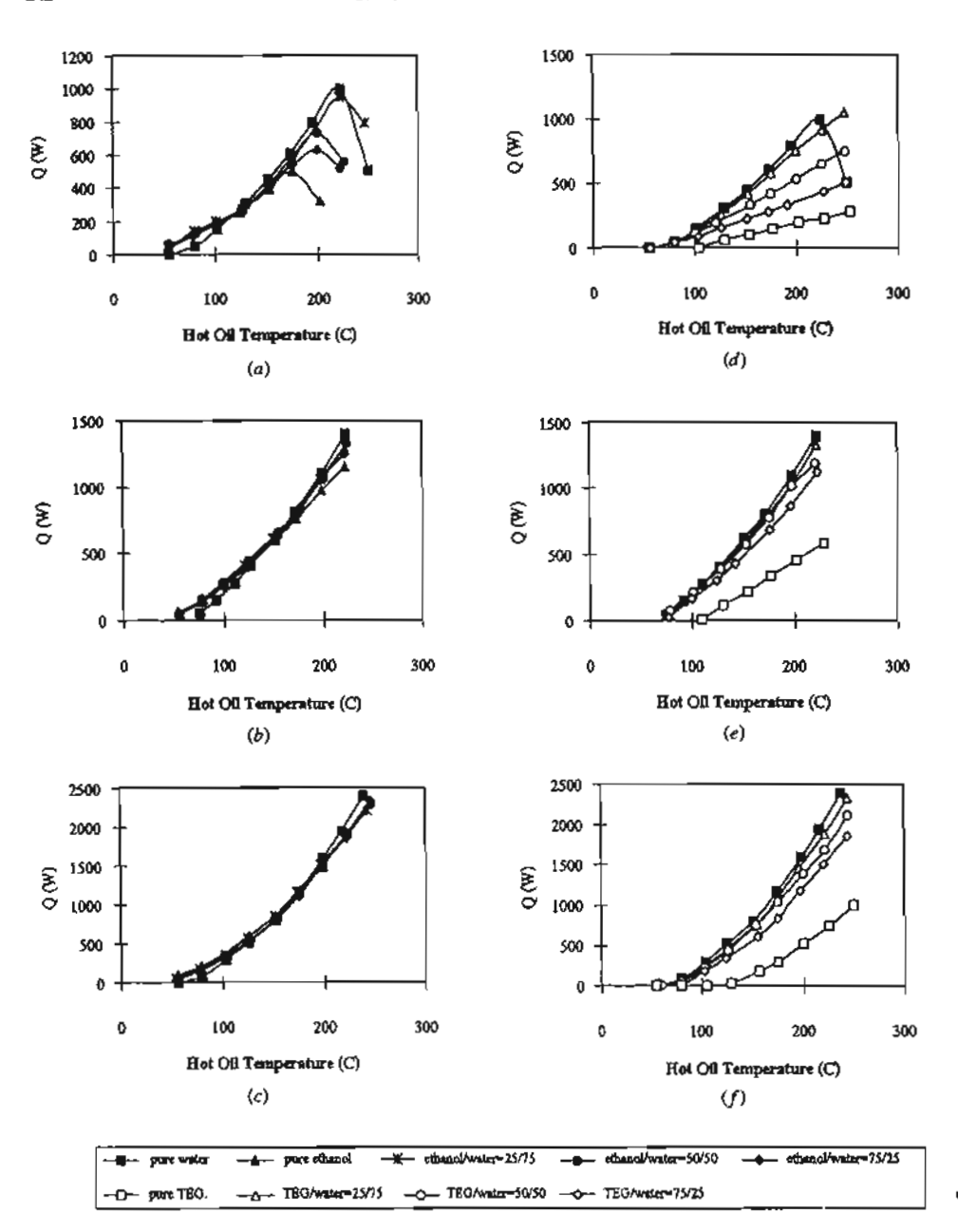


Figure 4. The relations between heat transfer rate of the thermosyphon heat pipe with binary mixtures and the hot oil temperature at various conditions: (a) working fluid ethanol-water, tube diameter 12.7 mm; (b) working fluid ethanol-water, tube diameter 19.05 mm; (c) working fluid ethanol-water, tube diameter 25.4 mm; (d) working fluid TEG-water, tube diameter 12.7 mm; (e) working fluid TEG-water, tube diameter 19.05 mm; (f) working fluid TEG-water, tube diameter 25.4 mm.

temperature, both ethanol and water can be boiled, and since the latent heat of vaporization of water is higher than that of ethanol, at this condition the thermosyphon with pure water can transfer more heat than those of ethanol or mixtures.

Flooding of working fluid in a small thermosyphon (12.70 mm diameter) has been found in the experiment. This phenomenon is due to the interaction between the countercurrent liquid and vapor flows occurring at the liquid-vapor interface in the thermosyphon. The viscous shear force at the interface may retard the return of liquid to the evaporator [4]. From Figure 4a, as the hot-oil temperature increases, the heat transfer rate of each working fluid also increases until the flooding limit has been obtained. After that the heat transfer rate drops drastically. This phenomenon always occurs when using a small thermosyphon with high temperature [4]. The critical heat flux at the flooding limit also depends on the composition of the mixtures.

The latent heat of vaporization of the working fluid plays an important role in controlling the flooding limit [4], and higher latent heat results in higher critical heat flux. In the case of ethanol—water mixtures, the latent heat of vaporization of water is very high compared to that of pure ethanol. Therefore, higher water content in the mixtures results in higher critical heat flux at the flooding limit.

TEG has a high boiling point, therefore the TEG-water mixtures could be vaporized well at high temperature. The heat transfer rate increases as the content of TEG in the mixture decreases. The results are shown in Figures 4d-4f. It was also found that no flooding occurs or the flooding limit is retarded in the working temperature range. From Figure 4d, it is found that with a small amount of TEG (25%) content in the mixture, the heat transfer rate is nearly the same as with pure water and no flooding occurs at high temperature even if the syphon diameter is small.

Thermal Resistance

The thermal resistance, Z, of the thermosyphon is calculated from

$$Z = \frac{T_{se,ave} - T_{sc,ave}}{O}$$
 (2)

where $T_{se,ave}$ and $T_{sc,ave}$ are the average outside surface temperatures at the evaporator and the condenser, respectively.

For ethanol-water mixtures (Figures 5a-5c), it is found that at low heat source temperature the resistance is very high, especially for water because a low amount of vapor could be generated. The thermal resistance of pure ethanol and the ethanol-water mixtures are lower than that of pure water because ethanol has a lower boiling point than water. For the high-temperature heat source, a large amount of both ethanol and water could be vaporized and transfer heat at the condenser, resulting in low thermal resistance. The resistances for all the working fluids are close to the values at high temperature. However, the resistance for pure water is lower than the others because of its high latent heat. Moreover, it is found

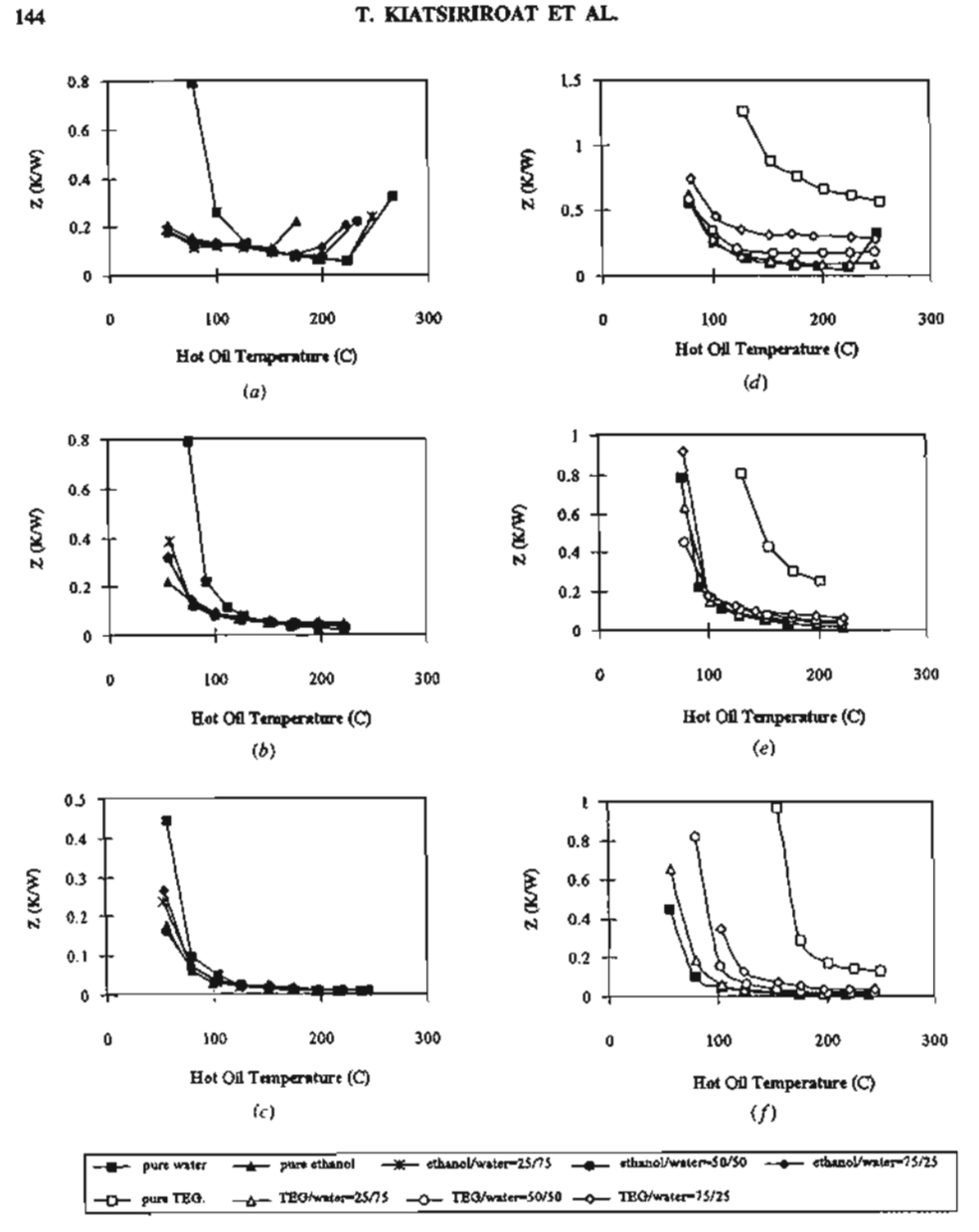


Figure 5. The relation between thermal resistance of the thermosyphon heat pipe with binary mixtures and the hot oil temperature at various conditions: (a) working fluid ethanol-water, tube diameter 12.7 mm; (b) working fluid ethanol-water, tube diameter 19.05 mm; (c) working fluid ethanol-water, tube diameter 25.4 mm; (d) working fluid TEG-water, tube diameter 12.7 mm; (e) working fluid TEG-water, tube diameter 19.05 mm; (f) working fluid TEG-water, tube diameter 25.4 mm.

that, as the diameter of the thermosyphon increases, the thermal resistance decreases, since a bigger thermosyphon results in a larger heat transfer area.

From Figure 5a, it is found that for the high-temperature heat source, the thermal resistance increases again because of flooding inside the thermosyphon.

In the case of TEG-water mixtures (Figures 5d-5f), it is found that the thermal resistance of pure water is the lowest, since water can be vaporized more easily than TEG. The effects of diameter and temperature on the thermal resistance are similar to those of ethanol-water mixtures. Again, for 25% volume content of TEG in the mixture, the performance is close to that of pure water but flooding does not occur even when the thermosyphon is operated at high temperature and the pipe diameter is small.

Heat Transfer Models

The heat transfer model of heat transfer coefficient of pure working fluids has been correlated. The pool boiling equation of Rohsenow [5] is modified to predict the boiling heat transfer coefficient inside the thermosyphon. The equation is

$$h_{\epsilon} = \frac{C_1}{\Delta T_{\epsilon} A} \left[\left(\frac{\Delta T_{\epsilon}}{B} \right)^3 \right]^{C_2} \tag{3}$$

where

$$A = \frac{1}{\mu_1 \lambda} \sqrt{\frac{g_c \sigma}{g(\rho_l - \rho_c)}}$$

and

$$B = \frac{\lambda \Pr_{I}}{C_{p_1}}$$

where h, is the boiling heat transfer coefficient of the thermosyphon, ΔT_e is the temperature difference between the fluid inside and the surface at the evaporator section, g_c is a conversion factor (in SI units, g_c is equal to 1 kg m/N s²), and C_1 and C_2 are empirical constants. Rohsenow's equation is developed for pure pool boiling, but in a thermosyphon, parts of the liquid return from the condenser sections also evaporate.

The factors C_1 and C_2 of each pure substance in Eq. (3) modified for the thermosyphon can be found from our experiments and are shown in Table 1.

Table 1. Factors C_1 and C_2 from the experiments

Working fluid	C_1	C2
Water	18.688	0.3572
Ethanol	17.625	0.3300
TEG	20.565	0.3662

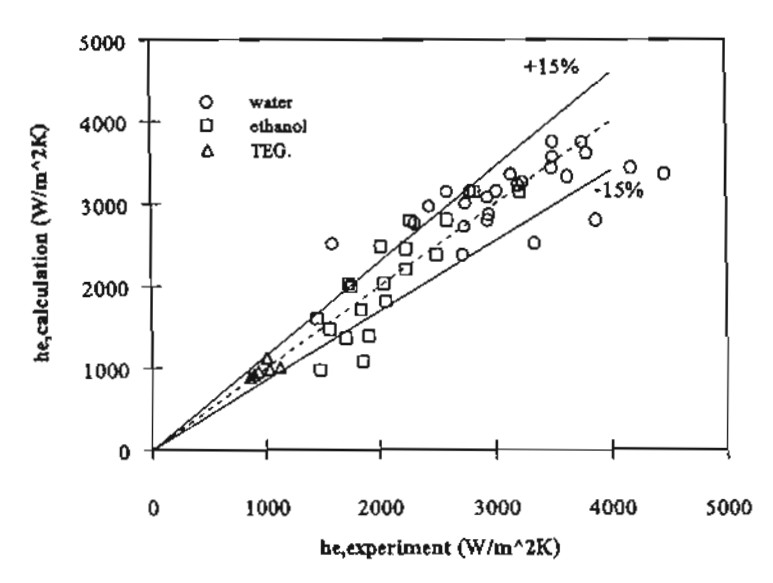


Figure 6. Comparisons of boiling heat transfer coefficients from the experiments and Eq. (3).

Figure 6 shows the results of the heat transfer coefficients of the pure working fluids, calculated from Eq. (3) and compared with those of the experimental data. Most of the calculated values are within $\pm 15\%$ of the experimental data.

At the condenser section, Nusselt's equation of condensation [5] is modified to predict the heat transfer coefficient of the condenser section. The equation is

$$h_c = C_3 \left(\frac{\rho_1^2 g \lambda k_1^3}{\mu_1 L_c \Delta T_c} \right)^{C_4} \tag{4}$$

where h_c is the condensation heat transfer coefficient, L_c is the length of condenser section, ΔT_c is the temperature difference between the fluid inside and the surface at the condenser section, and C_s and C_s are empirical constants.

the surface at the condenser section, and C_3 and C_4 are empirical constants. With our experimental results, the constants C_3 and C_4 for the pure working fluids are shown in Table 2. Comparison of the calculated condensation heat transfer coefficients with those of the experiments are shown in Figure 7. It is found that the boiling and condensation heat transfer coefficients of pure water and pure ethanol are close to those of Shiraishi et al.'s experiment [6].

Table 2. Factors C_3 and C_4 from the experiments

Working fluid	C ₃	C₄
Water	0.943	0.233
Ethanol	0.930	0.260
TEG	0.943	0.180

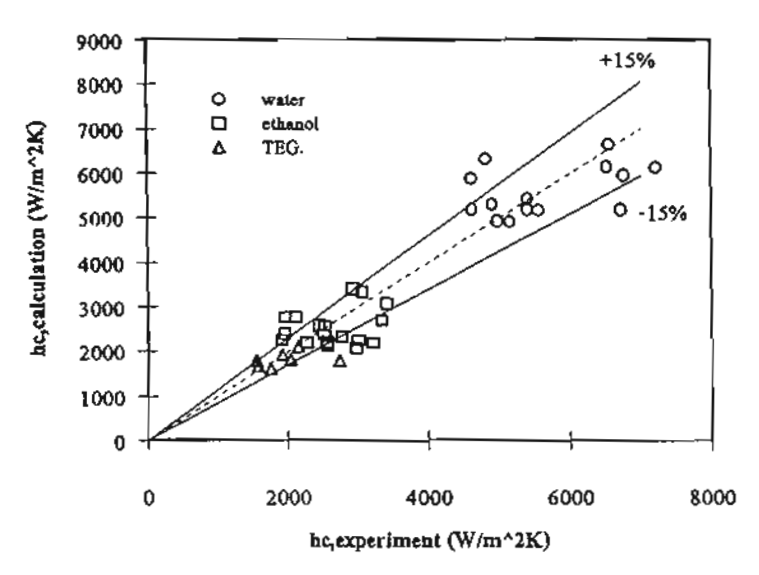


Figure 7. Comparisons of condensation heat transfer coefficients from the experiments and Eq. (4).

Heat Transfer Model of Binary Working Fluids

For a binary mixture, a method to evaluate the mixture heat transfer coefficient from each component [7] has been proposed as

$$h_m = x_1 h_1 + (1 - x_1) h_2 (5)$$

where h_m is the total heat transfer coefficient of the mixture, h_1 and h_2 are the heat transfer coefficients of high- and low-volatile components, respectively, and x is the mole fraction of the high-volatile component.

Normally the heat transfer coefficient of the binary mixture calculated from Eq. (5) could be predicted precisely for very low working pressure (ideal case) [7-10]. In the case of the experimental thermosyphon, the partial pressure of each working fluid inside the pipe is found to be very low, thus Eq. (5) can be used to predict the heat transfer coefficient very well. The results are shown in Figures 8 and 9 for boiling and in Figures 10 and 11 for condensation.

The composition of each component in liquid and vapor phases can be evaluated by Raoult's law and Dalton's law [11], and from the heat transfer coefficient of each pure component the heat transfer coefficient of the binary mixtures can be evaluated. The comparison of the heat transfer coefficients from the experiments and those from Eq. (5) are shown in Figures 8-11 for boiling and condensation at the evaporator and the condenser, respectively. It is found that the weighted-average method can be used to predict both boiling and condensation heat transfer coefficient within $\pm 15\%$ of the experimental values. Moreover, it is found that the heat transfer coefficients of those mixtures are between those of the pure working fluids.

T. KIATSIRIROAT ET AL.

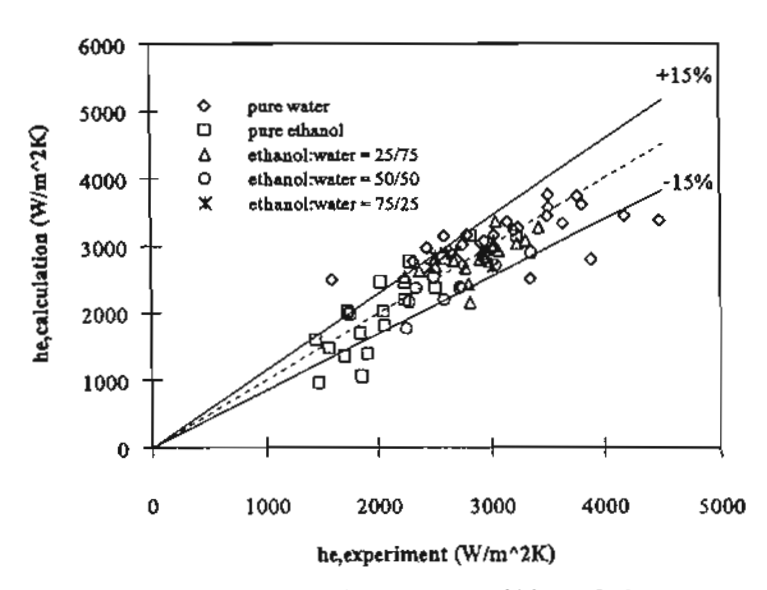


Figure 8. Comparisons of boiling heat transfer coefficients of ethanol-water mixtures from the experiments and Eq. (5).

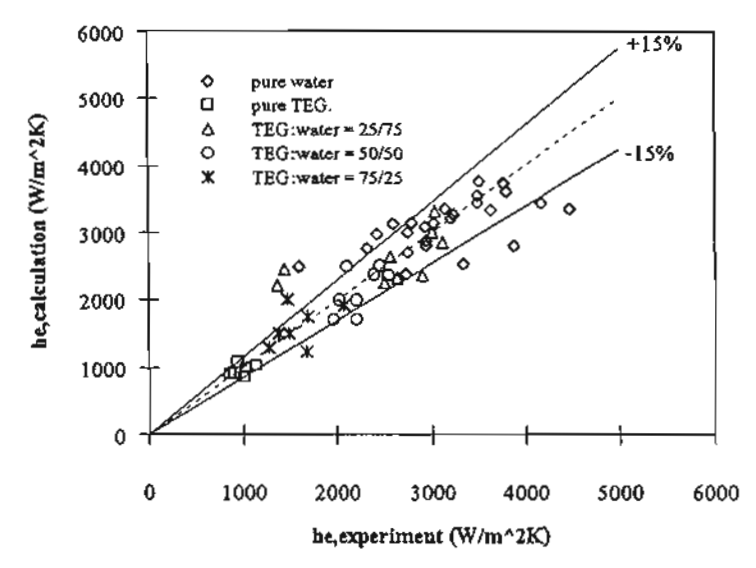


Figure 9. Comparisons of boiling heat transfer coefficients of TEG-water mixtures from the experiments and Eq. (5).

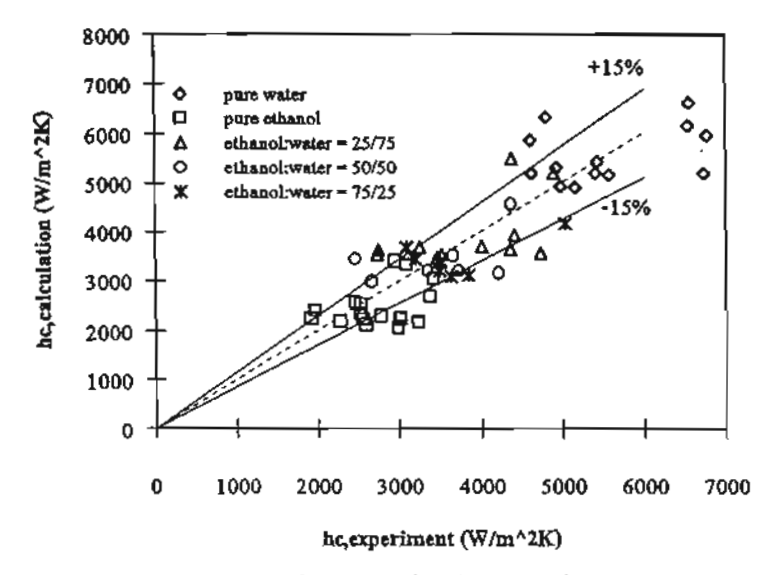


Figure 10. Comparisons of condensation heat transfer coefficients of ethanol-water mixtures from the experiments and Eq. (5).

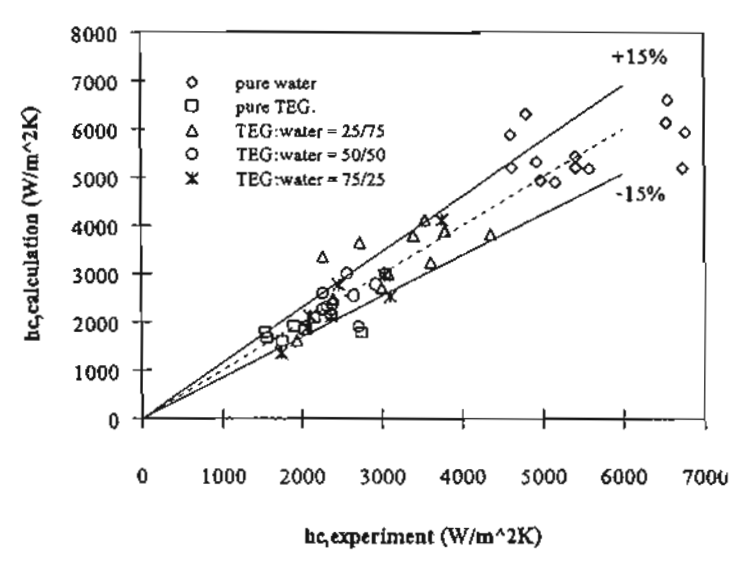


Figure 11. Comparisons of condensation heat transfer coefficients of TEG-water mixtures from the experiments and Eq. (5).

150

Flooding Limit of the Thermosyphon

Flooding always occurs in small thermosyphons with high temperature. Faghri's equation is normally used to calculate the critical heat flux due to the flooding limit [1] and is of the form

$$Q_{\text{max}} = K\lambda A_{\text{cs}} [g\sigma(\rho_l - \rho_v)]^{-0.25} (\rho_v^{-0.25} + \rho_l^{-0.25})^{-2}$$
 (6)

where

$$K = \left(\frac{\rho_l}{\rho_c}\right)^{0.14} \tanh^2 Bo^{0.25}$$

and

$$Bo = D_i \left[\frac{g(\rho_l - \rho_c)}{\sigma} \right]^{0.5}$$

where A_{cs} is the cross-sectional area of the thermosyphon, D_i is the inside diameter of the pipe, and Bo is the Bond number.

Faghri's equation has been applied for single working fluids. In this research work, for a binary mixture, ethanol-water, the properties of the mixture [12-17] have been used and it could be found that the prediction of the maximum heat transfer evaluated from the equation could be applied quite well (Figure 12).

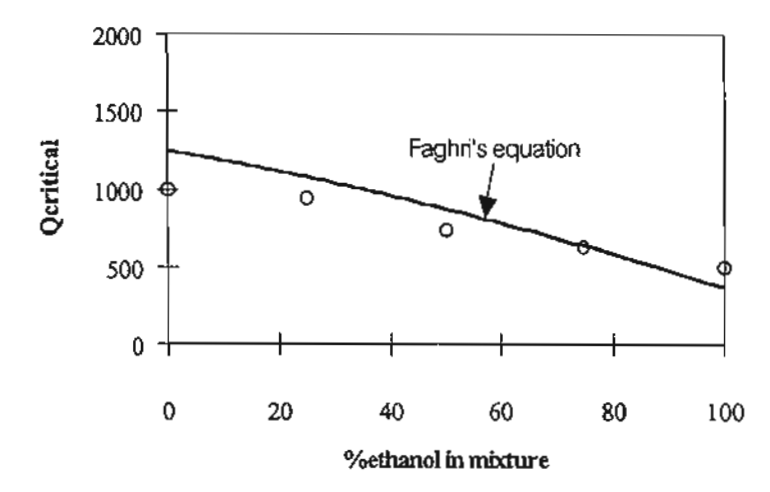


Figure 12. Prediction of the maximum heat transfer rate due to the flooding limit. The binary mixture is ethanol-water.

CONCLUSION

There is a high potential to improve performance of a thermosyphon heat pipe by using binary mixtures. Ethanol-water mixtures give a higher heat transfer rate than water at the low-temperature heat source (less than 80°C). In the case of TEG-water mixtures, the heat transfer rate of the thermosyphon decreases with the content of TEG in the mixture and it is found that a small amount of TEG in the mixture (25%) can enlarge the critical heat flux due to the flooding limit of the small size of the thermosyphon while the heat transfer rate is reduced slightly.

The boiling equation of Rohsenow and the condensation equation of Nusselt can be used to predict the heat transfer coefficients of boiling and condensation inside the thermosyphon. In the case of binary mixtures, the weighted average of the heat transfer coefficient of each component can be used to predict the total heat transfer coefficient. At the critical limit for flooding of the thermosyphon, it is found that Faghri's equation can be applied to calculate the maximum heat transfers of both pure water and ethanol-water mixtures.

REFERENCES

- 1. A. Faghri, Heat Pipe Science and Technology, Taylor & Francis, Philadelphia, PA, 1995.
- A. Nuntaphan, K. Pearce, and T. Kiatsiriroat, Second Law Analysis of Thermosyphon Air Preheater with Binary Mixtures, 6th Tri-University Joint Seminar and Symposium, Jiangsu University of Science and Technology, Jiangsu, People's Republic of China, 1999.
- A. Nuntaphan, J. Tiansuwan, and T. Kiatsiriroat, Thermal Behavior Analysis of Thermosyphon Heat Pipe Using Binary Working Fluids, 13th National Mechanical Engineering Conference, Chonburi, Thailand, 1999.
- G. P. Peterson, An Introduction to Heat Pipes Modeling, Testing and Applications, Wiley, New York, 1994.
- M. Amornkitbamrung, S. Wangnippanto, and T. Kiatsiriroat, Performance Studies on Evaporation and Condensation of a Thermosyphon Heat Pipe, 6th ASEAN Conference on Energy Technology, Bangkok, 1995.
- M. Shiraishi, K. Kikuchi, and T. Yamanishi, Investigation of Heat Transfer Characteristics of a Two Phase Closed Thermosyphon, in *Heat Recovery Systems*, vol. 1, pp. 287-297, Pergamon Press, 1981.
- E. U. Schlunder, Heat Transfer in Nucleate Boiling of Mixtures, Int. Chem. Eng. vol. 23, no. 4, pp. 589-599, 1983.
- H. C. Unal, Prediction of Nucleate Pool Boiling Heat Transfer Coefficients for Binary Mixtures, Int. J. Heat Mass Transfer, vol. 29, no. 4, pp. 637-640, 1986.
- J. R. Thome and S. Shakir, A New Correlation for Nucleate Pool Boiling of Aqueous Mixtures, AIChE Symp. Ser., vol. 83, no. 257, pp. 46-51, 1987.
- C. B. Chiou, D. C. Lu, and C. C. Wang, Investigation of Pool Boiling Heat Transfer of Binary Refrigerant Mixtures, J. Heat Transfer Eng., vol. 18, no. 3, pp. 61-72, 1997.
- N. Vorayos and T. Kiatsiriroat, Simplified Method for Estimating Thermodynamic Properties of Refrigerant Mixture, Proc. Tri-University International Joint Seminar and Symp., Mie University, Japan, 1997.
- C. L. Yaws, Handbook of Thermodynamic Diagrams, vol. 2, pp. 240, 378, Gulf Publishing, Houston, TX, 1996.
- R. H. Perry and C. H. Chilton, Chemical Engineer's Handbook, 5th ed., McGraw-Hill, New York, 1973.

- 14. R. C. Reid, J. M. Pransnitz, and B. E. Poling, *The Properties of Gases and Liquids*, 4th ed., McGraw-Hill, New York, 1986.
- A. L. Kohl and C. F. Riesenfeld, Gas Purification, 3d ed., pp. 595-629, Gulf Publishing, Houston, TX, 1979.
- 16. D. T. Jamieson, J. B. Irving, and J. S. Tudhope, Liquid Thermal Conductivity, a Data Survey to 1973, p. 140, National Engineering Laboratory, Scotlant, Germany, 1973.
- J. F. Kuong, Applied Nomography, vol. 1, pp.114-115, Gulf Publishing, Houston, TX, 1965.

Nuntaphan A., Tiansuwan J., Kiatsiriroat T. and Wang C.C., 2001, Performance Improvement of Thermosyphon Heat Exchangers by Using Two Kinds of Working Fluids, paper accepted for publication in **Heat Transfer Engineering**.



heat transfer engineering

AN INTERNATIONAL JOURNAL

Cir. Affebier J. Chajur, Balling de Claim Calabara Bain (Alexandra Alberta, Cir. 1400) 1400 -

November 16, 2000

Dr. Chi-Chuan Wang
Buergy & Resources Laboratories
Industrial Technology Research Institute
D400 ERL/ITRI; Bldg. 64, 195-6 Sec. 4
Chung Haing Rd., Chutung,
Heinchu, Taiwan 310, R. O. C.

Ref: Paper No. 0020, Nuntaphan, Tiansuwan, Kintsirirost, & Weng "Performance Improvement of Thermosyphon Heat Exchangers by Using Two Kinds of Working Fluids"

Dear Dr. Wang:

This will acknowledge receipt of the re-revised version of the above-inferenced paper submitted for publication in *Heat Transfer Engineering*. After reviewing the corrections to the re-revised version of the paper, I am forwarding the paper to the Production Editor of *Heat Transfer Engineering*. Your paper is scheduled for publication in Volume 22(4) to appear about June 2001 or Volume 22(5) to appear about August 2001. You will receive proofs of the paper as soon as they are available (about one month before the publication date).

Thank you very much for considering Heat Transfer Engineering as a suitable place to publish your work and congramlations. Please contact me at the above address if I can be of any assistance to you in connection with this manuscript.

Sincerely,

Afshin J. Ghajer, Ph.D., P.R.

Editor-in-Chief and

Regents Professor of Mechanical Engineering



Performance Improvement of Thermosyphon Heat Exchangers by Using Two Kinds of Working Fluids

A. NUNTAPHAN and J. TIANSUWAN

School of Energy and Materials, King Mongkut's University of Technology Thonburi Bangkok 10140 Thailand

T. KIATSIRIROAT

Department of Mechanical Engineering, Chiang Mai University Chiang Mai 50202 Thailand

C.C. WANG

Energy & Resources Laboratories, Industrial Technology Research Institute Chutung Hsinchu Taiwan 310 R.O.C.

ABSTRACT

In this study, the concept of introducing two-fluid thermosyphons is examined. Calculations were performed for both low and high temperature ranges with parallel and counter flow arrangements. For lower temperature application, $125 \, ^{\circ}\text{C} > T_{hi} > 75 \, ^{\circ}\text{C}$, use of ammonia in some rows and water in the rest of the thermosyphon can slightly improve the associated heat transfer performance for balanced counter flow arrangement. However, for balanced parallel flow arrangement at both low and high temperature applications, the concept of using two-fluid thermosyphons may not feasible. The use of two-fluid thermosyphons is especially advantageous for high temperature application. For instance, in the range of 375 $^{\circ}\text{C} > T_{hi} > 350 \, ^{\circ}\text{C}$, the two-fluid thermosyphons (dowtherm A-water) shows a $15\sim99\%$ increase of heat transfer performance relative to dowtherm A alone.

Keywords: Thermosyphon, two-fluid, heat transfer augmentation

INTRODUCTION

The thermosyphon is the heat exchanger that carries heat from the higher temperature heat source to the lower temperature heat sink via boiling and condensation of the working fluid inside the tube. Advantages of the thermosyphon heat exchangers include high thermal conductivity, low cost, and easy construction. The thermosyphon heat exchanger shows potential in energy recovery from industrial waste heat and has become an interesting topic for energy conservation.

The thermosyphon heat pipe shown in Figure 1a can be divided into three parts, namely the evaporator, the adiabatic, and the condenser section. When heat is added to the evaporator section, the working fluid inside the thermosyphon is vaporized. The vapor carries heat from the heat source, flows to the condenser section and rejects heat to the heat sink. The condensate of the working fluid then returns to the evaporator section by gravity.

In practical application, multi-row thermosyphon heat exchangers filled with one kind of working fluid are employed. For applications involved with a medium temperature heat source (40-350 °C), water is known as the best working fluid because of its high latent heat and low investment cost [1]. But it should be noticed that for temperature in the range of 40-100 °C, water may not be the best choice for its comparatively lower heat transfer coefficient than other work fluids (e.g. ammonia). In addition, for other applications having heat source higher than 350 °C, water thermosyphon may be inappropriate due to possible occurrence of critical heat flux. Hence, to enlarge the application scope, we propose to use two kinds of substances in the multi-row thermosyphon heat exchangers application. For low temperature application ($T_{hl} < 100$ °C), combination of ammonia and water heat pipes may be applicable. For application in the higher temperature range ($T_{hl} > 300$ °C), it is likely that the water thermosyphon may fail due to the occurrence of local dry out and

flooding. To avoid this condition, it is possible to apply thermosyphons using dowtherm A in several initial rows to reduce the hot-gas temperature and then use water thermosythons in the rest of tube row to effectively increase the heat transfer performance. It is the main objective of this study to present the feasibility of this two-fluid thermosyphons implementation.

HEAT TRANSFER ANALYSIS

Figure 1b shows the thermal resistances of the thermosyphon heat exchangers. In the present modeling, the pressure drops from the evaporator to the condenser end and the axial conduction along the pipe wall are assumed negligible. Detailed evaluations of the thermal resistance are described as follows.

The external air-side thermal resistance of the evaporator (Z_{eo}) and the condenser (Z_{co}) section can be calculated from

$$Z_{eo} = \frac{1}{h_{eo}A_{eo}} \tag{1}$$

$$Z_{co} = \frac{1}{h_{co}A_{co}} \tag{2}$$

where h_{eo} and h_{co} denote the external air-side heat transfer coefficient in the evaporator and condenser, respectively. For circular finned tube having staggered array, Hewitt et al. [2] proposed the following correlation:

$$\overline{Nu} = 0.242 \,\mathrm{Re}^{0.658} \left(\frac{f_s}{f_h}\right)^{0.297} \left(\frac{S_t}{S_t}\right)^{-0.091} \mathrm{Pr}^{0.333}$$
 (3)

where S_l and S_l are the transverse and longitudinal pith of the staggered array. Related information for calculating the fin surface area A_f , bare tube surface A_b , and fin efficiency η_l are given as:

$$A_{f} = \frac{nL\pi}{f_{s} + f_{t}} \left(0.5 \left(D_{f}^{2} - D_{r}^{2} \right) + D_{f} f_{t} + D_{r} f_{s} \right) \tag{4}$$

$$A_b = \frac{nL\pi}{f_s + f_s} \left(D_r f_s \right) \tag{5}$$

$$\eta_f = \frac{\tanh\left(\sqrt{2h_o/f_t k_f} \times \varphi\right)}{\sqrt{2h_o/f_t k_f} \times \varphi} \tag{6}$$

$$\varphi = \frac{D_r}{2} \left(\frac{D_f}{D_r} - 1 \right) \left(1 + 0.35 \ln \frac{D_f}{D_r} \right)$$
 (7)

Note that the fin efficiency η_f is computed from Schmidt's approximation [3].

The wall resistance in the evaporator and condenser can be calculated from Equations (8) and (9), respectively.

$$Z_{et} = \frac{\ln(r_o/r_i)}{2\pi k_i L_o} \tag{8}$$

$$Z_{cl} = \frac{\ln(r_o / r_i)}{2\pi k_c L_c} \tag{9}$$

The related in-tube resistances in the evaporator (Z_{ei}) and condenser (Z_{ci}) can be calculated from:

$$Z_{ei} = \frac{1}{h_{ei}A_{ei}} \tag{10}$$

$$Z_{ci} = \frac{1}{h_{ci}A_{ci}} \tag{11}$$

Notice that the internal resistance is around 3-5% of the outside resistance. For applications of the thermosyphon, there are many correlations for evaluation of the intube heat transfer coefficients for boiling and condensation. Depending on the flow condition, heat transfer mechanism in the evaporator may involve pool boiling or falling film evaporation. Therefore it is necessary to select the suitable correlation in association with heat transfer mechanism. Relevant correlations are described as follows: For lower temperature application ($T_s < 80$ °C), the Rohsenow [4] correlation for pool boiling is used:

$$\left[\frac{Cp_i\Delta T_e}{\lambda}\right] = C_{sf} \left[\frac{q}{\mu_i\lambda} \left(\frac{\sigma}{g(\rho_i - \rho_\nu)}\right)^{1/2}\right]^{C_1} \left[\frac{Cp_i\mu_i}{k_i}\right]^{C_2+1}$$
(12)

where $C_{sf} = 0.013$, $C_1 = 0.33$, and $C_2 = 0$ for water and 0.7 for another fluids.

In addition, in the case of falling film evaporation in the evaporator section for lower temperature, Nusselt's equation [5] can be also used for calculation [6], i.e.,

$$h_{el,f} = 0.943 \left[\frac{g\rho_l(\rho_l - \rho_v) \lambda k_l^3}{\mu_l(T_w - T_s) L_{e,f}} \right]^{1/4}$$
 (13)

where h_{eif} is the evaporation heat transfer coefficient of the falling film.

The heat transfer coefficient in the condenser can be calculated from Nusselt's theoretical results [5]:

$$h_{ci} = 0.943 \left[\frac{g \rho_t (\rho_t - \rho_v) \lambda k_t^3}{\mu_t (T_w - T_s) L_c} \right]^{1/4}$$
 (14)

For application of water at higher temperature ($T_s \ge 80$ °C), the correlation for boiling and condensation developed by Kiatsiriroat et al. [7] is adopted, i.e.,

Boiling heat transfer coefficient of water:

$$h_e = \frac{18.688}{\Delta T_e X} \left[\left(\frac{\Delta T_e}{Y} \right)^3 \right]^{0.3572},\tag{15}$$

where
$$X = \frac{1}{\mu_i \lambda} \sqrt{\frac{g_c \sigma}{g(\rho_i - \rho_v)}}$$
 and $Y = \frac{\lambda \Pr_i}{Cp_i}$.

Condensation heat transfer coefficient for water;

$$h_{ci} = 0.943 \left[\frac{g \rho_t^2 \lambda k_i^3}{\mu_t (T_w - T_s) L_c} \right]^{0.233}$$
 (16)

For high temperature application, dowtherm A is regarded as the working medium in this study. ESDU [8,9] proposed several correlations for both evaporator and condenser that is also applicable for downterm A, and is given as below:

Thermal resistance due to pool boiling in the evaporator section:

$$Z_{e_{i,p}} = \frac{1}{\phi_1 g^{0.25} Q^{0.4} (\pi D_i L_e)^{0.6}}$$
 (17)

$$\phi_1 = 0.32 \frac{\rho_i^{0.65} k_i^{0.3} C p_i^{0.7}}{\rho_v^{0.25} \lambda^{0.4} \mu_i^{0.3}} \left[\frac{P_v}{P_a} \right]^{0.23}$$
(18)

Thermal resistance due to falling film evaporation in the evaporator section:

$$Z_{ei,f} = \frac{0.235Q^{1/3}}{D_{i}^{4/3}g^{1/3}L_{e}\phi_{2}^{4/3}}$$
 (19)

$$\phi_2 = \left(\frac{\lambda k_i^3 \rho_i^2}{\mu_i}\right)^{1/4} \tag{20}$$

The total thermal resistance due to boiling in the evaporation can be calculated as:

$$Z_{e_{i}} = Z_{e_{i},f}(1-F) + Z_{e_{i},p}F$$
(21)

where F is filling ratio of the working fluid.

Thermal resistance in the condenser:

$$Z_{ci} = \frac{0.235Q^{1/3}}{D_i^{4/3}g^{1/3}L_c\varphi_2^{4/3}}$$
 (22)

The overall heat transfer resistance of the thermosyphon heat exchanger is then the summation from separate resistance described above,

$$\frac{1}{(UA)_{total}} = \frac{1}{h_{eo}A_{eo,total}} + \frac{\ln(r_o/r_i)}{2\pi k_i L_{e,total}} + \frac{1}{h_{ei}A_{ei,total}} + \frac{1}{h_{co}A_{co,total}} + \frac{\ln(r_o/r_i)}{2\pi k_i L_{c,total}} + \frac{1}{h_{ci}A_{ci,total}} (23)$$

Note that the properties to evaluate the inside heat transfer coefficients are based on the saturated temperature inside the thermosyphon [8], i.e.

$$T_{mside} = T_{hl} - \frac{Z_{ci} + Z_{ci} + Z_{co}}{Z_{total}} (T_{hi} - T_{ci})$$
 (24)

Figures 2(a) and 2(b) show the schematic of the arrangement of the thermosyphon heat exchanger considered in the calculations. Both counter and parallel flow arrangement is investigated. The sample heat exchanger consists of seven rows of heat pipe. The overall heat transfer rate of the sample heat exchangers can be calculated

$$Q_{total} = \sum_{i=1}^{7} Q = Q_1 + Q_2 + Q_3 + Q_4 + Q_5 + Q_6 + Q_7$$

$$= (UA)_{total} (LMTD)$$

$$= \dot{m}_h C p_h (T_{h_l} - T_{h_0})$$

$$= \dot{m}_c C p_c (T_{c0} - T_{ci})$$
(25)

where LMTD is log mean temperature difference.

SIMULATION PROGRAM

For better understanding of applicable temperature range of related applications, different simulation algorithms were adopted in the implementation of the thermosyphon heat exchanger. In the first part, performance of the thermosyphon heat exchanger at low temperature range is investigated (T_{hi} < 100 °C). In this part, the working fluids in the thermosyphons are ammonia and water. As mentioned in the introduction section, the thermosyphon heat exchanger that uses water in this range may possess a poor heat transfer characteristics. Therefore, it would be beneficial to use the thermosyphons that containing ammonia in some rows of the heat exchanger. This is because of better heat transfer performance of ammonia than water at this temperature range. The simulation program is capable of selecting the suitable working fluid for each row between water and ammonia, and of calculating the overall performance of the heat exchanger. Detailed flow chart for low temperature application can be seen from Figure 3.

As seen in Figure 3, both counter and parallel flow arrangements are implemented. For the counter flow arrangement at the starting stage of iteration, temperatures of the inlet hot and cold streams are prescribed and the inlet and outlet

temperatures of the fluids at each row are assumed by considering all rows to be water. Iteration then starts by setting ammonia to the first row. Comparison is made with original water thermosyphon. Ammonia is selected if the related heat transfer performance outperforms the original water thermosyphon. The selection process continues from the second row to the last row. In case of the parallel flow, similar process has been carried out from the first row to the last row. As a result, appropriate fluid in every row of the thermosyphon heat exchanger is obtained.

In the second part of higher temperature application ($T_{hi} > 300$ °C), water and dowtherm A were used as working fluids. The computer programs were constructed to calculate the performance of the heat exchanger and also to find the suitable working fluid from row to row of the thermosyphon heat exchanger subjected to the constraint of critical heat flux of water thermosyphon. The basic rule of thumb for water is the temperature limit of interior saturation temperature should be less than 300 °C (the highest recommend temperature for water [1]). Beyond this temperature, some critical conditions such as flooding or dry out may occur [1,8,10,11]. These critical conditions not only considerably deteriorate the performance of the heat exchanger but also may damage the thermosyphon as well. In this connection, for higher temperature application, dowtherm A may be chosen as an alternative. However, its heat transfer performance is relatively low when comparing with water [8,9]. For optimization the system performance, it is necessary to make a combination of two-fluid thermosyphons. Figure 4 shows the related flow chart for the high temperature application. Relevant conditions for the heat exchanger are tabulated in Table 1.

The procedure in Figure 4 is similar to that in Figure 3 but the selection of the working fluid in each row has been carried out subjected to critical temperature constraint. When the inside temperature is lower than 300°C, water should be used as a working fluid and when the inside temperature is over 300°C, dowtherm A is chosen instead.

RESULTS AND DISCUSSION

Part 1 - Results of Low Temperature

Table 2 shows calculated results from the simulation program in the case of the balanced counter flow arrangement $(\dot{m}_h = \dot{m}_c)$ at various working conditions. Calculations were performed at a fixed T_{ci} of 20 °C. Range of T_{hi} is from 75 °C to 125 °C with a mass flow rate of 0.1 ~ 0.4 kg/s. As can be seen from Table 2, one can see that all-water thermosyphons would be the best choice for $T_{hi} = 125$ °C while all-ammonia thermosyphons show the highest performance for $T_{hi} < 75$ °C. For 75 °C $< T_{hi} < 125$ °C, it can be shown that use of both kinds of thermosyphons would be advantageous. However, one can see that only a slight increase of performance is observed. This is because that the heat transfer coefficient for water and ammonia are comparable in this range. It should be pointed out that water thermosyphons should be placed at the hot air inlet consecutively in order to get the best performance. For detailed evaluations the appropriate number of water thermosyphons of various T_{hi} , one can see Figure 5. As seen in the figure, the appropriate number of the number of tube row of water thermosyphons increases with T_{hi} and m. For an application condition of m < 0.1kg/s

and T_{hi} < 90°C, performance improvement by use of water thermosyphons is not attainable. Meanwhile, for an application of $\dot{m} \ge 0.4$ kg/s and $T_{hi} > 90$ °C, it would be better to use all-water thermosyphons to achieve optimal performance.

In the case of thermosyphon heat exchanger with balanced parallel flow arrangement $(\dot{m}_h = \dot{m}_c)$, the calculation indicates that use of ammonia and water is not beneficial throughout the range when comparing to water or ammonia thermosyphon alone. Explanation of this phenomenon can be seen from Figure 6. As depicted from Figure 6, in the case of balanced parallel flow, the temperature profiles of hot and cold stream are quite symmetric and lead to nearly uniform inside temperature of the thermosyphons from the first to the last row. Therefore, the inside resistance for this situation is almost fixed from row to row. Therefore, use of two kinds of thermosyphon is not so beneficial when comparing to those of counter flow arrangement.

Unlike those of balanced parallel flow arrangement, for the case of unbalanced parallel flow thermosyphon heat exchanger $(\dot{m}_h \neq \dot{m}_c)$, the temperature profiles of hot and cold stream are not symmetric. The concept of employing the two-fluid thermosyphons is still feasible. Table 3 and Figure 7 shows the calculated results of $\dot{m}_h = 0.2$ kg/s with $\dot{m}_c = 0.1$, 0.2, and 0.4 kg/s, respectively. Analogous to the results of counter-flow arrangements, the calculated results show a detectable influence of the inlet temperature and mass flow. However, it should be pointed out that the applicable temperature range of using two-fluid thermosyphons for unbalanced parallel flow is comparatively small than those encountered in counter flow arrangement. For instance, the applicable range for the un-balanced parallel flow arrangement shown in Figure 7 is

80 °C < T_{hl} < 110 °C relative to 75 °C < T_{hl} < 125 °C for the balanced counter flow arrangement. The results are not surprising due to change of inner temperature of the thermosyphon is more pronounced for counter flow arrangement. The concept of using two-fluid thermosyphon is especially advantageous for large variation of temperatures.

Part 2 - Results of High Temperature

Results of the high temperature application using dowtherm A and water for balanced counter current flow thermosyphon heat exchanger are tabulated in Table 4. The inlet temperature of cold gas is 200 °C and 250 °C, respectively. The calculated results indicate that use of two-fluid thermosyphon is much more beneficial than those in low temperature application. Typical increase of heat transfer rate for waterdowtherm A thermosyphons relative to dowtherm A thermosyphon alone is from 15 ~ 99%. However, use of water thermosyphon is subjected to the constraint that the interior saturation temperature of water should be less than 300 °C. Therefore, in the case of water- dowtherm A, the heat transfer rate tends to decrease for increase of T_{hi} . In addition, one can experience a further drop of heat transfer performance when T_{ct} is raised to 250°C at $\dot{m} = 0.3$ or 0.4 kg/s. These phenomena come from the effect of the number of tube row that uses water as a working fluid. At higher inlet temperature of hot air, the number of tube row containing water thermosyphons are eventually decreased while the number of tube row for downterm A thermosyphons is increased. Figure 8 shows the variation of saturated temperature inside each row of thermosyphon vs. tube row at various conditions. As seen, when the interior saturation temperature

drops below the constraint temperature of 300°C, it would be beneficial to employ the water thermosyphons in these tubes. Because of the considerable improvement of the heat transfer performance of water thermosyphon, the associated hear transfer rate can be increased dramatically. However, it should be noted that for $T_{hi} > 375$ °C, no water thermosyphons can be inserted. In summary, for the counter flow arrangement, the applicable range of the two-fluid thermosyphons concept is limited to $T_{hi} = 325 \sim 375$ °C.

Similar results for the parallel flow thermosyphon heat exchanger using water-dowtherm A as working fluids are tabulated in Table 5. Figures 9 and 10 shows the change of interior saturation temperature vs. the number of tube row for balanced and un-balanced parallel flow arrangement. For balanced parallel flow arrangement shown in Figure. 9, the concept of two-fluid thermosyphon is not feasible. Explanation is identical to those of low temperature application due to the constant temperature situation. Thus for balanced parallel flow arrangement, if the inside saturation temperature is higher than 300 °C, all-dowtherm A thermosyphons may be used. On the other hand, if the inside temperature is lower then 300 °C, all-water thermosyphon would be more suitable. However, in the case of un-balanced parallel flow arrangement, as seen in Figure 10, the temperature profile of hot and cold stream are not symmetric, thus the inside temperature of each row can vary from row to row. Thus the concept of two-fluid thermosyphons is applicable. From the temperature distribution of Figure 10, one can see that it would be very beneficial to insert some rows of water thermosyphons into the heat exchanger (especially in row 5, 6, and 7).

CONCLUSION

In this study, the concept of using two-fluid thermosyphons is implemented for examining the performance improvement of thermosyphon heat exchangers.

Calculations were made for both low temperature and high temperature application.

Major results are summarized as follows:

- (1) For lower temperature application and 75 °C < T_{hi} < 125 °C, use of ammonia in some rows can slightly improve the associated heat transfer performance for balanced counter flow arrangement.</p>
- (2) For balanced parallel flow arrangement at low and high temperature application, the concept of using two-fluid thermosyphons may not be feasible.
- (3) For un-balanced counter flow arrangement, the concept of using two-fluid thermosyphons is also applicable. However, the associated range of T_{hi} is comparatively smaller than those of counter flow arrangement.
- (4) For un-balanced parallel flow arrangement, the concept of using two-fluid thermosyphons is applicable.
- (5) For higher temperature application, benefits of using two-fluid thermosyphons are much more pronounced than those in lower temperature application. However, the related applicable range of T_{ht} may be smaller than those in high temperature application due to the constraint of critical heat flux of water.

ACKNOWLEDGEMENT

The authors gratefully acknowledge the support provided by the Thailand Research Fund for carrying out this study. Part of the finacial support provided by the Energy R&D foundation funding from the Energy Commission of the Ministry of Economic Affairs, Taiwan is also appreciated.

NOMENCLATURE

```
area, m<sup>2</sup> (ft<sup>2</sup>)
A
```

 C_{1-2} empirical constants

specific heat, J/kg°C (Btu/lbm°F) $C_{\mathcal{D}}$

 C_{sf} liquid-surface constant

D diameter of tube, m (ft)

fh fin hight, m (ft)

 f_s fin gap, m (ft)

fin thickness, m (ft) f_t

F filling ratio of working fluid

gravitational acceleration, 9.81 m/s² (ft/s²) g

conversion factor, 1 kg m/N s² (32.17 lbm·ft/lbf sec²) g_c

heat transfer coefficient, W/m² °C (Btu/h ft² °F) h

thermal conductivity, W/m °C (Btu/h ft °F) k

L length, m (ft)

LMTD log mean temperature difference, °C (°F)

mass flow rate, kg/s (lb_m/s) m

n number of tube

NuNusselt number

P pressure, Pa (lb/in²)

Prandtl number Pr

heat flux, W/m² (Btu/h ft²)

Q heat transfer rate, W (Btu/h)

radius of tube, m (ft)

Re Reynolds number

 S_d diagonal pith of staggered

Array, m (ft)

 S_I longitudinal pith of staggered array, m (ft)

 S_t transverse pith of staggered

Array, m (ft)

 T_{ci} inlet temperature of cold gas, °C (°F)

 T_{co} outlet temperature of cold gas, °C (°F)

inlet temperature of hot gas, °C (°F) T_{hi}

- T_{ho} outlet temperature of hot gas, °C (°F)
- ΔT_c temperature difference between inside surface and liquid at condenser section, °C (°F)
- ΔT_e temperature difference between inside surface and liquid at evaporator section, °C (°F)
- UA overall heat transfer coefficient-area, W/°C (Btu/h °F)
- Z thermal resistance, °C/W (°F h/Btu)

Greek symbols

- ϕ function
- η efficiency
- φ function
- λ latent heat of vaporization, J/kg (Btu/lb_m)
- μ dynamic viscosity, Pa s (lb_m/ft s)
- ρ density, kg/m³ (lb_m/ft³)
- σ surface tension, N/m (lb_f/ft)

Subscripts

- a air, atmospheric
- b bare tube
- c condenser, cold
- e evaporator
- f fin, film
- h hot
- i inlet, inside
- l liquid
- o outlet, outside
- r root
- s saturated
- t tube
- w wall
- v vapor

REFERENCES

- [1] Faghri A., Heat Pipe Science and Technology, Taylor & Francis, Philadelphia, USA, 1995.
- [2] Hewitt G.F., Shires G.L. and Bott T.R., *Process Heat Transfer*, CRC Press, Boca Raton, Florida USA, 1994.
- [3] Schmidt, Th. E., Heat Transfer Calculations for Extended Surfaces, Refrigerating Engineering, pp. 351-357, April, 1949.

- [4] Rohsenow W.M., A Method of Correlating Heat Transfer Data for Surface Boiling of Liguids, *Trans. ASME*, 74, pp.969-975, 1952.
- [5] Nusselt W., Die Oberflachenkondensation des Wasserdampfes, Zeitschr. Ver. Deutsch. Ing., 60, pp.541-569, 1916.
- [6] Tanthapanichakoon W., Design of Heat Pipe Heat Exchanger, in Thai, Chulalongkorn University, Bangkok, Thailand, 1986.
- [7] Kiatsiriroat T., Nuntaphan A. and Tiansuwan J., Thermal Performance Enhancement of thermosyphon heat pipe with binary working fluids, *Experimental Heat Transfer*, Vol. 13, No.2, pp.137-152, 2000.
- [8] Engineering Data Science Unit No.81038, Heat Pipes-Performance of Two-phase Closed Thermosyphons, ESDU Int. Plc., London, UK,1983.
- [9] Engineering Data Science Unit No.80017, Thermophysical Properties of Heat Pipe Working Fluids: Operating Range Between -60°C and 300°C, ESDU Int. Plc., London, UK, 1980.
- [10] Lock G.S.H., The Tubular Thermosyphon Variations on a Theme, Oxford Engineering Science Series 33, Oxford University Press, New York, USA, 1992.
- [11] Peterson G.P., An Introduction to Heat Pipes Modeling, Testing and Applications, John Wiley & Sons, New York, USA, 1994.

Captions of Tables and Figures

- Table 1 Testing conditions and related geometrical parameters of the thermosyphon heat exchanger.
- Table 2 Results of simulation in the case of balanced counter flow arrangement for low temperature application; working fluid: ammonia (NH₃) water (H₂O).
- **Table 3** Results of simulation in the case of unbalanced parallel flow arrangement for low temperature application; working fluid: ammonia (NH₃) water (H₂O), $\dot{m}_h = 0.2 \, \text{kg/s}$.
- Table 4 Results of simulation in the case of balanced counter flow arrangement for high temperature application; working fluid: water-dowtherm A.
- **Table 5** Results of simulation in the case of unbalanced parallel flow arrangement for high temperature application; working fluid: water-dowtherm A.
- Figure 1 Schematic of the thermosyphon heat pipe (a). Operating principle; (b). Thermal resistance circuit.
- Figure 2 Flow arrangement of the thermosyphon heat exchanger.

- Figure 3 The flow chart of the two-fluid thermosyphons in low temperature application.
- Figure 4 The flow chart of the two-fluid thermosyphons in high temperature application.
- Figure 5 Relation of the appropriate number of water thermosyphons vs. inlet conditions for balanced counter flow arrangement at $T_{ci} = 20$ °C.
- Figure 6 Temperature profiles of the balanced parallel flow thermosyphon heat exchanger using water and ammonia as working fluids.
- Figure 7 Relation of the appropriate number of water thermosyphons vs. inlet conditions for unbalanced parallel flow arrangement at $T_{ci} = 20$ °C and $\dot{m}_b = 0.2$ kg/s.
- Figure 8 Interior saturation temperatures of each row of counter flow heat exchanger at various conditions; mass flow rate of air = 0.3 kg/s.
- Figure 9 Temperature profile of the balanced parallel flow heat exchanger using water and dowtherm A as working fluids.
- Figure 10 Temperature profile of the unbalanced parallel flow heat exchanger using water and dowtherm A as working fluids.

Table 1 Testing conditions and related geometrical parameters of the thermosyphon heat exchanger.

	Items	Conditions
1.	Flow arrangement	Parallel and counter flow
2.	Temperature of hot air	50-125 °C for low temperature
		325-400 °C for high temperature
3.	Temperature of cold air	20 °C for low temperature
)		200-250 °C for high temperature
1		0.05-0.4 kg/s
5.	Thermosyphon arrangement	Staggered array
_		$S_t = 0.053 \text{ m}, S_d = 0.053 \text{ m}, S_i = 0.046 \text{ m}$
6.	Number of tube row	7
7.	Number of column	7
1	Diameter of thermosyphon (bare tube)	0.027 m
	Type of fin	Circular fin
10	. Size of fin	Fin height = 0.1 m and fin pitch = 10
		fins/inch
1	. Filling ratio of working fluid	50%
12	. Material of pipe and fin	Stainless steel 304

Table 2 Results of simulation in the case of balanced counter flow arrangement for low temperature application; working fluid: ammonia (NH_3) – water (H_2O) .

T_{ci}	T _{hi}	m	0	0	0	No. of t	ube row	% inc	crease
(°C)	(°C)	(kg/s)	Q _{H,O} (W)	Q_{NH} , (W)	$Q_{H_2O-NH_3}$ (W)	H ₂ O	NH ₃	Relative to H ₂ O	Relative to NH ₃
20	125	0.1	5155.09	4872.82	5155.09	7	0	0.00	5.79
20	125	0.2	7456.00	6779.58	7456.00	7	0	0.00	9.98
20	125	0.3	8882.18	7850.84	8882.18	7	0	0.00	13.14
20	125	0.4	9865.96	8553.55	9865.96	7	0	0.00	15.34
20	100	0.1	3761.03	3778.79	3826.01	3	4	1.73	1.25
20	100	0.2	5467.49	5319.22	5488.06	5	2	0.38	3.17
20	100	0.3	6506.54	6201.61	6506.54	7	0	0.00	4.92
20	100	0.4	7223.34	6787.23	7223.34	7	0	0.00	6.43
20	95	0.1	3491.61	3552.24	3575.62	2	5	2.41	0.66
20	95	0.2	5071.65	5012.1	5113.46	4	3	0.82	2.02
20	95	0.3	6033.43	5851.68	6043.20	6	1	0.16	3.27
20	95	0.4	6696.93	6410.27	6696.93	7	0	0.00	4.47
20	90	0.1	3222.87	3323.42	3330.90	2	5	3.35	0.23
20	90	0.2	4676.74	4700.36	4749.82	3	4	1.56	1.05
20	90	0.3	5561.43	5495.50	5596.36	4	3	0.63	1.84
20	90	0.4	6171.70	6025.85	6182.09	5	2	0.17	2.59
20	85	0.1	2954.92	3092.44	3092.44	0	7	4.65	0.00
20	85	0.2	4283.02	4384.14	4398.77	2	5	2.70	0.33
20	85	0.3	5090.79	5133.17	5170.42	3	4	1.56	0.73
20	85	0.4	5647.95	5634.03	5696.8	4	3	0.86	1.11
20	80	0.1	2687.93	2859.42	2859.42	0	7	6.38	0.00
20	80	0.2	3890.70	4063.53	4063.53	0	7	4.44	0.00
20	80	0.3	4621.82	4764.77	4768.35	1	6	3.17	0.08
20	80	0.4	5126.02	5234.94	5243.41	2	5	2.29	0.16
20	75	0.1	2422.11	2624.39	2624.39	0	7	8.35	0.00
20	75	0.2	3500.14	3738.65	3738.65	0	7	6.81	0.00
20	75	0.3	4154.91	4390.43	4390.43	0	7	5.67	0.00
20	75	0.4	4606.35	4828.61	4828.61	0	7	4.83	0.00

Table 3 Results of simulation in the case of unbalanced parallel flow arrangement for low temperature application; working fluid: ammonia (NH₃) – water (H₂O), $\dot{m}_h = 0.2 \, \text{kg/s}$.

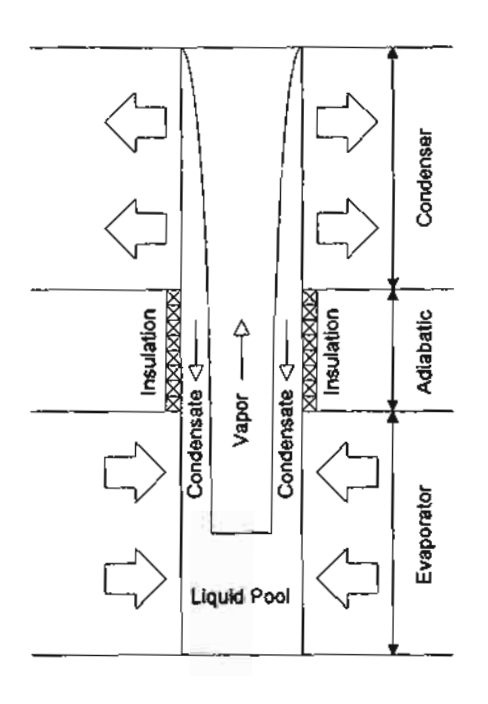
	T.	rin .	0	0	0	No. of t	ube row	% inc	crease
T _c , (°C)	T _{hi} (°C)	m _c (kg/s)	Q_{H_2O} (W)	Q_{NH_3} (W)	$Q_{H_2O-NH_3}$ (W)	H ₂ O	NH ₃	Relative to H ₂ O	Relative to NH ₃
20	110	0.1	4587.09	4444.08	4587.09	7	0	0.00	3.22
20	110	0.3	6500.33	6219.93	6500.33	7	0	0.00	4.51
20	110	0.4	6859.51	6559.15	6859.51	7	0	0.00	4.58
20	100	0.1	4016.58	3976.97	4033.43	5	2	0.42	1.42
20	100	0.3	5676.76	5582.6	5705.28	5	2	0.50	2.20
20	100	0.4	5988.52	5889.68	6024.55	5	2	0.60	2.29
20	90	0.1	3447.36	3499.02	3508.11	2	5	1.76	0.26
20	90	0.3	4856.82	4927.58	4957.25	3	4	2.07	0.60
20	90	0.4	5121.66	5201.31	5236.26	3	4	2.24	0.67
20	80	0.1	2880.37	3011.31	3011.31	0	7	4.55	0.00
20	80	0.3	4042.06	4255.73	4255.73	0	7	5.29	0.00
20	80	0.4	4260.53	4494.78	4494.78	0	7	5.50	0.00

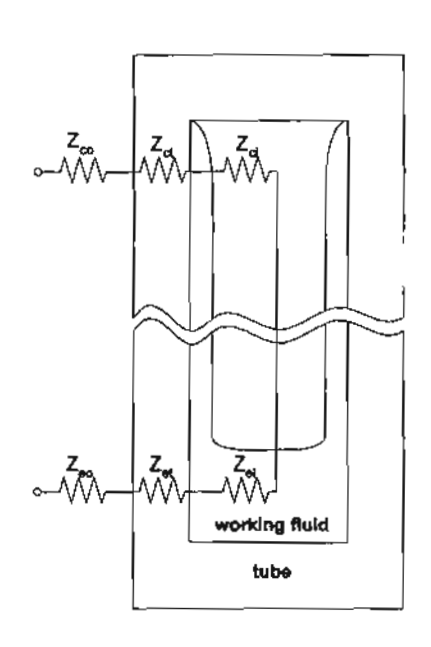
Table 4 Results of simulation in the case of balanced counter flow arrangement for high temperature application; working fluid: water-dowtherm A.

T _c ,	T_{hi}	m	0	0	Q _{dowthermA} No. of tube row		% increase
(°C)	(°C)	(kg/s)	$Q_{H_2O-dowthermA} \ ext{(W)}$	∠dowthermA (W)	H ₂ O	dowtherm A	relative to dowtherm A
200	325	0.2	14,801.24	8,586.18	7	0	72.38
200	325	0.3	19,733.14	9,924.58	7	0	98.83
200	325	0.4	23,910.64	10,794.05	7	0	121.52
200	350	0.2	16,278.12	10,180.31	5	2	59.90
200	350	0.3	21,261.08	11,722.44	5	2	81.37
200	350	0.4	25,367.74	12,717.51	5	2	99.47
200	375	0.2	16,695.81	11,734.56	3	4	42.28
200	375	0.3	21,136.80	13,464.64	3	4	56.98
200	375	0.4	24,643.56	14,574.15	3	4	69.09
250	325	0.2	8,215.36	5,311.22	4	3	54.68
250	325	0.3	10,749.66	6,183.04	4	3	73.86
250	325	0.4	12,843.12	6,756.87	4	3	90.07
250	350	0.2	8,912.57	6,977.37	2	5	27.74
250	350	0.3	11,077.11	8,078.91	2	5	37.11
250	350	0.4	12,735.22	8,796.64	2	5	44.77
250	375	0.2	9,937.70	8,591.39	1	6	15.67
250	375	0.3	9,900.76	9,900.76	0	7	0.00
250	375	0.4	10,746.83	10,746.83	0	7	0.00

Table 5 Results of simulation in the case of unbalanced parallel flow arrangement for high temperature application; working fluid: water-downterm A.

$T_{c'}$	Thi	\dot{m}_h/\dot{m}_c	Q _{H2O-dowthermA}	Q _{dowthermA}	No. of tube row		% increase
(°C)	(°C)	(kg/s)	(W)	(W)	H ₂ O	dowtherm A	relative to dowtherm A
250	375	0.1/0.3	9,581.41	7,255.79	7	0	32.05
250	375	0.15/0.3	12,172.92	8,349.21	6	1	* 45.80
250	375	0.17/0.3	11,597.18	8,639.07	3	4	34.24
250_	375	0.2/0.3	9,070.19	9,070.19	0	7	0.00
250	400	0.05/0.3	6,752.08	6,036.20	7	0	11.86
250	400	0.1/0.3	11,404.50	8,654.23	6	1	31.78
250	400	0.12/0.3	11,769.60	8,309.16	3	4	41.65
250	400	0.2/0.3	10,629.87	10,629.87	0	7	0.00

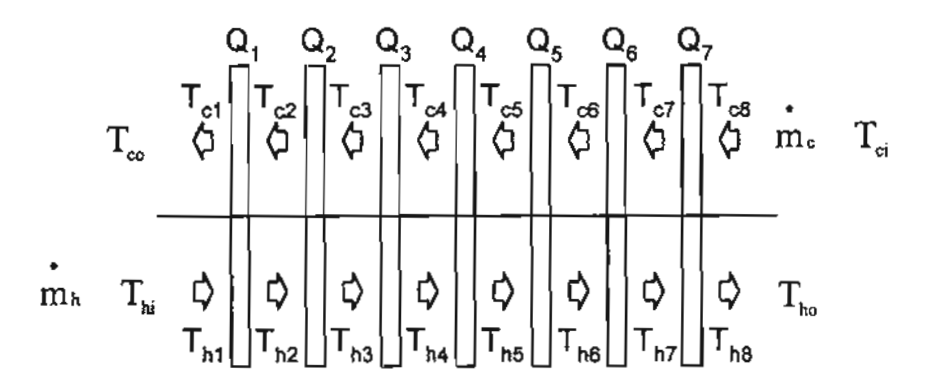




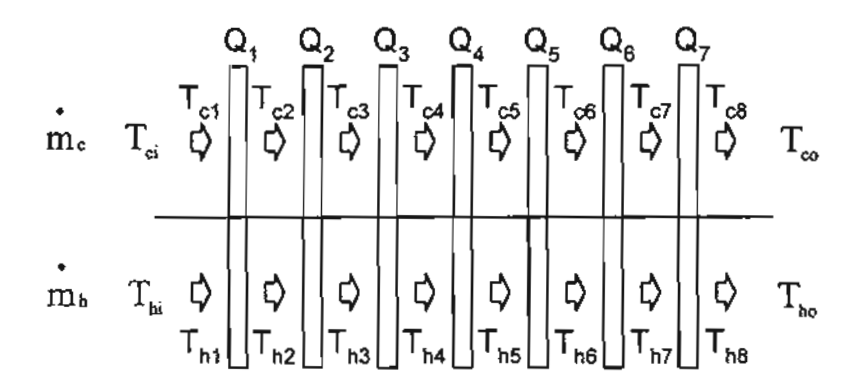
a. Operating principle

b. Thermal resistance circuit

Figure 1 Schematic of the thermosyphon heat pipe.



a. Counter flow thermosyphon heat exchanger.



b. Parallel flow thermosyphon heat exchanger.

Figure 2 Flow arrangement of the thermosyphon heat exchanger.

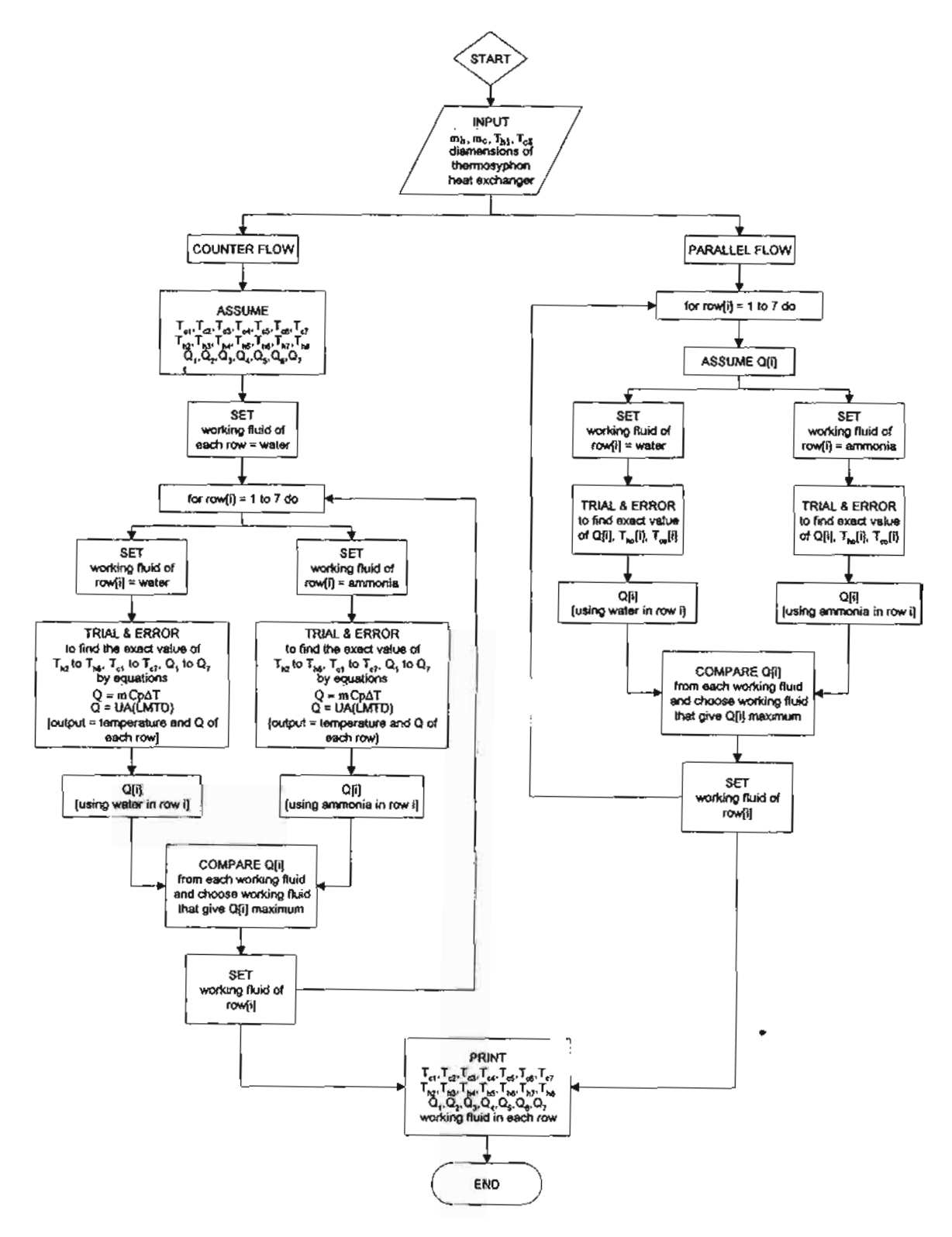


Figure 3 The flow chart of the two-fluid thermosyphons in low temperature application.

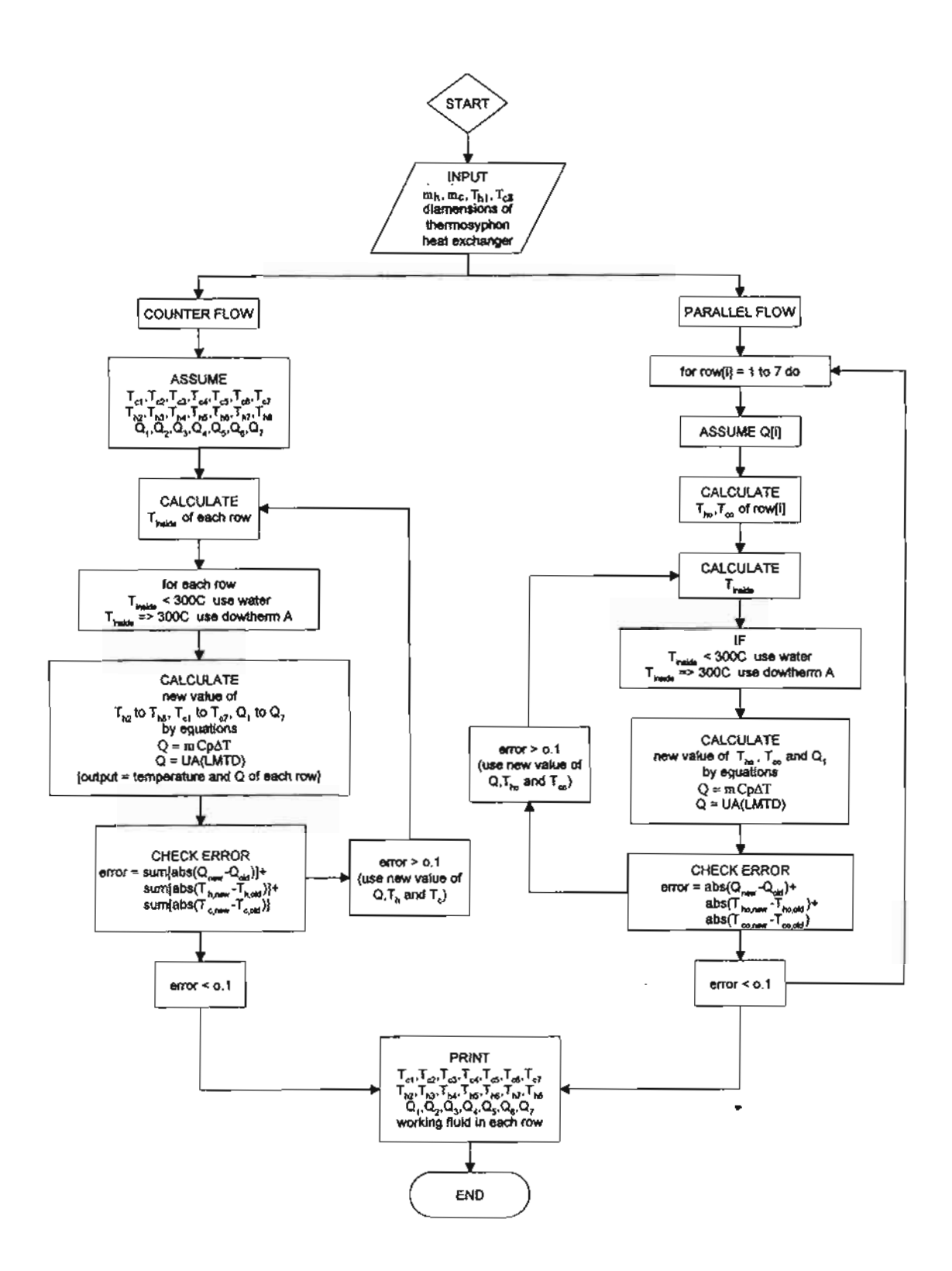


Figure 4 The flow chart of the two-fluid thermosyphons in high temperature application.

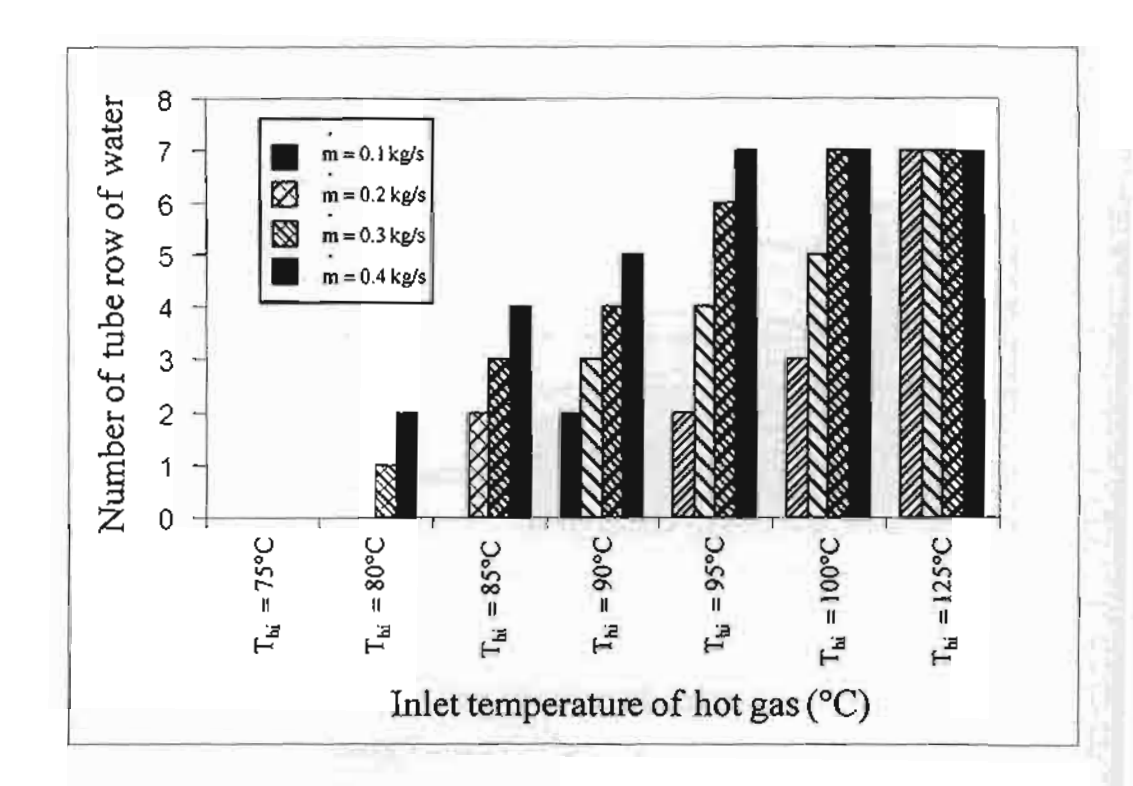


Figure 5 Relation of the appropriate number of water thermosyphons vs. inlet conditions for balanced counter flow arrangement at $T_{ci} = 20$ °C.

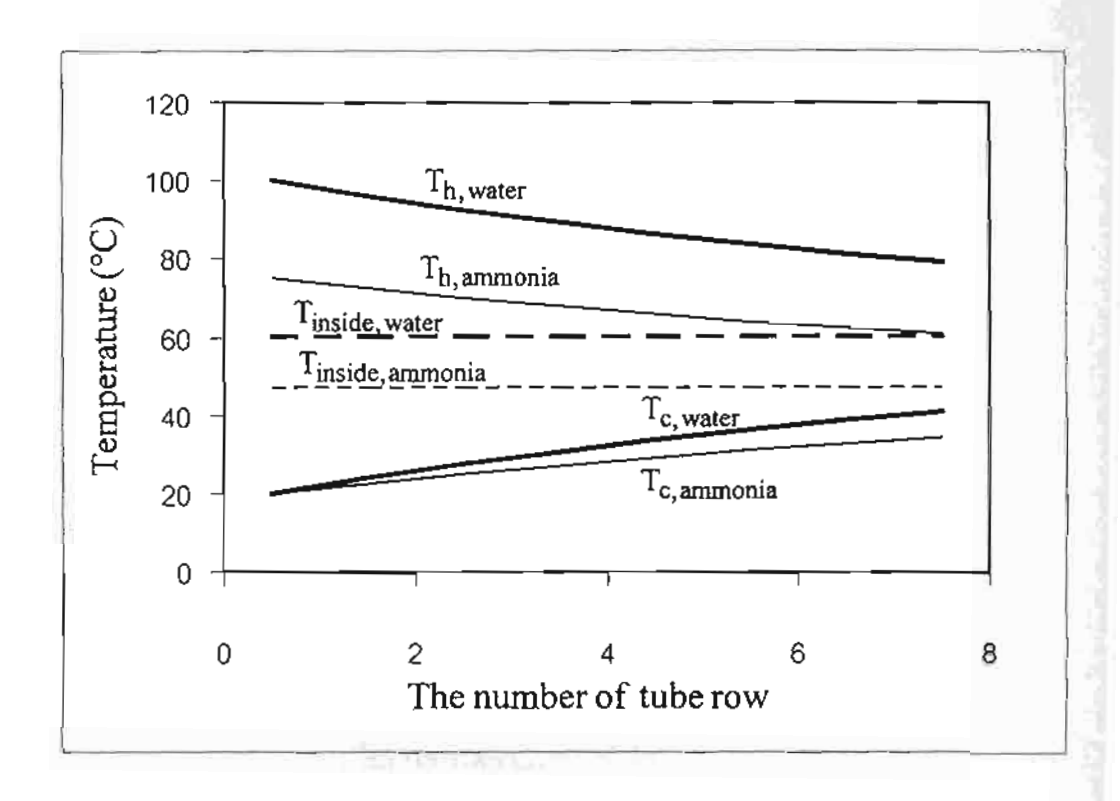


Figure 6 Temperature profiles of the balanced parallel flow thermosyphon heat exchanger using water and ammonia as working fluids.

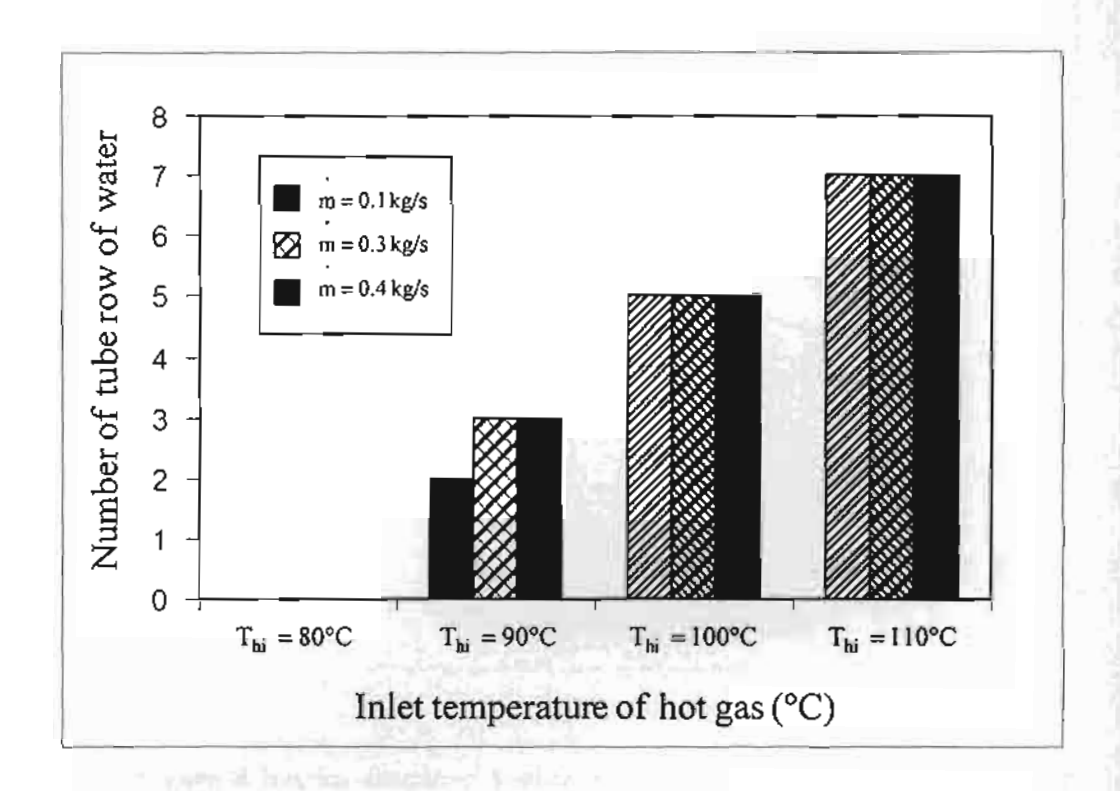


Figure 7 Relation of the appropriate number of water thermosyphons vs. inlet conditions for unbalanced parallel flow arrangement at $T_{ci} = 20$ °C and $\dot{m}_h = 0.2$ kg/s.

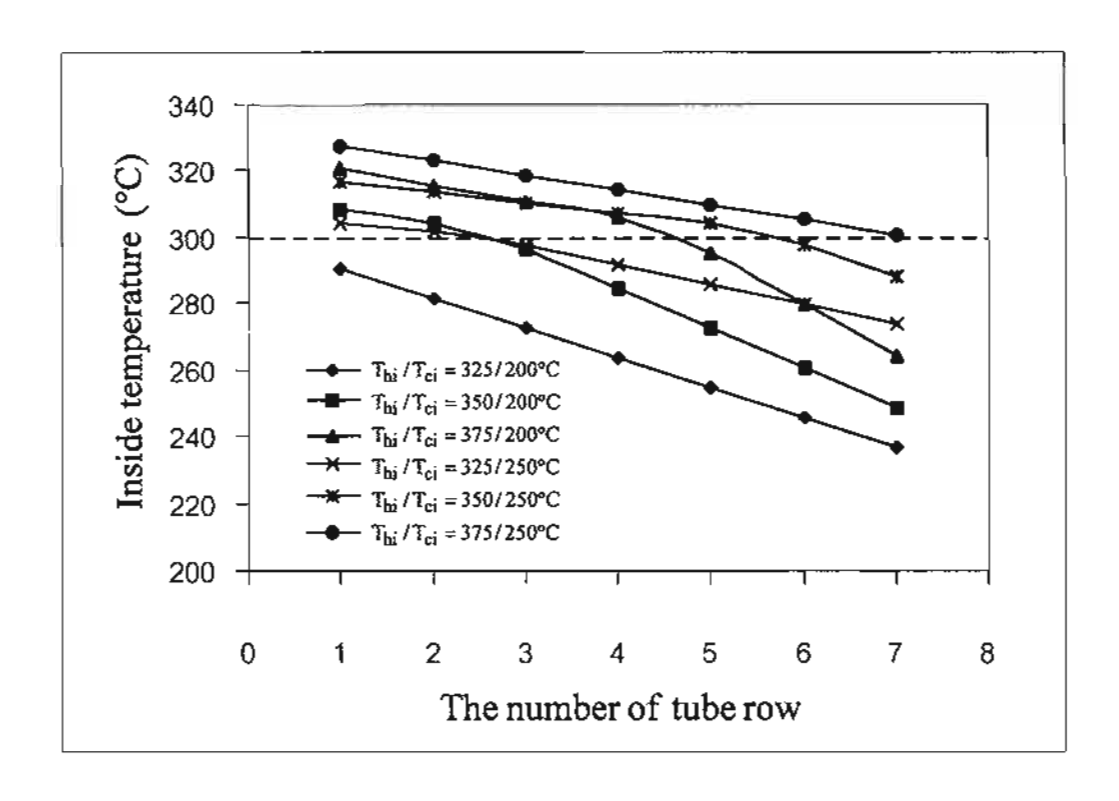


Figure 8 Interior saturation temperatures of each row of counter flow heat exchanger at various conditions; mass flow rate of air = 0.3 kg/s.

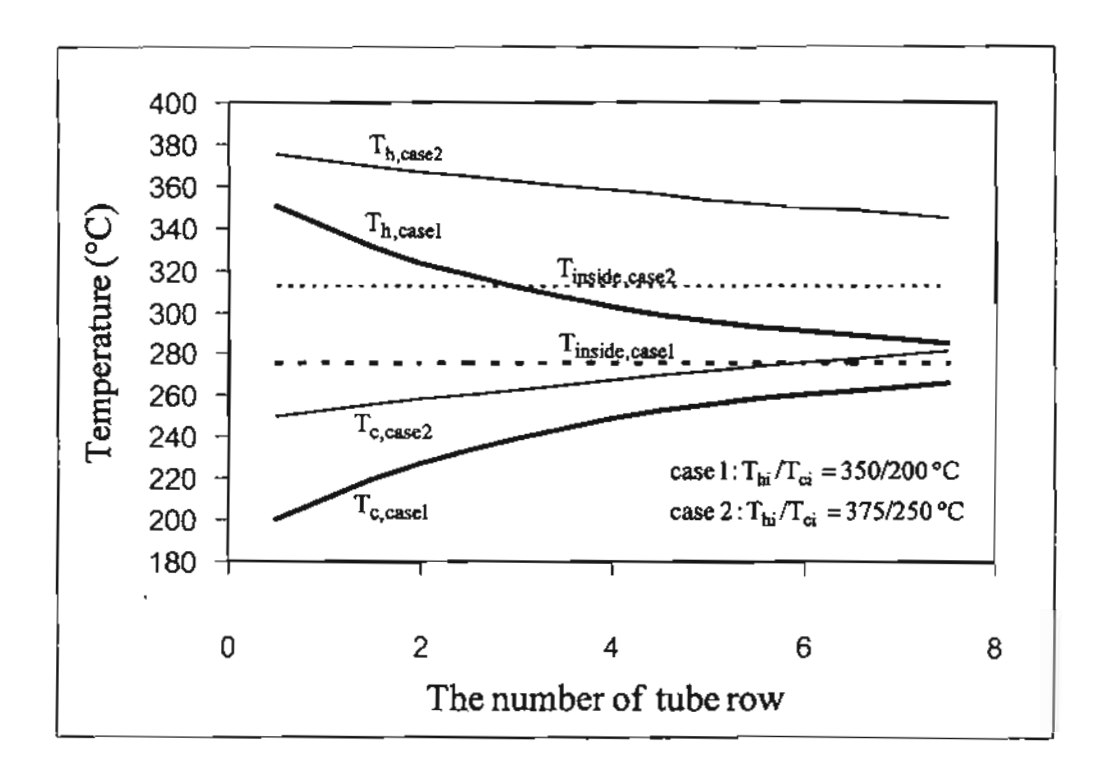


Figure 9 Temperature profile of the balanced parallel flow heat exchanger using water and dowtherm A as working fluids.

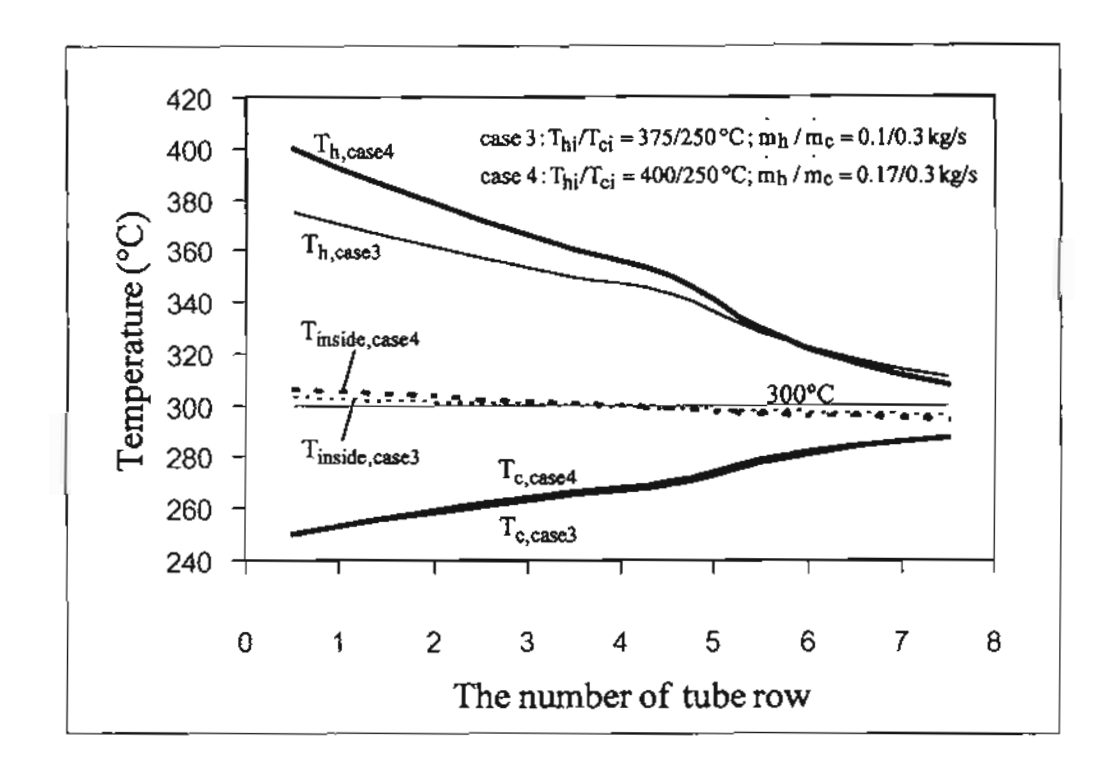


Figure 10 Temperature profile of the unbalanced parallel flow heat exchanger using water and dowtherm A as working fluids.

Nuntaphan A., Tiansuwan J. and Kiatsiriroat T., 2001, Enhancement of Heat Transport in Thermosyphon Air Preheater at High Temperature With Binary Working Fluid: A Case Study of TEG-water, paper submitted for publication in **Applied Thermal Engineering**.

Enhancement of Heat Transport in Thermosyphon Air Preheater at High Temperature with Binary Working Fluid: A Case Study of TEG-water

A. Nuntaphan and J. Tiansuwan

School of Energy and Materials, King Mongkut's University of Technology Thonburi, Bangkok 10140, Thailand

T. Kiatsiriroat

Department of Mechanical Engineering, Chiang Mai University, Chiang Mai 50200, Thailand

Abstract - In this research, the critical heat flux due to flooding limit of thermosyphon

heat pipe using TEG-water mixture has been investigated. From the experiment it is

found that, use of TEG-water mixture can extend the heat transport limitation compared

with pure water and higher heat transfer is obtained compared with pure TEG at high

temperature applications. Moreover it is found that ESDU equation can be used to

predict the critical heat flux of the thermosyphon in case of TEG-water mixture.

For thermosyphon air preheater at high temperature applications, it is found that

with selected mixture content of TEG-water in each row of the thermosyphon the

performance of the system could be increased approximately 30-80% compared with

pure TEG for parallel flow and 60-115% for counter flow configurations. The

performances also increase approximately 80-160% for parallel flow and 140-220% for

counter flow compared with those of pure dowtherm A which is the common working

fluid at high temperature applications.

Keywords: thermosyphon air preheater, critical heat flux

1. INTRODUCTION

The thermosyphon air preheater, at present, has become an important equipment for energy recovery from industrial waste heat because of its low investment cost and high thermal conductivity.

The thermosyphon air preheater consists of many tubes of thermosyphon heat pipes. The thermosyphon heat pipe shown in Fig. 1a can be divided into three parts, evaporator, adiabatic and condenser. When heat is added to the evaporator section, the working fluid inside the tube boils, vaporises and carries heat from the high temperature heat source to the low temperature heat sink where the working fluid condenses. The condensate from the condenser returns to the evaporator by gravitational force.

Water, normally, has been used as a working fluid inside the thermosyphon because of its high latent heat of vaporization and wide working temperature range, (approximately 50-300°C) [1-3]. However, in some conditions of waste heat such as the flue gas from ceramic furnace, the temperature of hot gas is higher than 300°C and the critical heat flux (CHF) due to flooding limit may occur when using pure water as the working fluid. Dowtherm A is recommended for this high temperature range [4] however the heat transfer rate when using dowtherm A is very low compared to the water [5].

From a previous study [6], it was found that using Triethylene glycol (TEG; $C_6H_{14}O_4$) – water mixture as a working fluid could reduce the flooding phenomenon of the thermosyphon while the heat transfer rate slightly decreases. However, the information of the TEG concentration effect on the heat transport is very limited. In this

research work the critical limit of the thermosyphon heat pipe using TEG-water has been investigated. Selection of the suitable fraction of TEG in the working fluid mixture in each row of a thermosyphon air preheater operated at high temperature has also been carried out.

2. FLOODING LIMIT OF THE THERMOSYPHON

2.1. Critical heat flux equation

Flooding phenomenon of working fluid inside the thermosyphon always occurs at high operating temperature. ESDU [7] proposes a the correlation to calculate this critical heat flux due to flooding limit and is in the form of

$$Q_{max} = f_1 f_2 f_3 \lambda A_{rs} \left(g \sigma(\rho_1 - \rho_{\nu}) \right)^{0.25} \rho_{\nu}^{0.5}, \tag{1}$$

where A_{cs} is cross-sectional area of the thermosyphon, D_l is inside pipe diameter. The factor f_l is the function of Bond number (Bo) and it can be evaluated from

$$f_1 = -0.0331Bo^2 + 0.8161Bo + 3.2134, (2)$$

where

$$Bo = D_i \left(\frac{g(\rho_i - \rho_v)}{\sigma} \right)^{0.5}. \tag{3}$$

The factor f_2 is a function of the dimensionless pressure parameter (K_p) which is defined as

$$K_{\rho} = \frac{P_{\nu}}{(g(\rho_{I} - \rho_{\nu})\sigma)^{0.5}} \tag{4}$$

and

$$f_2 = K_p^{-0.17}$$
 if $K_p \le 40000$ (5)

$$f_2 = 0.165$$
 if $K_p > 40000$. (6)

The function f_3 is unity if the pipe is in vertical direction.

2.2. Experimental Set-up

The CHF due to flooding limit of a TEG-water thermosyphon has been investigated and Fig. 2 shows a schematic diagram of the experimental apparatus. A 9.5 mm diameter copper tube with 1 mm thickness has been used as a thermosyphon. The length of evaporator, adiabatic and condenser sections are 40, 20 and 40 cm respectively. Four K-type thermocouples are attached at the outer surface of the tube along the length of the evaporator section and the others four are also attached at the condenser section for measuring the surface temperature. The pressure gage is mounted on the top of the tube for measuring inside pressure. Hot paraffin oil bath with an electric heater and a temperature control box is used as the heat source of the evaporator section. The air bubble is also injected to the paraffin oil to make a uniform temperature. The condenser section is inserted into the cooling jacket. The mass flow rate of cooling water is controlled by a constant head tank and the water flows through the jacket to absorb heat from the condenser section. The inlet and the outlet temperatures of cooling water are measured by a set of thermocouples and a flow meter is used to measure the mass flow rate. These values are used to calculate the heat transfer rate of the thermosyphon.

In this study, the temperature of hot paraffin oil is controlled from 90-200°C and the temperature of the cooling water is kept constant at 30°C and the mass flow rate is 0.0054 kg/s. The working fluid inside the thermosyphon is TEG-water mixture at 0, 25, 50, 75 and 100% by volume of TEG. The filling ratio is 50% of the evaporator volume. The experiments have been carried out under steady-state conditions.

2.3. Critical heat flux of TEG-water mixture

Fig. 3 shows the critical heat flux of the thermosyphon heat pipe using various contents of TEG-water mixture. It is found that using TEG-water can extend CHF due to flooding limit and this limit is proportional to the content of TEG in the mixture. The heat transfer rate of the thermosyphon using pure TEG is the lowest compared to those of pure water and the binary mixture because of very low latent heat of pure TEG and its high normal boiling point (278°C at normal pressure for TEG).

Fig. 4 shows the comparison of the experimental results critical heat flux with those calculated from the ESDU correlation. Both results agree quite well. Note that the properties of the binary mixture can be evaluated from the methods in references [8-13].

3. THERMOSYPHON AIR PREHEATER USING TEG-WATER – A CASE STUDY

3.1. Thermal resistances of the thermosyphon air preheater

Fig. 1b shows the thermal resistance circuit of the thermosyphon. In this research work, the pressure drops from the evaporator to the condenser end and the axial

conduction along the pipe wall are assumed to be negligible. Evaluation methods of the thermal resistance are described as follows:

The external air-side thermal resistances of the evaporator (Z_{eo}) and the condenser (Z_{co}) section can be calculated from

$$Z_{eo} = \frac{1}{h_{eo}A_{eo}},\tag{7}$$

$$Z_{co} = \frac{1}{h_{co}A_{co}}. (8)$$

 h_{eo} and h_{co} are the external air-side heat transfer coefficient at the evaporator and the condenser, respectively. For plain plate finned tube having staggered array, Webb [14] proposed a following correlation as

$$j = 0.14 Re^{-0.328} \left(\frac{S_t}{S_t}\right)^{-0.502} \left(\frac{f_s}{D_o}\right)^{0.031}, \tag{9}$$

where j is Colburn factor which is defined as:

$$j = \frac{h_o}{\rho V_{max} C \rho_I} P r^{2/3} . \tag{10}$$

Related information for calculating the fin surface area A_f , the bare tube surface A_b , and the fin efficiency η_f are given as:

$$A_{f} = 2n_{f} \left((n_{c} + 0.5) S_{t} S_{i} - 0.25 \pi n_{c} D_{o}^{2} \right), \tag{11}$$

$$A_b = \left(\frac{\pi n_c L_e}{f_s + f_t}\right) D_o f_s, \tag{12}$$

$$\eta_f = \frac{\tanh(\sqrt{2h_o/f_t k_f} \times \varphi)}{\sqrt{2h_o/f_t k_f} \times \varphi},\tag{13}$$

$$\varphi = (\phi - 1)(1 + 0.35 \ln \phi), \tag{14}$$

$$\phi = 12.7 \frac{X_M}{r} \left(\frac{X_L}{X_M} - 0.3 \right)^{1/2}, \tag{15}$$

$$X_{L} = 0.5\sqrt{\frac{S_{1}/2}{2}^{2} + S_{1}^{2}},$$
 (16)

$$X_M = 0.5S_t. \tag{17}$$

Note that the fin efficiency η_f is computed from Schmidt's approximation [15,16].

The wall resistances in the evaporator and the condenser sections can be calculated from

$$Z_{et} = \frac{\ln(r_o / r_i)}{2\pi k_t L_e},\tag{18}$$

$$Z_{ct} = \frac{ln(r_o / r_i)}{2\pi k_t L_c}.$$
 (19)

The boiling and condensation resistances in the evaporator (Z_{el}) and condenser section (Z_{cl}) can be calculated from

$$Z_{ei} = \frac{1}{h_{ei}A_{ei}} \tag{20}$$

$$Z_{\sigma} = \frac{1}{h_{\sigma} A_{\sigma}} \tag{21}$$

Kiatsiriroat et al. [6] has proposed correlations for calculating the boiling and condensation heat transfer coefficients inside the thermosyphon as Boiling:

$$h_e = \frac{C_1}{\Delta T_e X} \left[\left(\frac{\Delta T_e}{Y} \right)^3 \right]^{C_2}, \tag{22}$$

where
$$X = \frac{1}{\mu_l \lambda} \sqrt{\frac{g_c \sigma}{g(\rho_l - \rho_v)}}$$
 and $= \frac{\lambda P r_l}{C \rho_l}$.

Condensation:

$$h_{cl} = C_3 \left[\frac{g \rho_l^2 \lambda k_l^3}{\mu_l (T_w - T_s) L_c} \right]^{C_4}. \tag{23}$$

The correlation constants C_{I} - C_{4} for water and TEG are shown in Table 1.

In case of binary working fluid, Kiatsiriroat et al. [6] also proposed a correlation for predicting the heat transfer coefficient as

$$h_{mixture} = h_1 x_1 + h_2 (I - x_1),$$
 (24)

where x_1 means the mole fraction of component 1 in the mixture.

For high temperature application, dowtherm A, is normally used as the working fluid. ESDU [7] proposed correlations for calculating the thermal resistances due to boiling and condensation inside the thermosyphon.

Thermal resistance due to pool boiling in the evaporator section:

$$Z_{ei,p} = \frac{1}{\phi_i g^{0.25} Q^{0.4} (\pi D_i L_e)^{0.6}},$$
 (25)

where

$$\phi_{I} = 0.32 \frac{\rho_{I}^{0.65} k_{I}^{0.3} C p_{I}^{0.7}}{\rho_{v}^{0.25} \lambda^{0.4} \mu_{I}^{0.1}} \left[\frac{P_{v}}{P_{a}} \right]^{0.23}.$$
 (26)

Thermal resistance due to falling film evaporation in the evaporator section:

$$Z_{ei,f} = \frac{0.235Q^{1/3}}{D_i^{4/3}g^{1/3}L_e\phi_2^{4/3}},$$
 (27)

$$\phi_2 = \left(\frac{\lambda k_l^3 \rho_l^2}{\mu_l}\right)^{l/4}.$$
 (28)

The total thermal resistance due to boiling in the evaporation can be calculated

as:

$$Z_{ei} = Z_{ei,f}(I - F) + Z_{ei,p}F$$
(29)

where F is filling ratio of the working fluid.

Thermal resistance in the condenser:

$$Z_{ci} = \frac{0.235Q^{1/3}}{D_i^{4/3}g^{1/3}L_c\phi_2^{4/3}}$$
 (30)

The overall thermal resistance of the thermosyphon air preheater can be calculated from

$$\frac{I}{(UA)_{total}} = Z_{eo} + Z_{et} + Z_{et} + Z_{ct} + Z_{ct} + Z_{co}$$
 (31)

where (UA)total is the overall thermal resistance of the thermosyphon air preheater.

The overall heat transfer rate of the thermosyphon air preheater from Fig. 5 for parallel flow and counter flow arrangements can be evaluated as

$$Q_{total} = (UA)_{total} \Delta T_{LMTD}$$

$$= m_h C p_h (T_{hi} - T_{ho}).$$

$$= m_c C p_c (T_{co} - T_{ci})$$
(32)

 ΔT_{lmtd} could be calculated from

for parallel flow

$$\Delta T_{lmid} = \frac{(T_{hi} - T_{ci}) - (T_{ho} - T_{co})}{ln \left[\frac{T_{hi} - T_{ci}}{T_{ho} - T_{co}} \right]},$$
(33)

for counter flow

$$\Delta T_{lmtd} = \frac{(T_{hl} - T_{co}) - (T_{ho} - T_{cl})}{ln \left[\frac{T_{hl} - T_{co}}{T_{ho} - T_{cl}} \right]}.$$
 (34)

3.2. Simulation program

This part is the case study of using TEG-water as a working fluid in the thermosyphon air preheater. Table 2 shows testing conditions and related geometrical parameters of the thermosyphon air preheater using in the simulation program. The concept of the program is to find out the suitable mixture content of TEG-water in each row of the air preheater. Note that the contents of TEG in the binary mixture are 0, 25, 50, 75 and 100% by volume.

Fig. 6 shows the flow chart of the calculation method. It can be divided into two parts, counter flow and parallel flow. In the counter flow part, firstly input all of working conditions and also dimensions of the air preheater then assume values of inlet and outlet temperatures of the hot and the cold streams and also heat transfer rate in each row. Next, set the working fluid of each row as water and using trial and error technique for finding out the real value of the temperatures and the heat transfer rate of each row. Then check the critical heat flux of each row and select the suitable working fluid which gives the highest heat transfer rate. Re-calculate until all the computational values are constant. The calculation continues to the last row of the heat exchanger.

For the parallel flow part, starting with row 1 by assume the value of Q and using water as working fluid. Then, by trial and error technique, the real value of the outlet temperature of the hot and the cold air and also the heat transfer rate are obtained.

Next check the critical heat flux of this row and compute the heat transfer rate then select the suitable mixture content and recalculate again until every value is steady. Next starting with row 2 by the same method until the last row is carried out.

3.3. Results and discussion

Tables 3 and 4 show the results of the heat exchanger from the simulation program for the parallel flow and the counter flow respectively. It is found that the heat transfer rate increases significantly in some conditions compared to pure TEG when using suitable mixture content in each row of the air preheater. Normally water cannot be used as a working fluid in this temperature range (300-400°C) because of the flooding limit. However, TEG-water can extend this condition and the performance increases approximately 30-80% for parallel flow and 60-115% for counter flow compared to pure TEG. When compared with a common working fluid, dowtherm A, it is also found that using TEG-water can also increases the heat transfer rate approximately 80-160% for parallel flow and 140-220% for counter flow configurations.

In case of parallel flow, it is found that the content of TEG should be high in the first rows and water is a good working fluid in the last rows. These results can be explained by Fig. 7 which shows the temperature profiles of the parallel flow air preheater. Normally the gap between the hot and the cold streams is large at the initial rows and narrow at the last rows. Consequently the heat transfer rate of the initial row is higher than that of last row and it has a high opportunity to reach the critical limit and

therefore high content of TEG or pure TEG are the suitable working fluids in this range. On the other hand, water or lower content of TEG in the mixture is suitable for the last rows. In Fig. 7 it also shows the comparison between using TEG-water and pure TEG. This result comes from the simulation program shown in Table 3 (No.7). It is found that using 75% and 25% of TEG in rows 3 and 4 and pure water in row 5 and 6, the temperature difference between the hot and the cold air streams is smaller significantly compared with pure TEG, therefore, higher heat exchange is obtained.

In case of counter flow, from Table 4, it is found that in case of balance counter flow $(m_h = m_c)$ the mixture content in each row is nearly the same. This phenomenon can be explained by Fig. 8 which shows the comparison of temperature profiles of balance counter flow between using TEG-water mixture and pure TEG. Actually in this case the temperature gap of the hot and the cold streams is nearly constant in this case. Consequently the heat transfer rate of each row is also nearly constant and this value is suitable for only one mixture content. However, in case of unbalance counter flow $(m_h \neq m_c)$, the temperature difference is not constant including the heat transfer rate, therefore, the mixture content in each row will affect the performance. Fig. 9 shows the result obtained from Table 4 (No.18). Use of TEG content of 75% in row 1-3 and 100% in rows 4-6 shows better heat exchange compared with pure TEG in all rows.

It could be seen that, the system performance when using TEG-mixture is also higher than using dowtherm A which is a common working fluid of high temperatures. From Tables 3 and 4, the performance increases about 80-160% for parallel flow and 140-220% for counter flow.

4. CONCLUSIONS

In this research, the concept of using TEG-water in the thermosyphon heat pipe has been studied. Major results are summarized as follow:

- Using of TEG-water can extend the critical limit due to flooding inside the thermosyphon and the limit is directly proportional to the content of TEG in the mixture.
- Suitable mixture content of TEG-water in each row of the thermosyphon air preheater can increase the performance of the system approximately 30-80% for parallel flow and 60-115% for counter flow air preheater compared with pure TEG.
- 3. The heat exchanger with suitable content of TEG-water also shows better performance than that with dowtherm A.

Acknowledgement - The authors gratefully acknowledge the support provided by Thailand Research Fund for carrying out this study.

REFERENCES

- 1. Chi S.W., Heat Pipe Theory and Practice, Hemisphere, Washington, USA, 1976.
- Faghri A., Heat Pipe Science and Technology, Taylor & Francis, Philadelphia, USA, 1995.
- Peterson G.P., An Introduction to Heat Pipes Modeling, Testing and Applications,
 John Wiley & Sons, New York, USA, 1994.

- Engineering Data Science Unit No.80017, Thermophysical Properties of Heat Pipe Working Fluids: Operating Range Between -60 °C and 300 °C, ESDU Int. Plc., London, UK, 1980.
- Nuntaphan A., Tiansuwan J., Kiatsiriroat T. and Wang C.C., Performance
 Improvement of Thermosyphon Heat Exchangers by Using Two Kinds of Working
 Fluids, a paper accepted for publication in Heat Transfer Engineering, 2001.
- Kiatsiriroat T., Nuntaphan A. and Tiansuwan J., Thermal Performance Enhancement of Thermosyphon Heat Pipe with Binary Working Fluids, Experimental Heat Transfer, 2000;13(2):137-152.
- Engineering Data Science Unit No.81038, Heat Pipes-Performance of Two-Phase Closed Thermosyphons, ESDU Int. Plc., London, UK, 1983.
- C.L. Yaws, Handbook of Thermodynamic Diagrams, Vol.2, p.240,378, Gulf Publishing, Houston, Texas, USA, 1996.
- R.H. Perry and C.H. Chilton, Chemical Engineer's Handbook, 5th Edition, McGraw Hill, New York, USA, 1973.
- R.C. Reid, J.M. Pransnitz and B.E. Poling, The Properties of Gases&Liquids, 4th
 Edition, McGraw Hill, New York, USA, 1986.
- 11. A.L. Kohl and C.F. Riesenfeld, Gas Purification, 3rd Edition, p.595-629, Gulf Publishing, Houston, Texas, USA, 1979.
- D.T. Jamieson, J.B. Irving and J.S. Tudhope, Liquid Thermal Conductivity a Data Survey to 1973, p.140, National Engineering Laboratory, Edinburgh, Germany, 1973.

- J.F. Kuong, Applied Nomography, Vol.1, p.114-115, Gulf Publishing, Houston, Texas, USA, 1965.
- Webb R.L., Principles of Enhanced Heat Transfer, John Wiley & Sons, New York, USA, 1994.
- Schmidt Th. E., Heat Transfer Calculations for Extended Surfaces, Refrigerating Engineering, 1949:351-357.
- 16. Wang C.C., Lee C.J., Chang C.T. and Chang Y.J., Some Aspects of Plate Fin-and-Tube Heat Exchangers: With and Without Louvers, *Enhanced Heat Transfer*, 1999;6:357-368.

NOMENCLATURE

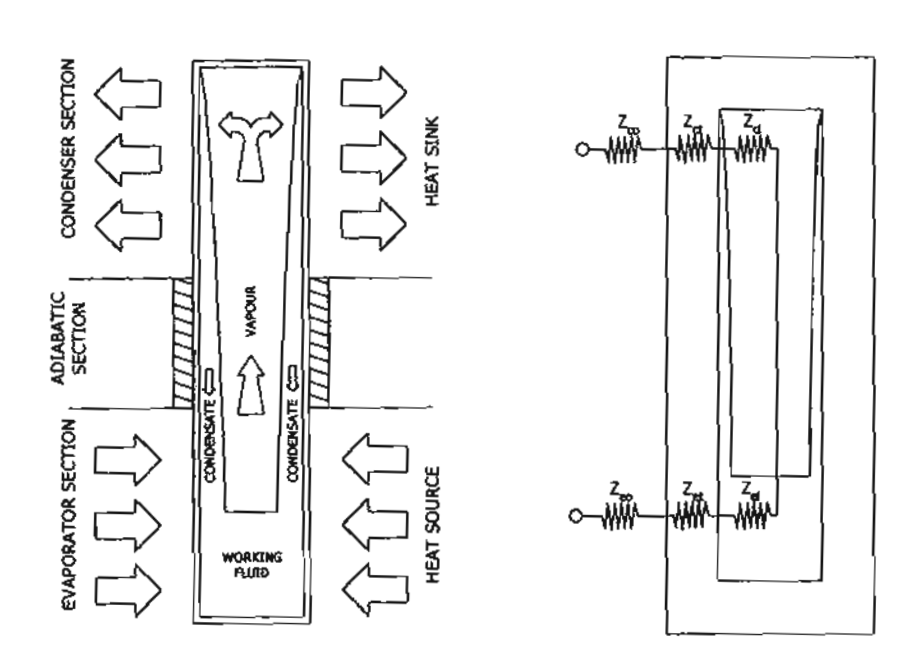
area (m²) \boldsymbol{A} cross sectional area (m²) A_{cs} Вo Bond number empirical constants C_{I-4} specific heat (J/kgK) CpĎ diameter (m) f_{1-3} parameter fin gap (m) f_s fin thickness (m) f_t gravitational acceleration (9.81 m/s²) g conversion factor (1 kgm/Ns²) g_c heat transfer coefficient (W/m²K) h Colburn factor thermal conductivity (W/mK) k K_p parameter L length (m) mass flow rate (kg/s) m number of column of tube bank n_c total number of fin

heat transfer rate (W)

```
radius (m)
S_{l}
        longitudinal pith of tube bank (m)
S_t
        transverse pith of tube bank (m)
T
        temperature (°C)
        temperature difference between inside surface
\Delta T_e
        of evaporator tube and working fluid (°C)
        temperature difference between inside surface
\Delta T_c
        of condenser tube and working fluid (°C)
ΔT<sub>lmtd</sub> log mean temperature difference (°C)
        mole fraction
х
X
        factor
        factor
X_{L}
X_{M}
        factor
Y
        factor
Z
        thermal resistance (K/W)
Greek symbols
        factor
        efficiency
η
        factor
φ
λ
        latent heat (J/kg)
        dynamic viscosity (Pas)
μ
        density (kg/m<sup>3</sup>)
ρ
        surface tension (N/m)
\sigma
Subscripts
        bare tube
        condenser section, cold air
с
        evaporator section
е
        fin, film evaporation
f
h
        hot air
i
       inside, inlet
l
       liquid
       outside, outlet
0
       pool boiling
p
       surface
s
       vapor
ν
       working fluid
w
```

CAPTIONS OF FIGURES AND TABLES

- Fig. 1. Schematic of the thermosyphon heat pipe. a. Operating principle. b. Thermal resistance circuit.
- Fig. 2. The experimental set-up.
- Fig. 3. Critical heat flux of thermosyphon heat pipe using TEG-water mixtures.
- Fig. 4. Comparison of critical heat flux from the experiment and the ESDU model at various mixtures content of TEG.
- Fig. 5. Thermosyphon air preheater, a. Parallel flow arrangement, b. Counter flow arrangement.
- Fig. 6. Flow chart for calculating the suitable mixture content of TEG-water in each row of the thermosyphon air preheater.
- Fig. 7. Comparison of temperature profile of parallel flow thermosyphon air preheater between using TEG-water mixtures and pure TEG (no. 7 in Table 3).
- Fig. 8. Comparison of temperature profile of balance counter flow thermosyphon air preheater between using TEG-water mixtures and pure TEG (no. 3 in Table 4).
- Fig. 9. Comparison of temperature profile of unbalance counter flow thermosyphon air preheater between using TEG-water mixtures and pure TEG (no.18 in Table 4).
- Table 1. Empirical constants of Kiatsiriroat et al. Correlation.
- Table 2. Testing conditions and related geometrical parameters of the thermosyphon air preheater.
- Table 3. Results of simulation in case of parallel flow arrangement; inlet temperature of cold air = 30°C.
- Table 4. Results of simulation in case of counter flow arrangement; inlet temperature of cold air = 30°C.



- a. Operating principle
- b. Thermal resistance circuit

Fig. 1. Schematic of the thermosyphon heat pipe.

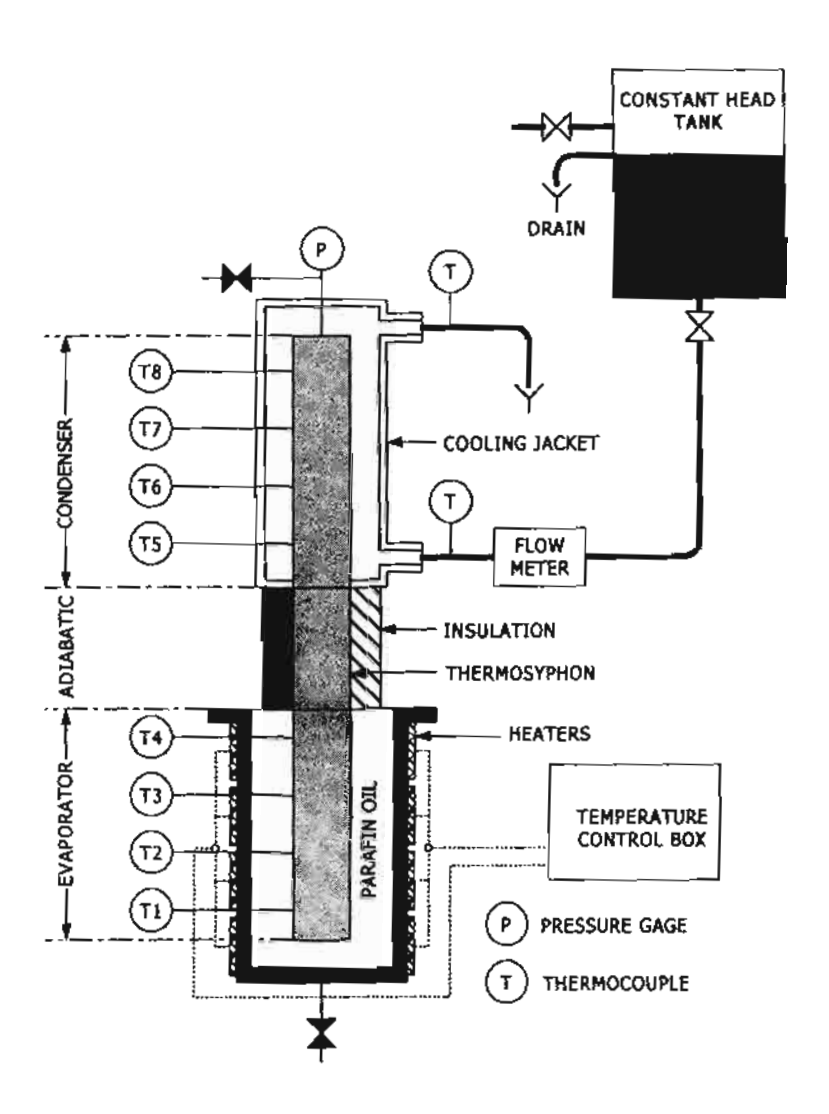


Fig. 2. The experimental set-up

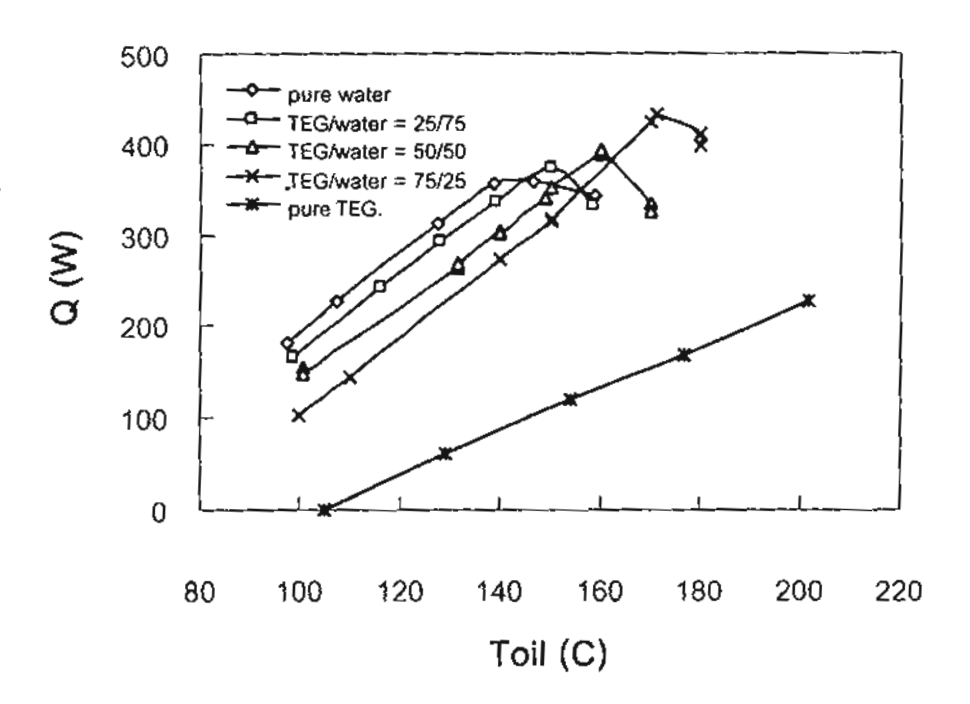


Fig. 3. Critical heat flux of thermosyphon heat pipe using TEG-water mixtures.

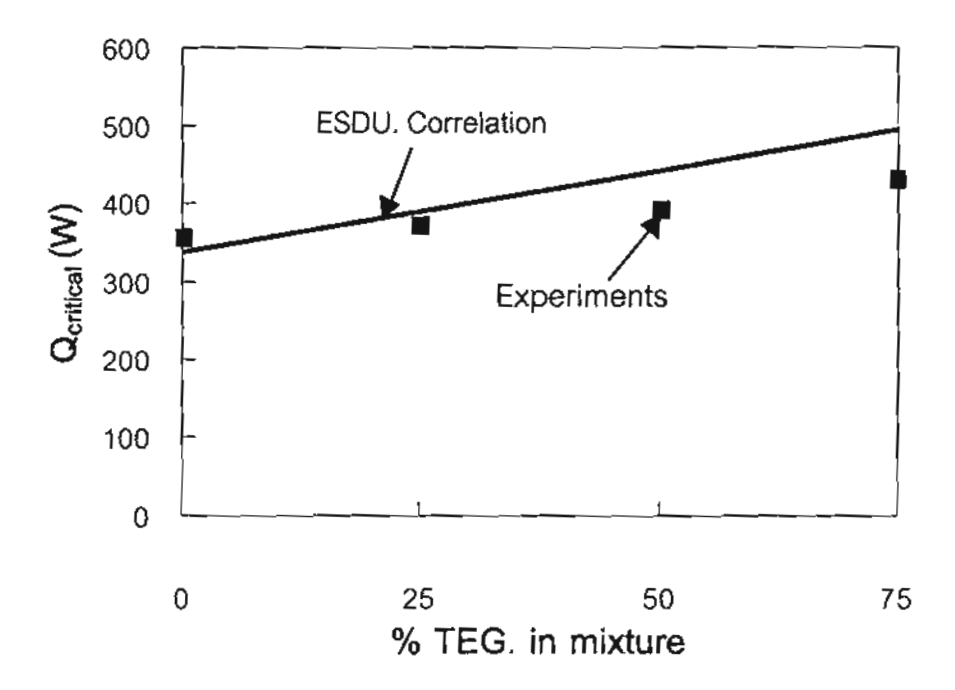
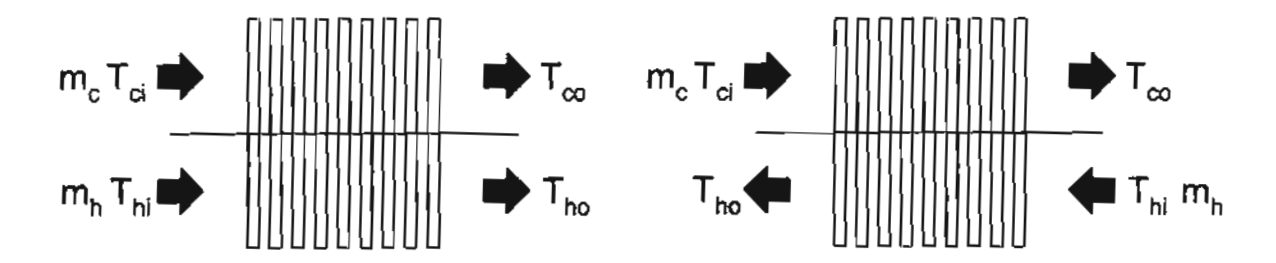


Fig. 4. Comparison of critical heat flux from the experiment and the ESDU model at various mixtures content of TEG.



a. Parallel flow arrangement

b. Counter flow arrangement

Fig. 5. Thermosyphon air preheater.

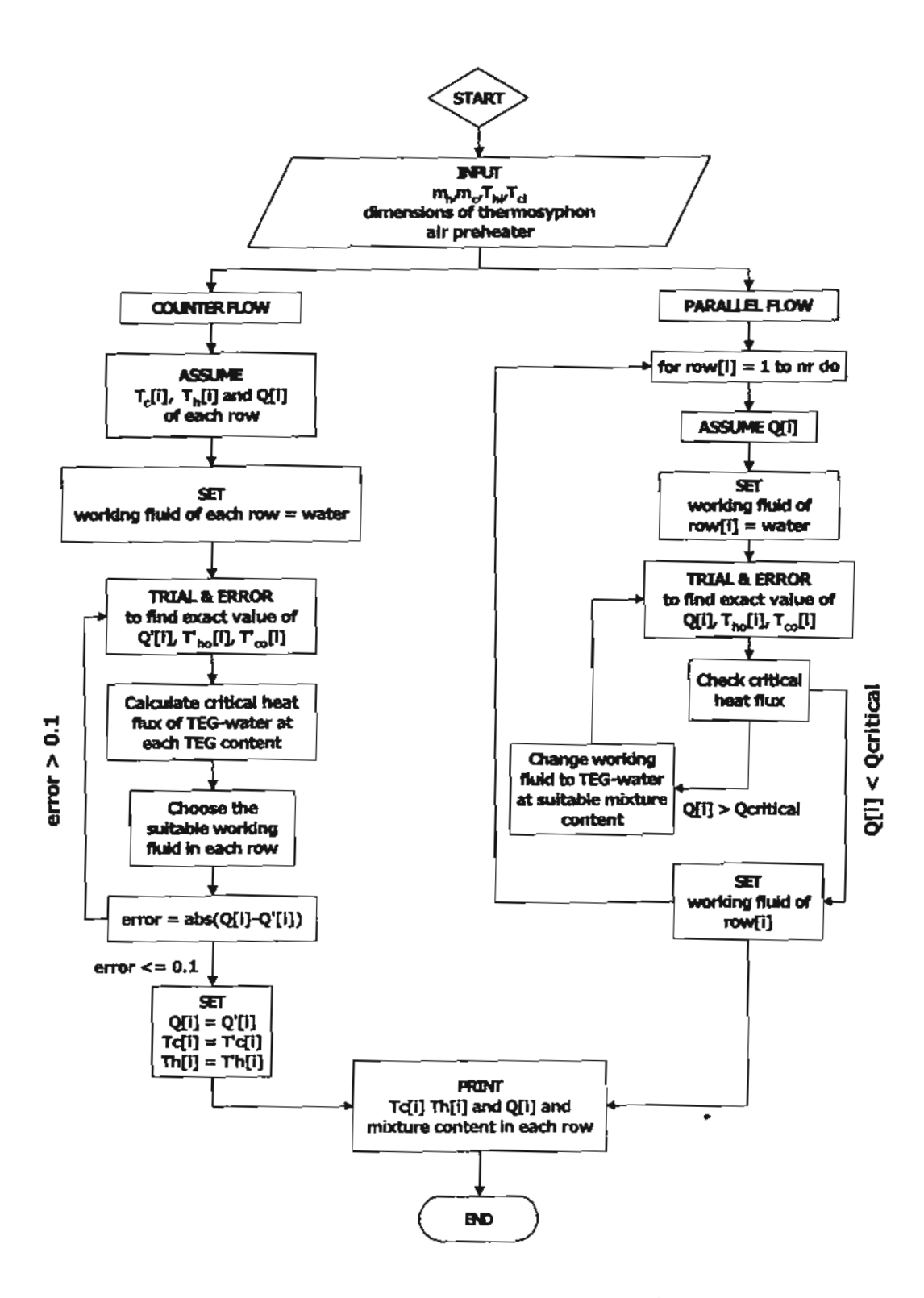


Fig. 6. Flow chart for calculating the suitable mixture content of TEG-water in each row of the thermosyphon air preheater.

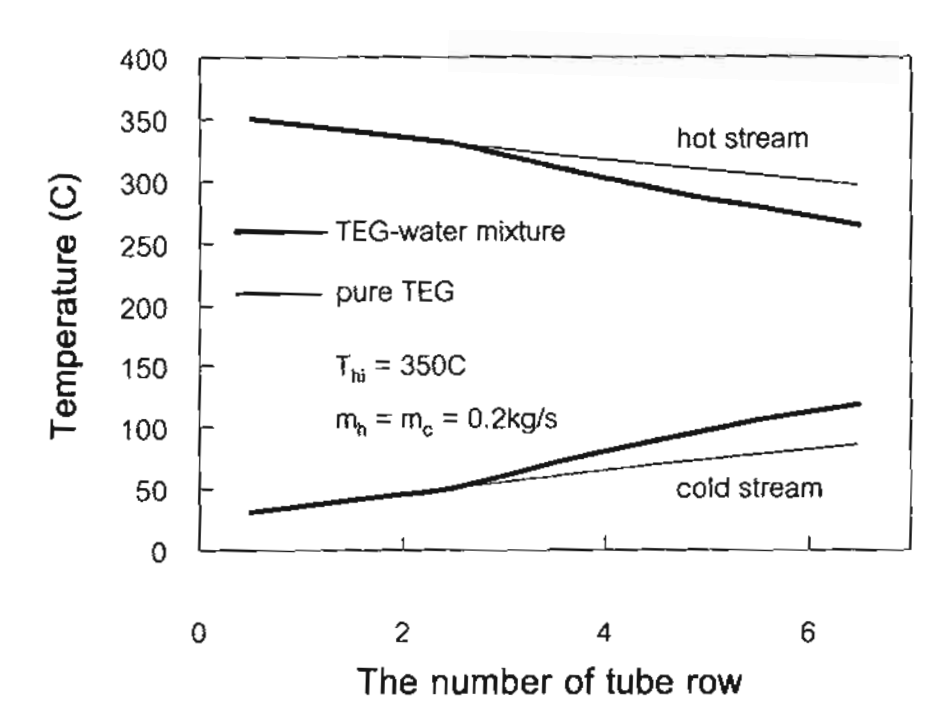


Fig. 7. Comparison of temperature profile of parallel flow thermosyphon air preheater between using TEG-water mixtures and pure TEG (no. 7 in Table 3).

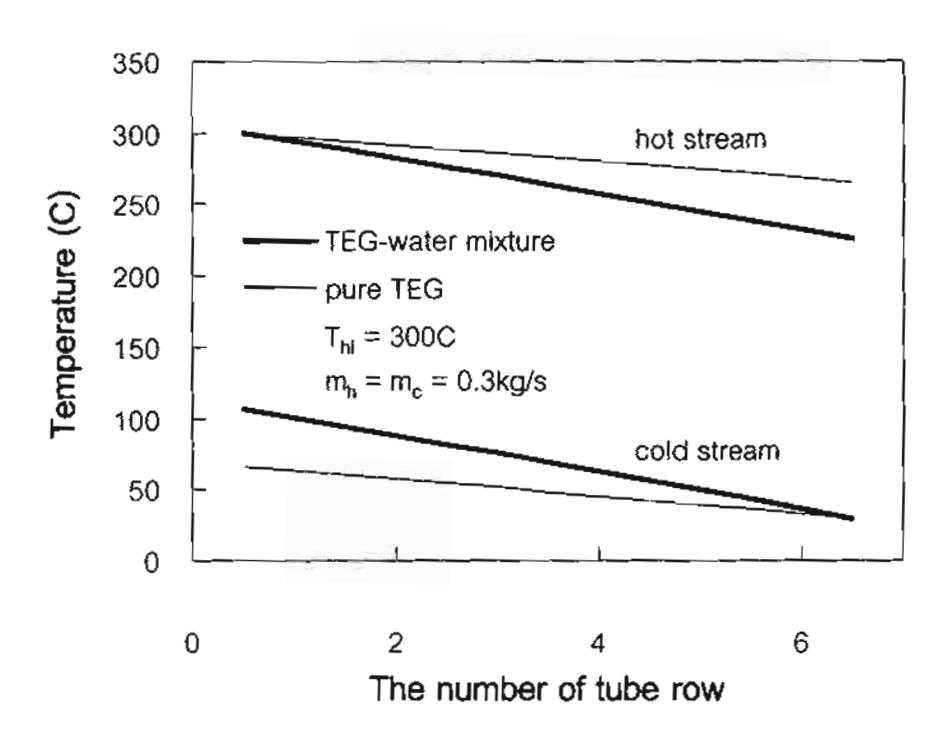


Fig. 8. Comparison of temperature profile of balance counter flow thermosyphon air preheater between using TEG-water mixtures and pure TEG (no. 3 in Table 4).

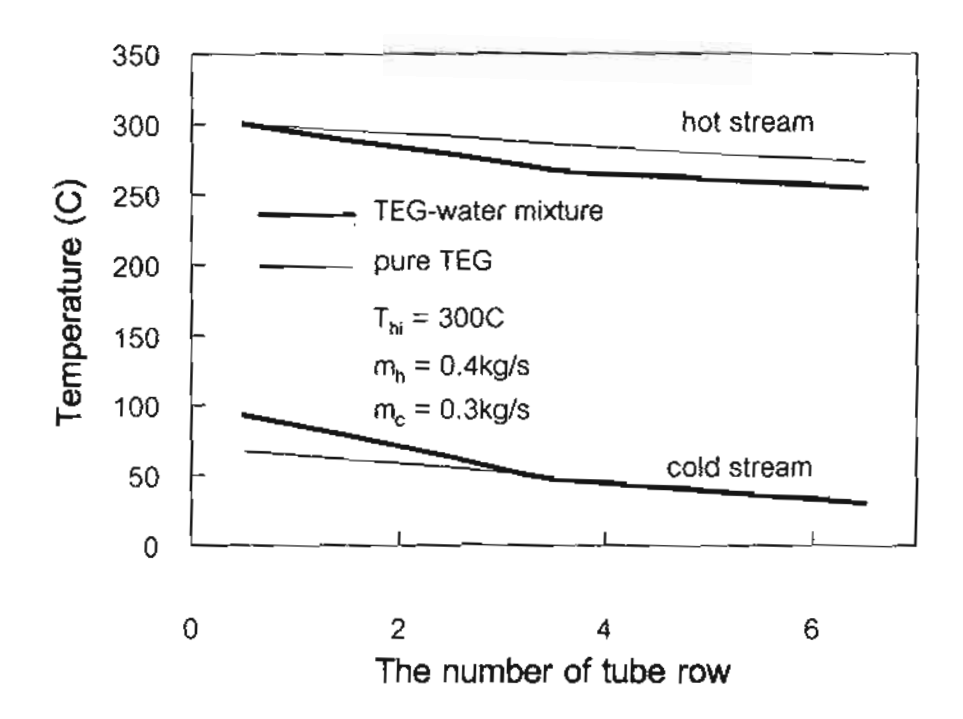


Fig. 9. Comparison of temperature profile of unbalance counter flow thermosyphon air preheater between using TEG-water mixtures and pure TEG (no.18 in Table 4).

Table 1. Empirical constants of Kiatsiriroat et al. correlation.

Working fluid	C_L	C_2	C_3	C4
Water	18.688	0.3572	0.943	0.233
TEG	20.565	0.3662	0.943	0.180

Table 2. Testing conditions and related geometrical parameters of the thermosyphon air preheater.

Items	Conditions
Flow arrangement	Parallel and counter flow
2. Temperature of hot air	300-400 °C
3. Temperature of cold air	30 °C
4. Mass flow rate of air	0.1-0.5 kg/s
5. Thermosyphon arrangement	Staggered array
	$S_t = 0.02 \text{ m}, S_d = 0.02 \text{ m}, S_l = 0.0173 \text{ m}$
6. Number of tube row	6
7. Number of column	10
8. Diameter of thermosyphon (bare tube)	0.0095 m
9. Type of fin	Plain plate fin
10. Size of fin	fin pitch $= 6$ fins/inch
	fin thickness = 0.0005 m
11. Filling ratio of working fluid	50%
12. Material of pipe and fin	Copper for pipe and Aluminum for fin

Table 3. Results of simulation in case of parallel flow arrangement; inlet temperature of cold air = 30°C.

_		_			_	_													_					_	_	-			
% increase	Relative to	dowtherm A	87.01	159.92	111.21	53.74	57.04	86'38	128.48	49.53	54.16	57.44	91.36	87.10	50.31	54.94	58.21	124.20	164.71	51.42	52.98	126.11	96.75	51.84	53.39	115.85	46.35	52.62	54.15
% inc	Relative to	TEG	45.00	83.16	41.68	00.0	0.00	46.49	60.52	0.00	0.00	0.00	47.34	30.74	0.00	0.00	0.00	64.15	82.41	0.00	0.00	65.10	35.16	0.00	0.00	56.83	0.00	0.00	0.00
	Showtherm A	(w)	5377	9999	7263	7626	7871	6371	7846	8539	8952	9231	7340	0668	9758	10215	10521	6102	6917	7459	7586	7227	8151	8757	6688	8324	9338	9994	10146
,	Creo	(<u>w</u>)	6934	9446	10827	11724	12361	8236	11168	12768	13801	14533	9533	12865	14668	15827	16646	8335	10038	11294	11605	8686	11866	13297	13650	11456	13666	15253	15640
(Q75G-water	<u>*</u>	10055	17301	15340	11724	12361	12065	17926	12768	13801	14533	14046	16820	14668	15827	16646	13681	18311	11294	11605	16341	16038	13297	13650	17967	13666	15253	15640
	,	0	0	0	25	100	001	0	0	100	100	001	0	25	100	100	100	0	0	100	100	0	25	001	001	0	901	100	001
 *	1	<u></u>	0	0	75	8	100	0	0	100	100	100	0	75	100	100	100	0	0	001	100	0	75	100	100	0	100	001	100
each ro		4	0	0	100	100	100	0	25	001	001	100	0	001	100	100	001	0	0	100	100	0	100	001	001	0	100	100	100
% TEG in each row	,	m	0	0	100	100	100	0	75	100	801	100	0	001	100	001	100	0	25	100	100	0	100	100	001	25	100	100	100
8	[,	7	0	25	100	100	100	0	100	100	100	100	0	100	100	100	100	0	7.5	100	100	0	100	100	8	75	001	100	100
L		_ 	٥	20	100	100	100	0	100	100	100	100	25	100	100	100	100	0	100	100	100	20	100	100	100	001	100	100	100
E	I HI	္ဌာ	300	300	300	300	300	350	350	350	350	350	400	400	400	400	400	300	300	300	300	350	350	350	350	400	400	400	400
	m ^c ,	(kg/s)	0.1	0.2	0.3	0.4	0.5	0.1	0.2	0.3	4.0	0.5	0.1	0.2	0.3	0.4	0.5	0.3	0.3	0.3	0.3	0.3	0.3	0.3	0.3	0.3	0.3	0.3	0.3
	m,	(Kg/s)	0.1	0.2	0.3	0.4	0.5	0.1	0.2	0.3	4.0	0.5	0.1	0.2	0.3	0.4	0.5	0.1	0.2	4.0	0.5	0.1	0.2	0.4	0.5	0.1	0.2	9.4	0.5
	No		_	2	٣	4	Š	9	7	∞	6	10	11	12	13	14	15	16	17	82	19	20	21	22	23	24	25	56	27

Table 4. Results of simulation in the case of counter flow arrangement; inlet temperature of cold air ≈ 30 °C.

_		_								_				_			_								_			_
% increase	Relative to dowtherm A	82.66	176.24	220.70	54.09	57.29	102.76	167.03	50.03	54.50	57.68	106.36	166.20	50.81	55.27	58.45	133.11	192.47	154.16	92.46	135.00	187.72	52.27	53.74	136.89	47.00	53.03	54.49
% inc	Relative to TEG	52.86	93.49	114.37	0.00	00.0	54.75	86.47	0.00	0.00	0.00	26.77	84.92	0.00	0.00	0.00	69.59	100.63	67.38	25.51	70.50	96.76	0.00	00.0	71.02	0.00	0.00	0.00
	Edowiherm A (W)	5448	6684	7278	7635	7878	6452	7877	8555	8962	9237	7429	9023	9116	10225	10529	6133	6937	7470	7596	7262	8174	8770	8910	8362	9362	10008	10157
	25 25 25 25 25 25 25 25 25 25 25 25 25 2	7120	9543	10888	11765	12391	8453	11280	12836	13847	14566	9778	12989	14743	15877	16682	8430	10113	11344	11648	10009	11952	13354	13698	11582	13762	15314	15692
(CTEC-water (W)	10884	18465	23340	11765	12391	13081	21033	12836	13847	14566	15330	24019	14743	15877	16682	14296	20290	18987	14619	17065	23517	13354	13698	19808	13762	15314	15692
	9	0	0	20	001	100	0	25	100	001	100	0	75	8	100	100	0	0	001	001	0	25	100	001	0	100	100	001
*	5	0	0	20	100	100	0	25	001	100	001	0	75	100	100	100	0	0	81	100	0	20	901	100	•	100	100	100
each ro	4	0	0	20	100	100	0	25	100	001	100	0	75	100	100	100	0	0	001	100	0	20	100	100	0	100	100	100
% TEG in each row	8	0	0	50	001	100	0	25	9	100	100	0	75	100	100	100	0	25	75	100	0	20	001	100	0	001	100	100
%	7	0	0	20	100	100	0	25	100	001	801	0	20	001	100	001	0	25	75	100	0	7.5	100	100	25	100	100	100
	-	0	0	20	100	100	0	25	100	100	100	0	20	100	100	100	0	25	7.5	75	25	7.5	100	100	20	100	001	100
٤	(C) (C)	300	300	300	300	300	350	350	350	350	350	400	400	400	400	400	300	300	300	300	350	350	350	350	400	400	400	400
 -	mc (kg/s)	0.1	0.2	0.3	0.4	0.5	0.1	0.2	0.3	0.4	0.5	0.1	0.2	0.3	0.4	0.5	0.3	0.3	0.3	0.3	0.3	0.3	0.3	0.3	0.3	0.3	0.3	0.3
	/// (kg/s)	0.1	0.2	0.3	0.4	0.5	0.1	0.2	0.3	0.4	0.5	0.1	0.2	0.3	4.0	0.5	0.1	0.2	4.0	0.5	0.1	0.2	0.4	0.5	0.1	0.2	0.4	0.5
	No	-	~	~	4	Ś	9	7	••	0	10	11	12	- 13	14	15	16	17	18	61	20	21	22	23	24	25	56	27

Kiatsiriroat T., Nuntaphan A. and Tiansuwan J., Parameters Affecting Exergy Loss of Thermosyphon Air Preheater, The 6th International Heat Pipe Symposium, 5-9 November 2000, Chiang Mai, Thailand.

Parameters Affecting Exergy Loss of Thermosyphon Air Preheater

T. Kiatsiriroat

Department of Mechanical Engineering Chiang Mai University Chiang Mai Thailand 50202

A. Nuntaphan and J. Tiansuwan

School of Energy and Materials King Mongkut's University of Technology Thonburi Bangkok Thailand 10140

ABSTRACT

The parameters affecting the exergy loss of the thermosyphon air preheater was studied in this research work. The effect of the ratio of mass capacity flow rate, the inlet temperature ratio, the pipe arrangement and the flow direction had been considered as the parameters and the simulation program was used to calculate the exergy loss of the system. The dimensionless of exergy loss per dimensionless heat transfer rate formulated from the simulation program was used as the criteria for various conditions.

From the simulation program, it was found that the parallel flow and aligned array give more exergy loss than the counter current flow and staggered array respectively. Moreover it was found that the exergy loss per unit heat transfer vary in reverse direction with the ratio of mass capacity flow rate but directional to the inlet temperature ratio.

Key Words: Exergy analysis, Thermosyphon air preheater.

INTRODUCTION

At present, the second law efficiency of thermodynamic that used for evaluate the performance of the mechanical system has become interesting topic of a new research work. The entropy generation or the exergy loss is used as a scale to determine quantitatively the quality of thermal energy transformation.

Gool [1] used the exergy concept for analysis the industrial processes to find the exergy loss and the second law efficiency. Nikolaidis and Probert [2] studied the behavior of two-stage compound compression cycle, with flash intercooling, using R-22 by exergy method. Kotas and Jassim [3] and McGovern [4] analyzed the exergetic cost with the optimization

technique to find the suitable condition and size of the thermal system.

In the case of heat exchanger, normally the effectiveness is used as a parameter to determine the performance. However this quality gives very limited information on the quality of energy transformation in the system [5]. Consequently, in this research, the concept of second law efficiency of thermodynamic is applied to evaluate the performance of the thermosyphon air preheater. The thermosyphon air preheater is an economic type of heat exchanger because of its many advantages such as low investment cost, high thermal conductivity, no energy consumption and moving part. Normally this equipment is used to recover heat from the exhaust gas to produce hot air. So it can improve the performance of overall system.

THEORETICAL ANALYSIS

The method for analysis of exergy loss of Teke et al. [6] had been used in this research work and the details are as follow.

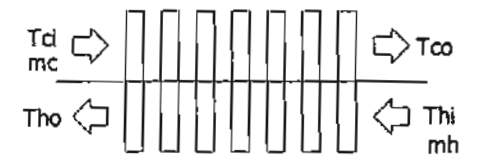


Figure 1 Flow direction of the thermosyphon air preheater.

Figure 1 shows the flow pattern of the thermosyphon air preheater and the exergy loss from the heat transfer is

$$E = T_0 \left[m_h C p_h \ln \left(\frac{T_{ho}}{T_{hi}} \right) + m_c C p_c \ln \left(\frac{T_{co}}{T_{ci}} \right) \right]$$

[1]

where E is the exergy loss of the air preheater. The effectiveness of the air preheater when the heat capacity flow rate of hot fluid is minimum, can be evaluated as

$$\varepsilon = \frac{\mathsf{T}_{\mathsf{h}\mathsf{i}} - \mathsf{T}_{\mathsf{h}\mathsf{o}}}{\mathsf{T}_{\mathsf{h}\mathsf{i}} - \mathsf{T}_{\mathsf{c}\mathsf{i}}} \qquad [2]$$

The inlet temperature ratio and the ratio of heat capacity flow rate is defined as

$$Tr = \frac{T_{hi}}{T_{ci}}$$
 [3]

$$Cr = \frac{m_h Cp_h}{m_c Cp_c}$$
 [4]

where Tr is inlet temperature ratio and Cr is heat capacity flow rate ratio. A dimensionless exergy loss and a dimensionless heat transfer rate are defined as

$$e = \frac{E}{m_h C p_h T_0}$$
 [5]

$$q = \frac{Q}{m_h C p_h T_{ci}}$$
 [6]

where e is a dimensionless exergy loss and q is a dimensionless heat transfer rate.

From equations 1-6 the dimensionless of exergy loss per dimensionless heat transfer rate can be evaluated as

$$\frac{e}{q} = \frac{\ln[1 - \varepsilon(1 - (1/Tr))] + (1/Cr)\ln[1 + \varepsilon Cr(Tr - 1)]}{\varepsilon(Tr - 1)}$$

where e/q is the dimensionless of exergy loss per dimensionless heat transfer rate. Higher e/q is mean that the irreversibility of system increases.

The simulation program had been constructed by the method of Nuntaphan et al. [7] to calculate the e/q at various conditions such as the inlet temperature, the flow pattern of the air preheater, the pipe arrangement and the mass flow rate of hot and cold streams.

EXPERIMENTAL SETUP

In this research work, the counter and parallel flow heat pipe air preheaters with staggered and aligned arrangement had been used to calculate the exergy loss per dimensionless heat transfer rate. Importance conditions of these heat exchangers are shown in Table 1.

RESULTS AND DISCUSSION

Figure 2 shows the relation between the dimensionless of exergy loss per dimensionless heat transfer rate (e/q) and the inlet temperature ratio (Tr) at various conditions of heat capacity flow rate ratio (Cr), pipe arrange and flow pattern.

From figure 2, it was found that the factor e/q vary with the inlet temperature ratio. It means that higher difference of inlet

temperature of hot and cold stream gives higher e/q. The increase of factor e/q indicates that the irreversibility of the system increase. In the case of the heat exchanger, the second low efficiency equals to unity in the reversible process. It means that no exergy loss. From equation 1, no exergy loss occurs when the inlet temperature of hot stream equals to the outlet temperature of cold stream and on the other hand the outlet temperature of hot stream equals to the inlet temperature of cold stream. Moreover the heat capacity flow rate ratio must equals to unity. These mean that there is no gap between the temperature profile of hot and cold stream. So, it can be concluded that the exergy loss can be reduced by reduce the gap of the temperature profile of both stream.

The effect of the inlet temperature ratio plays an important role on the factor e/q and the increase of this factor creates the enlargement of the temperature gap between hot and cold stream. Consequently, high e/q is obtained.

The same affect as the inlet temperature, the heat capacity flow rate ratio equals to unity give lowest factor e/q. Because the rate of flow can decreases the temperature gap of hot and cold stream. In the case of flow pattern, counter flow has lower factor e/q than parallel flow because of it nature of the flow pattern. Counter flow can reduces the temperature gap more efficiently than parallel flow. It means that the area between the two stream of counter flow is lower than that of parallel flow. However at low ratio of heat capacity flow rate, factor e/q of parallel flow is slightly higher than counter flow because the unbalance of the flow pattern.

The pipe arrangements have also affect to the factor e/q. Staggered array gives lower factor e/q than aligned array. Normally staggered array has high heat transfer rate than aligned array. Therefore, the temperature change of both streams is greater than that of aligned array and it means that the gap of temperature or both

streams is reduced and the irreversibility of system is decreased.

CONCLUSION

The exergy loss of the thermosyphon air preheater can be decreased by reduce the temperature gap of hot and cold stream. The increase in the inlet temperature different and decrease the heat capacity flow rate bring to enlarge this temperature gap and high exergy loss is obtained.

The counter flow air preheater has lower exergy loss than that of parallel flow because of it's more efficiently transfer of heat and the area of gap between two streams is lower than that of parallel flow. The staggered array arrangement of pipe in the thermosyphon air preheater give lower exergy loss than that of aligned arrangement because of its high efficiency of heat.

ACKONWLEDGEMENT

The Authors gratefully acknowledge the support provided by the Thailand Research Fund for carrying out this study.

NOMENCLATURE

Cp = specific heat (J/kgK)

Cr = heat capacity flow rate ratio

e = dimensionless exergy loss

E = exergy loss (W)

T = temperature(K)

 $T_0 =$ ambient temperature (K)

Tr = inlet temperature ratio

q = dimensionless heat transfer

rate

Q = heat transfer rate (W)

Subscripts

c = cold stream

h = hot stream

m = mass flow rate (kg/s)

Greek symbol

 ε = effectiveness

i = inlet

o = outlet

REFERENCES

- Gool W.V., "Exergy Analysis of Industrial Processes", J. of Energy, Vol.17, No.8, P.791-803, 1992
- Nikolaidis C. and Probert D., "Exergymethod Analysis of a Two-stage Vaporcompression Refrigeration-plants Performance", Applied Energy, Vol.60, P.241-256, 1998
- Kotus T.J. and Jassim R.K., "Cost of Exergy Flows in the Thermodynamic of Optimisation of the Geometry of Rotary Regenerators", Energy Systems and Ecology, Cracow Poland, July 5-9, 1993
- 4. McGovern J.A., "Exergetic Cost Analysis of a Mechanical Exergy

- Recycle", Energy Systems and Ecology, Cracow Poland, July 5-9, 1993
- Sekulic D.P., "The Second Law Quality of Energy Transformation in a Heat Exchanger", J. of Heat Transfer, Vol.112, P.295-300, 1990
- Teke I., Kincay O. and Temir G., "Determination of Economic Heat Exchanger Type According to Exergy Loss", Energy Systems and Ecology, Cracow Poland, July 5-9, 1993
- Nuntaphan A., Tiansuwan J. and Kiatsiriroat T., "Performance Analysis of Thermosyphon Air Preheater with Variable Heat Transfer Coefficient", 14th National Mechanical Engineering Conference, Chiang Mai Thailand, 2000

Table 1 Testing condition of heat exchangers.

Items	Conditions
Flow arrangement	Parallel and counter flow
2. Thermosyphon arrangement	
Staggered array	$S_t = 0.053 \text{ m}, S_d = 0.053 \text{ m}, S_1 = 0.046 \text{ m}$
Aligned array	$S_t = 0.053 \text{ m}, S_1 = 0.053 \text{ m}$
3. Number of tube row	7
4. Number of column	7
5. Diameter of thermosyphon (bare tube)	0.027 m
6. Length	
Evaporator section	0.4 m
Condenser section	0.4 m
Adiabatic section	0.2 m
7. Type of fin	Circular fin
8. Size of fin	Fin height $= 0.1 \text{ m}$
	fin pitch = 10 fins/inch
9. Filling ratio of working fluid	50%
10. Material of pipe and fin	Stainless steel 304

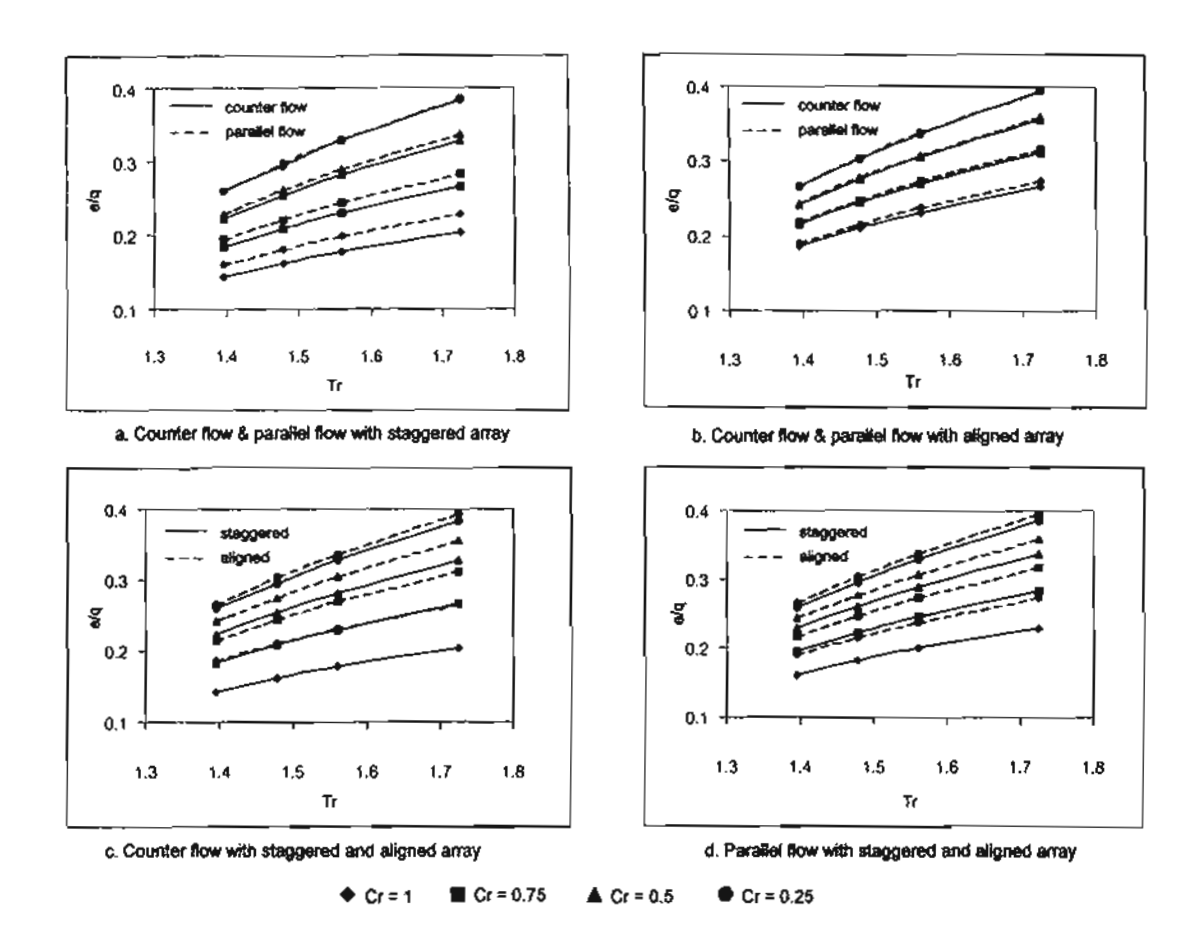


Figure 2 The dimensionless of exergy loss per dimensionless heat transfer rate at various working conditions of the thermosyphon air preheater.

5. Nuntaphan A., Pearce K. and Kiatsiriroat T., Second Law Analysis of a Thermosyphon Air Preheater with Binary Mixtures, **The 6th Tri-University International Joint Seminar & Symposium**, October 1999, Jiansu University of Science and Technology, China PRC.

SECOND LAW ANALYSIS OF A THERMOSYPHON AIR PREHEATER WITH BINARY MIXTURES

A. Nuntaphan School of Energy and Materials King Mongkut's University of Technology Thonburi Bangkok Thailand

K. Pearce Dept. of Chemical Engineering Melbourne University Melbourne Australia

T. Kiatsiriroat Dept. of Mechanical Engineering Chiangmai University Chiangmai Thailand ABSTRACT Performance of different binary working fluids in a thermosyphon heat exchanger has been considered by evaluating the 2nd law efficiency. The binary working fluids used are ethanol-water and TEG.-water and the heat exchanger is designed as an air preheater of a longan dryer; ambient air is considered as the cold stream and the flue gas from the dryer as the hot stream. The performances have been compares with that of pure water.

It was found that the ethanol-water working fluid resulted in the highest second law efficiency. An efficiency of 0.34 was found at 57 rows for the 19.05 mm. thermosyphon size, and at 90 rows for the 12.7 mm. thermosyphon size at a flue gas temperature of 80°C.

1. INTRODUCTION

A longan dryer is used to removed moisture from longan, an important fruit of Thailand. Normally consumes a lot of thermal energy. To save such energy, a heat exchanger is designed to recover waste heat from the dryer by using the exhaust flue gas from the dryer is the input hot stream which ranges from 60-80°C. The cold stream gas is the ambient air ranging 25-40°C.

A thermosyphon heat exchanger is used to recover the waste heat. The simple working fluid inside is water. However, there is an idea to improve the heat exchanger by using binary mixture and the fluid pairs of ethanolwater and TEG.-water have been selected. In this paper, comparison of the heat exchanger performance of the binary mixtures with the pure water have been carried out and the second law efficiency is the tool to estimate the system.

2. THERMOSYPHON HEAT EXCHANGER

2.1 The Longan Dryer

Longan is an important fruit of Thailand. In order to increase the life of the fruit, and decrease the weight and volume of the fruit for storage and handling they are often dried. A direct dryer is usually used to dry the whole fruit, outer skin and seed included. Ambient air is usually combusted with LPG and the resulting hot gas passed directly over the longans.

In order to conserve energy the flue gas ranges of about 60-80°C from the dryer may be used to pre-heat ambient air of about 25-40°C before it is combusted with LPG.

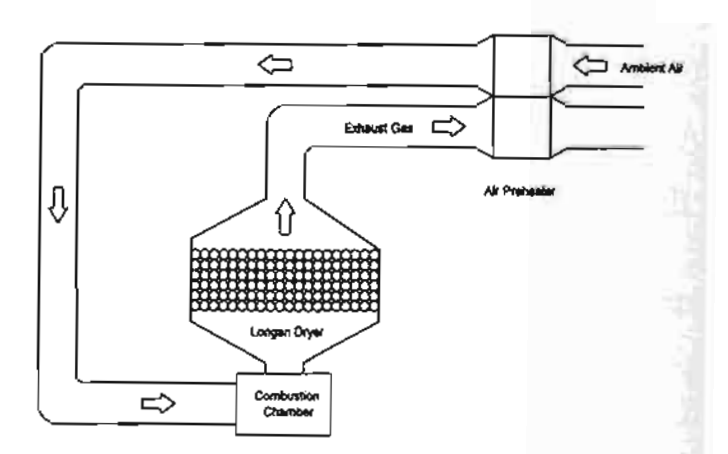


Fig. 1 The longan drying process and air preheater

2.2. Principals of Thermosyphon

A thermosyphon is a heat transfer device that utilizes the high heat transfer ability of boiling and condensation process. A small quantity of working fluid is placed in the bottom of a tube from which air has been evacuated. The tube is then sealed. Heat is applied to the lower end of the tube, causing vapor to form and move up to the cold end where it is condensed. The condensed liquid returns via gravity to the evaporator section. Because the latent heat of vaporization is large considerable quantities of heat may be transported with a small temperature difference. A thermosyphon has high effective thermal conductance.

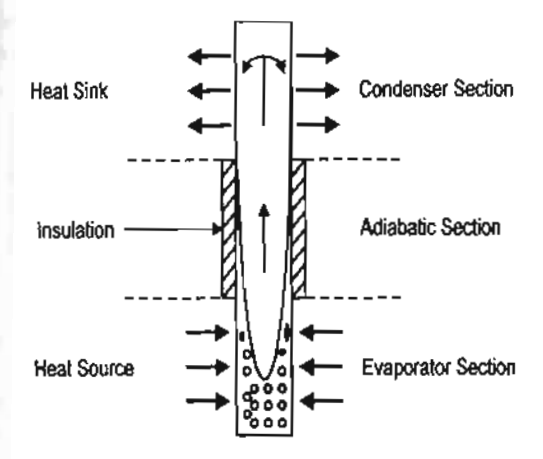


Fig. 2 Thermosyphon

2.3. Internal Resistance in Thermosyphon

In order to determine the amount of heat transferred through a heat pipe, the resistance in the heat pipe must be determined.

The internal resistance of the heat exchanger incorporates the boiling and condensing heat transfer resistance, an axial resistance, vapor/liquid interface resistance and pressure drop resistance and the wall resistance in the evaporator and condenser sections of the thermosyphon.

Experimental data tests were carried out on a single thermosyphon. The thermosyphon had cooling water flowing over the condenser section and the evaporator section was heated by a hot oil bath. The temperature of the oil bath, the evaporator wall, the inlet and outlet cooling water temperatures and the temperature of the condenser wall were measured. These were used to determine the internal resistance of the thermosyphon.

An energy balance over the condenser section enables Q, the heat transferred to be determined.

$$Q = m_w C_{pw} \Delta T_w$$
 (1)

This could then be used to determine internal thermal resistant of heat pipe from

$$R_{in} = \frac{\left(T_{ev} - T_{ed}\right)}{Q} \tag{2}$$

Where T_{ev} and T_{ed} are surface temperature of heat pipe at evaporator and condenser section respectively.

The relations between internal resistance and log mean temperature difference for ethanol-water, TEG.water and water are shown in equation 3 and table 1.

$$R_{in} = a(LMTD) + b (3)$$

Table 1 The values of a and b in equation 3

Substant	a	b
water (d = 12.7 mm.)	-0.0160	1.5798
ethanol-water (d = 12.7 mm.)	-0.0010	0.2195
TEGwater (d= 12.7 mm.)	-0.0100	1.2453
water (d = 19.05 mm.)	-0.0047	0.4989
ethanol-water (d = 19.05 mm.)	-0.0013	0.1774
TEGwater (d= 19.05mm.)	-0.0060	0.6353

2.4 Heat Exchanger Configuration

The heat exchanger was assumed to be of a staggered, counter-current configuration. The spacing between thermosyphons was set at 0.023m, in the direction of flow and perpendicular to the direction of flow.

The benefits of a thermosyphon heat exchanger over a the standard heat exchangers is that there is no opportunity for cross-contamination, there are no moving parts required, the design is compact, there is no need for an external energy supply and they have low maintenance and operating costs.

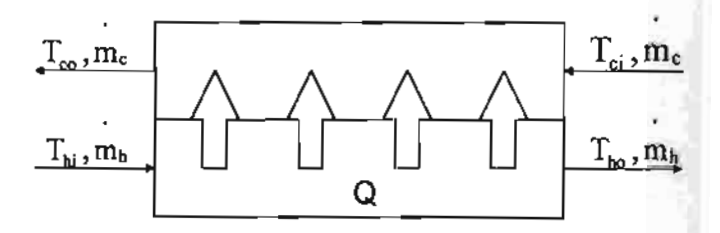


Fig 3 Counter-current Thermosyphon Heat Exchanger Configuration

2.5 Second Law Efficiency

The first law of thermodynamics states that energy must always be conserved. The concept of first law efficiency relates to minimizing energy losses from a process. In the case of a heat pipe the energy losses are minimal and the first law efficiency can be taken as 100%.

The second law of thermodynamics states the entropy of an isolated system cannot decrease. Thus, although energy must always be conserved, a given amount of energy will not always have the same potential for use. Potential for use or availability of a system can be destroyed by irreversibility. Irreversibility of a system may be due to a finite temperature difference, pressure differences and friction. In the case of a heat exchanger the main factor is that of minimizing the temperature difference.

The 2nd law efficiency uses the concept of availability in assessing the effectiveness of energy resource utilization. By comparing the second law efficiency obtained for various designs the most thermodynamically effective use of energy can be determined.

In a counter-current heat exchanger as considered here and assuming the pressure drop over the length of a heat pipe is negligible, the second law efficiency can be evaluated as

$$\varepsilon = \frac{\dot{m}_{c} \left(C_{pc} (T_{co} - T_{ci}) - T_{amb} C_{pc} \ln(\frac{T_{co}}{T_{ci}}) \right)}{\dot{m}_{h} \left(C_{ph} (T_{hi} - T_{ho}) - T_{amb} C_{ph} \ln(\frac{T_{hi}}{T_{bo}}) \right)}$$
(4)

2.6 External Resistance

The external resistance over the evaporator and condenser are evaluated according to convective heat transfer relations for the flow over a bank of tubes.

$$R_{ev,o} = 1 / (h_{ev,o} A_{ev,o})$$
 (5)

$$R_{cd,o} = 1/(h_{cd,o}A_{cd,o})$$
 (6)

The average heat transfer coefficient for the entire tube bundle can be found using the correlation

$$Nu = C_1 Re_{max}^m$$
 (7)

Where C₁ and m are empirical constants. This equation is valid for flow over 10 or more rows of tubes.

2.7 Simulation Program

Determination of the 2nd law efficiency was conducted using the Turbo Pascal computer program. A flow chart of input data and calculations is shown in the appendix

3. RESULT AND DISCUSSION

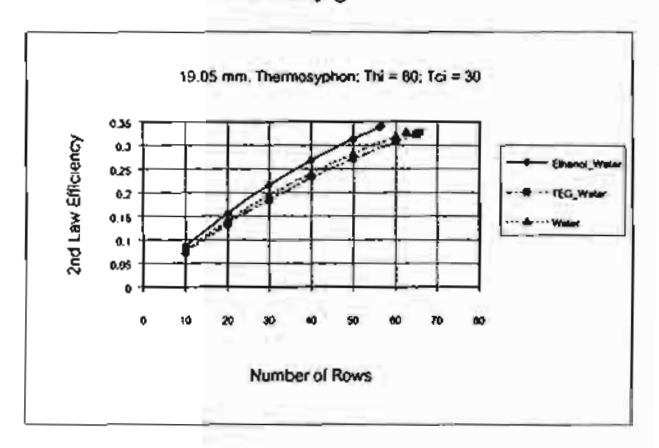
From the simulation program it is found that, as the number of rows was increased the resulting change in outlet temperatures was found to reduce until the addition of another row did not produce a significant change in temperature. At this point the second law efficiency plateaus, and the maximum obtainable second law efficiency is found.

Ethanol-water was found to be the better working fluid in the thermosyphons considered (Refer to Fig. 4). It produced the highest efficiency for the lowest number of rows in both the 19.05 and 12.7 mm. thermosyphon heat exchangers. The efficiency was found to plateau at a value of 0.34 in both cases. The number of rows required was 57 for the 19.05mm, and 89 for the 12.7 mm. at a flue gas temperature of 80° C, and ambient air temperature of 30°C.

The difference in performance between TEG-water and pure water was found to be minimal (Refer to Fig. 4). In addition to this TEG has a high boiling point and under the conditions of operation this component was probably not vaporizing. Hence the TEG-water mix was seen to behave in a similar way to the water.

A plot of the temperature profile for ethanol-water heat exchanger and pure water heat exchanger are shown in Fig. 5. From this it can be seen using the ethanol-water binary mixture reduces the temperature difference between the hot and cold streams. This in turn reduces the irreversibility of the system and increases the second law efficiency.

Because Ethanol has a lower boiling point than water the ethanol water mixture boils at a lower temperature. As the liquid is vaporized the pressure in the tube increases. In the case of ethanol-water more vapor is formed and therefore the pressure in the tube is greater than the pure water thermosyphon. As a result of this the ethanol-water vapor is able to condense at a lower temperature. The effect of this is that the temperature difference are lower for the ethanol-water mixture and hence the 2nd Law efficiency greater.



12.7 mm Thermosyphon; Thi = 80; Tci = 30

a

Fig. 4 Effect of number of rows on 2nd law efficiency

b

The two different thermosyphon sizes resulted in large differences in the number of rows required (Refer to Fig. 6). This difference is expected as the heat transfer surface area of the 19.05 mm. thermosyphon is 0.09 m² compared with 0.06 m² for the 12.7 mm. thermosyphon. Therefore a 33% increase in the number of rows can be expected. The choice of a 19.05 mm. thermosyphon is preferable, as capital investment cost would be lower for this sized thermosyphon.

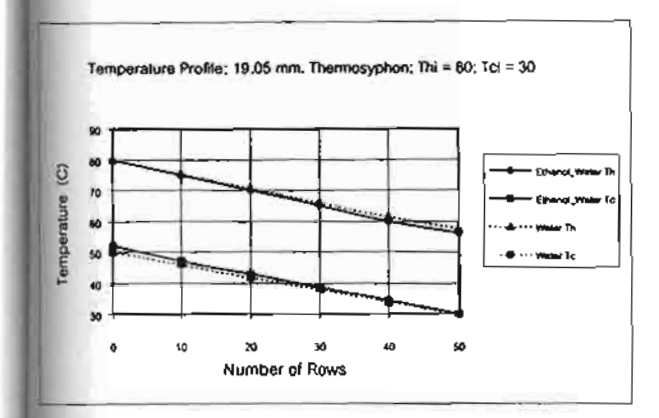


Fig. 5 Temperature profile along the heat exchanger

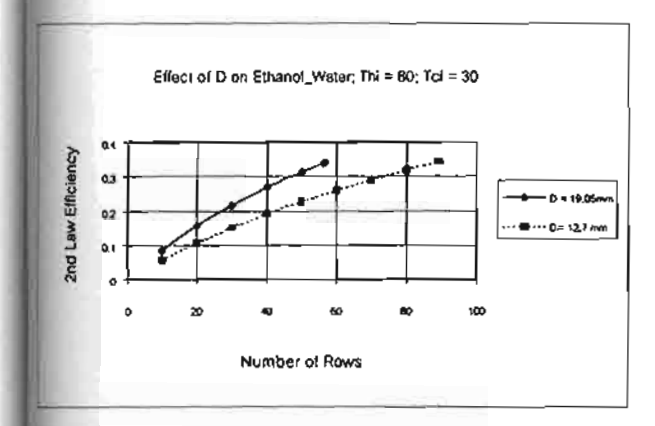


Fig. 6 Effect of diameter on the the 2nd law efficiency

4. CONCLUSION

It was found that the ethanol-water working fluid resulted in the highest second law efficiency. The use of ethanol-water reduced the temperature difference throughout the heat exchanger compared to the other working fluids; a reduction in a the temperature difference corresponds to a decrease in the irreversibility and an increase in the 2nd law efficiency. An efficiency of 0.34 was found at 57 rows for the 19.05 mm. thermosyphon size, at a flue gas temperature of 80°C and ambient air temperature of 30°C.

5 ACKNOWLEDGMENT

The Authors gratefully acknowledge the partial support provided by the Thailand Research Fund for carrying out this study.

6. REFERENCES

- Moran, M.J., Shapiro, H.N, "Fundamentals of Engineering Thermodynamics," 2nd Edition, 1993, John Wiley & Sons Inc., USA
- Incropera, F.P., De Witt, D.P., "Fundamentals of Heat and Mass Transfer," 3rd Edition, 1990, John Wiley & Sons, Inc., USA.
- Bejan, A., "Entropy Generation Minimization; The Method of Thermodynamic Optimization of Finite-

- Sized Systems and Finite-Time Processes," CRC Press.
- Wadowski, T., Akbarzadeh, A., Johnson, P., "Characteristics of Gravity-Assisted Heat Pipe based Heat Exchanger," Heat Recovery Systems and CHP, Volume 2, pp 69-77, 1991, Peragon Press, Great Britain.

7. NOMENCLATURES

7. NOME	NCL	ATURES
A	=	Area (m²)
C_{p}	=	Specific heat (J/kg-K)
LMTD	=	Log mean temperature difference
m'	=	Mass flow rate (kg/s)
Q	=	Heat transfer rate (W)
R	=	Thermal resistant (K/W)
Re	=	Reynold's Number
Υ	=	Temperature (°C)
Subscript		
amb	=	Ambient
С	÷	Cold
cd	=	Condenser
ev	=	Evaporator
h	=	Hot
i	=	Inlet
in	=	Inside
0	=	Outlet
w	=	Water
Greek Sym	ibol	
e =		2 nd Law Efficiency

BIODATA

Α	utho	r l
м	umo	ŗj

Name Mr. Atipoang Nuntaphan M.Eng.

Ph.D. Student

Thermal Technology Division School of Energy and Materials

KMUTT

Date of birth 15 October 1971

Author 2

Name Ms. Kristie Pearce

Undergraduate student

Dept. of Chemical Engineering

Faculty of Engineering Melbourne University

Author 3

Name Mr. Tanongkiat Kiatsiriroat D.Eng.

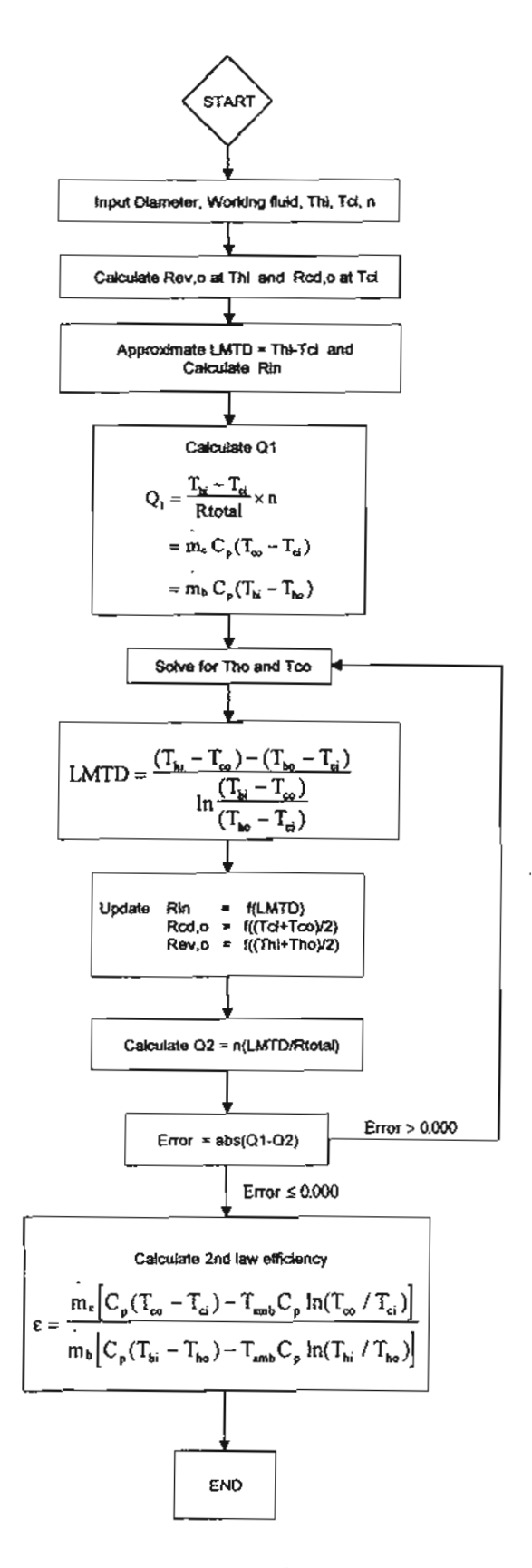
Professor

Dept. of Mechanical Engineering

Faculty of Engineering Chiangmai University

Date of birth 22 January 1955

APPENDIX



Simulation flowchart

Nuntaphan A., Tiansuwan J. and Kiatsiriroat T., Heat Transfer Coefficients of Thermosyphon Heat Pipe at Medium Operating Temperature, The 1st Regional Conference on Energy Technology Toward a Clean Environment, 1-2 December 2000, Chiang Mai, Thailand.

Heat Transfer Coefficients of Thermosyphon Heat Pipe at Medium Operating Temperature

A. Nuntaphan 1, J. Tiansuwan 1 and T. Kiatsiriroat 2

- School of Energy and Materials, King Mongkut's University of Technology Thonburi, Bangkok 10140, Thailand
- 2. Department of Mechanical Engineering, Chiang Mai University, Chiang Mai 50202, Thailand

Abstract

This research work studied the heat transfer coefficient of thermosyphon heat pipe at medium operating temperature. The pipe is 100 cm stainless steel tube with 40 cm evaporator and condenser sections and 20 cm for adiabatic section. Hot oil bath and cooling water are used as heat source and heat sink respectively. Nine points of thermocouples are inserted into the pipe for measuring inside temperatures along the thermosyphon and the other nine points also for measuring the surface temperature at the same positions. Water, ethanol, methanol and acetone are used as working fluids with 50% filling ratio. The hot oil temperature is varied from 40-120°C and the temperature of cooling water is kept at 30°C at constant flow rate. The measured inlet and outlet temperatures of cooling water are used to calculate the heat transfer rate of the thermosyphon.

From the experiments it is found that when the hot oil temperature is less than 60°C, the heat transfer rate of water is lower than those of other working fluids. However at higher temperature heat source, the heat transfer rate of water is the best. Boiling Equation of Rohsenow is modified to predict the boiling heat transfer coefficient of the thermosyphon at various types of working fluids. For the condenser section, it is found that modified Nusselt correlation of condensation agrees well with the experiments.

Introduction

The thermosyphon heat pipe, one type of heat exchanger, at present, plays an important role in the energy conservation program because of its good advantages such as high thermal conductivity, low operating cost and easy to construct. Figure 1 shows the schematic picture of the operating thermosyphon. When heat is added to the evaporator section, the working fluid inside the thermosyphon is boiled, vaporized and then the vapor flows to the condenser section where the condensation process occurs and rejects heat to the outside of the thermosyphon.

Because the heat transfer of the thermosyphon deals with boiling and condensation inside a tube, it is important to know the heat transfer coefficient of both processes. Many researches have been done to find the correlations to predict these phenomena. ESDU [1] collected many data and correlations of both boiling and condensation inside the thermosyphon and proposed these new correlations in term of the thermal resistance as follows:

Boiling

$$Z_b = Z_{pool}F + Z_{film}(1 - F), \qquad [1]$$

where

$$Z_{\rm film} = \frac{0.235 Q^{1/3}}{D^{4/3} g^{1/3} L_e \phi_1^{4/3}}, \quad Z_{\rm pool} = \frac{1}{\phi_2 g^{0.2} Q^{0.4} (\pi D L_e)^{0.6}},$$

$$\phi_1 = \left(\frac{\lambda k_i^3 \rho_i^2}{\mu_i}\right)^{0.25}, \quad \phi_2 = 0.32 \frac{\rho_i^{0.55} k_i^{0.3} C_{pi}^{0.7}}{\rho_a^{0.25} \lambda^{0.4} \mu_i^{0.1}} \left[\frac{P_v}{P_a}\right]^{0.23},$$

Condensation

$$Z_{cd} = \frac{0.235Q^{1/3}}{D^{4/3}g^{1/3}L_{cd}\phi_1^{4/3}}$$
 [2].

Although the correlation of ESDU can be used with in high operating range and various type of working fluid, however in some conditions, especially at low operating temperature, the use of ESDU correlations may give some errors. Shiraishi et al [2] found that at low operating temperature (32-60°C) equations 1 and 2 can predict the heat transfer coefficient of the thermosyphon within 70-150% of the experimental values. Hahne and Gross [3] found that at a working temperature between 37-76°C, the correlations of ESDU give a lower prediction of the heat transfer coefficient (31-76% for boiling and 46-86% for condensation).

At present there are attempt to use the thermosyphon to recover waste heat from agricultural industries in Thailand. The heat source is normally lower than 80°C. Therefore using correlations of ESDU may be give some error for predicting the heat transfer coefficient. In this research, correlations of boiling and condensation heat transfer coefficients have been reconstructed to predict the heat transfer rate of the thermosyphon heat exchanger at medium operating temperature with some common working fluids such as water, ethanol, methanol and acetone.

Materials and Methods

1. Experimental Setup

Figure 2 shows the schematic diagram of the experimental setup. Stainless 304 with 27 mm diameter, 2 mm thickness and 1 m length has been used as the thermosyphon heat pipe. This tube can be divided into 3 parts, 40 cm for evaporator, 20 cm for adiabatic section and 40 cm for condenser section. Nine K-type thermocouples are inserted into the thermosyphon for measuring inside temperatures at the length 5, 15, 25, 35, 50, 65, 75, 85 and 95 cm from the evaporator end. The other nine thermocouples are attached at the outside surface of the thermosyphon at the same positions of the inside measurement. The hot paraffin oil bath controlled by the electric heater is used as the heat source of the thermosyphon and the injection of bubble air into the hot oil is also used to make well mix of hot oil temperature. At the condenser section, there is a stream of cooling water to remove heat out of the thermosyphon. The flow rate of cooling water is kept constant at 0.0057 kg/s by the constant head tank at normal temperature (approximately 30°C). The inlet and outlet temperatures of cooling water are measured by the thermocouples to calculate the heat transfer rate of the thermosyphon.

Four types of common working fluids, water, ethanol, methanol and acetone, have been used with 50% filling ratio of the evaporator section.

2. Analysis

The heat transfer rate of the thermosyphon can be calculated as

$$Q = m_w C_{pw} (T_{wo} - T_{wt})$$
 [3].

The boiling and condensation heat transfer coefficient can be calculated as

$$h_b = \frac{Q}{A_{ei}\Delta T_e} \tag{4}$$

$$h_{cd} = \frac{Q}{A_{cdi} \Delta T_{cd}}$$
 [5]

where h_b and h_{cd} are the heat transfer coefficient of the evaporator and condenser respectively.

Rohsenow equation [4] is modified to predict the boiling heat transfer coefficient of the thermosyphon by find the new empirical constant as follow

$$Nu = C_1 Re^{C_2} Pr^{C_3}$$
 , [6]

where

$$Nu = \frac{h_b}{k_i} \left[\frac{\sigma}{g(\rho_i - \rho_g)} \right]^{1/2}, \quad Re = \frac{q}{\lambda \rho_i} \left[\frac{\sigma}{g(\rho_i - \rho_g)} \right]^{1/2} \frac{\rho_i}{\mu_i},$$

$$Pr = \frac{C_\rho \mu_i}{k_i}.$$

In this work factor C_3 was set as 0.40 [5].

For the condenser section, the modified heat transfer coefficient of Nusselt [4] has been used to calculate the heat transfer coefficient as

$$h_{cd} = C_4 \left(\frac{\rho_l (\rho_l - \rho_g) g k^3 \lambda}{\mu_l L_{cd} \Delta T_{cd}} \right)^{C_5}$$
 [7]

 ΔT_{cd} is the temperature difference between inside surface and inside temperature of the condenser section.

Results and Discussion

Figure 3 shows the heat transfer rate of the thermosyphon heat pipe, using water, ethanol, methanol and acetone at various temperatures of hot oil. From this Figure it is found that when the temperature is lower than 60°C, the heat transfer rate of water is lower than that of ethanol, methanol and acetone and the heat transfer rate of ethanol, methanol and acetone is slightly difference. These phenomena come from the higher boiling point of water and its difficulty to boil at this condition. However when the temperature is higher than this point, water can boil and the heat transfer rate of water higher than those of other working fluids because of high latent heat of the vaporization of water. The heat transfer rate of methanol and ethanol are the same at this range since the physical properties of these working fluids are slightly difference. However the heat transfer rate of acetone is lower than the other working fluids because of its very low latent heat of vaporization.

Figure 4 shows the comparison between the experimental and calculated data of the Nusselt number of boiling modified from the Rohsenow equation. It was found that the new correlation, with the correlation coefficient shown in Table 1 can predict 96.3% of the experimental value with in ±20%. Figures 5a and b show the comparison of Nusselt number of boiling of water and ethanol at various temperature of working fluid with the previous work [6]. It is found that, for water, when the temperature of working fluid lower than 50°C, the Nusselt number drop drastically with the reduction of working fluid temperature. However when the temperature more than 50°C the Nusselt number is comparatively constancy since the nucleate boiling of water has occurred. In case of boiling of ethanol inside the thermosyphon, it is found that the result from the present correlation agree well with Kiatsiriroat et al. correlation [6] because at this temperature range the ethanol can be boiled easily.

Table 1 The correlation coefficient C₁, C₂, C₄ and C₅

Working Fluids	C ₁	C ₂	Ċ ₄	C ₅
Water	41.27	0.37	0.94	0.245
Ethanol	14.64	0.15	0.94	0.275
Methanol	24.09	0.20	0.96	0.270
Acetone	27.44	0.22	0.95	0.280

For the condensation heat transfer coefficient it is found that modified Nusselt equation of condensation can predicts 73.6% of the experimental data within $\pm 30\%$ and Figure 6 also shows this results. Moreover it is found that the correlation constants C_4 and C_5 shown in Table 1 are slightly difference from the former Nusselt correlation, which equal to 0.943 and 0.25 respectively.

Conclusions

From the experiment it can be concluded that;

- 1. When the temperature of hot oil is lower than 60°C the heat transfer rate of water is lower than those of the other working fluids because of higher boiling point of water.
- 2. As the temperature of hot oil is over 60°C the heat transfer rate of water is the best because of its very high latent heat of vaporization.
- 3. Modified boiling equation of Rohsenow can predict 96.3% of the Nusselt number of boiling inside the thermosyphon with in ±20%.
- 4. Modified Nusselt equation of condensation can predict 73.68% of the condensation heat transfer coefficient inside the thermosyphon with in ±30%.

Acknowledgement

The authors gratefully acknowledge the support provided by Thailand Research Fund for carrying out this study.

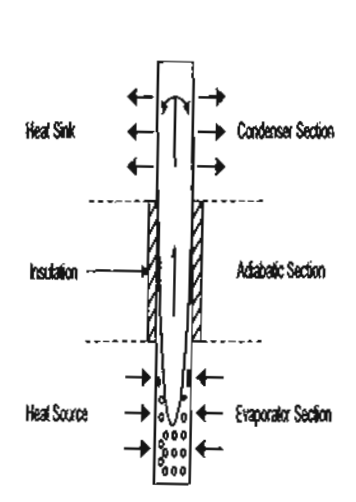
References

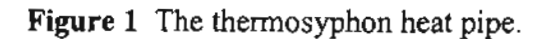
- [1] Engineering Sciences Data Unit Item Number 81038, "Heat Pipes- Performance of Two-Phase Closed Thermosyphons", (1983)
- [2] Shiraishi M., Kikuchi K. and Yamanishi T., "Investigation of Heat Transfer Characteristics of a Two-Phase Closed Thermosyphon", Advances in Heat Pipe Technology: IV International Heat Pipe Conference, London, September 1981, Pergamon Press, Oxford, (1982)
- [3] Hahne E. and Gross U., "The Influence of the Inclination Angle on the Performance of a Closed Two-Phase Thermosyphon", Advances in Heat Pipe Technology: IV International Heat Pipe Conference, London, September 1981, Pergamon Press, Oxford, (1982)
- [4] Collier J.G. and Thome J.R., "Convective Boiling and Condensation", 3rd edition, Clarendon Press, Oxford, (1994)
- [5] Gilmour C.H., "Nucleate boiling-a correlation", Chemical Progress Vol. 54, October (1958)
- [6] Kiatsiriroat T., Nuntaphan A. and Tiasuwan J., "Thermal Performance Enhancement of Thermosyphon Heat Pipe with Binary Working Fluids", Experimental Heat Transfer, Vol.13, p137-152, (2000)

[7] Engineering Sciences Data Unit Item Number 80017, "Thermophysical Properties of Heat Pipe Working Fluids: Operating Range Between -60°C and 300°C", (1983)

Nomenclatures

A	area, m ²	T	temperature (°C)
C_{1-5}	empirical constants	\boldsymbol{z}	thermal resistance, °C/W
C_{ρ}	specific heat, J/kg°C	Greel	k symbols
\vec{D}	diameter of tube, m	ϕ	function
F	filling ratio of working fluid	à	latent heat of vaporization, J/kg
g	gravitational acceleration,	μ	dynamic viscosity, Pa s
	9.81 m/s^2	ρ	density, kg/m ³
h	heat transfer coefficient, W/m ² °C	σ	surface tension, N/m
\boldsymbol{k}	thermal conductivity, W/m °C	Subsc	
L	length, m	a	ambient
m	mass flow rate, kg/s	ь	boiling
Nu	Nusselt number	cd	condenser, condensation
\boldsymbol{P}	pressure, Pa	e	evaporator
Pr	Prandtl number	film	film boiling
\boldsymbol{q}	heat flux, W/m ²	g	gas
Q	heat transfer rate, W	i	inlet, inside
Re	Reynolds number	1	liquid
ΔT_{cd}	temperature difference between	0	outlet, outside
	inside surface and liquid at	pool	pool boiling
	condenser section, °C	\$	surface
ΔT_e	temperature difference between	ν	vapour
	inside surface and liquid at	w	water
	evaporator section, °C		





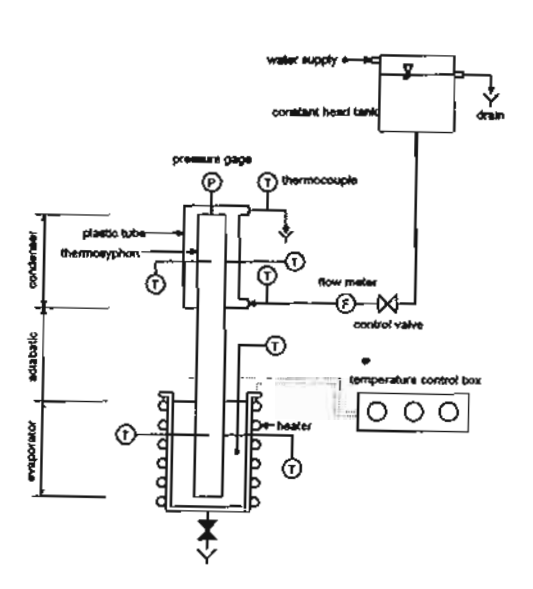
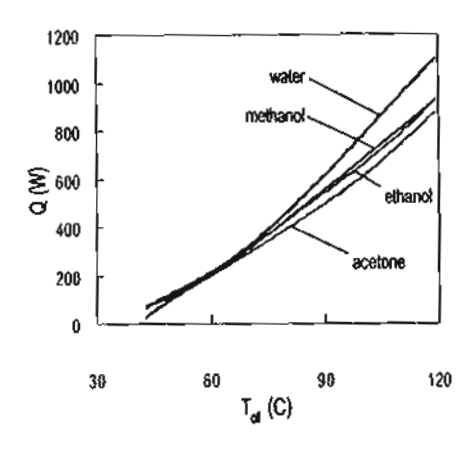


Figure 2 The experimental setup.



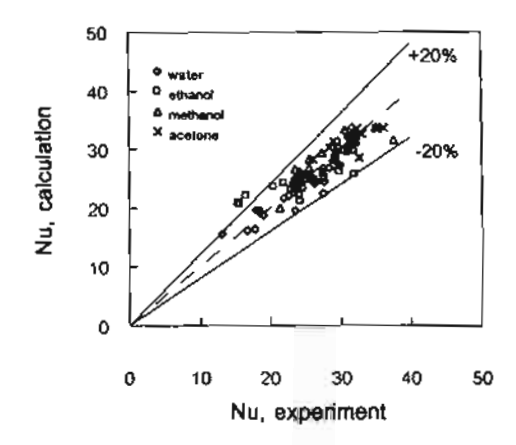


Figure 3 Variation of heat transfer rate of various kinds of working fluids with hot oil temperature.

Figure 4 Comparison of Nusselt number of boiling inside the thermosyphon between the experimental and calculation data.

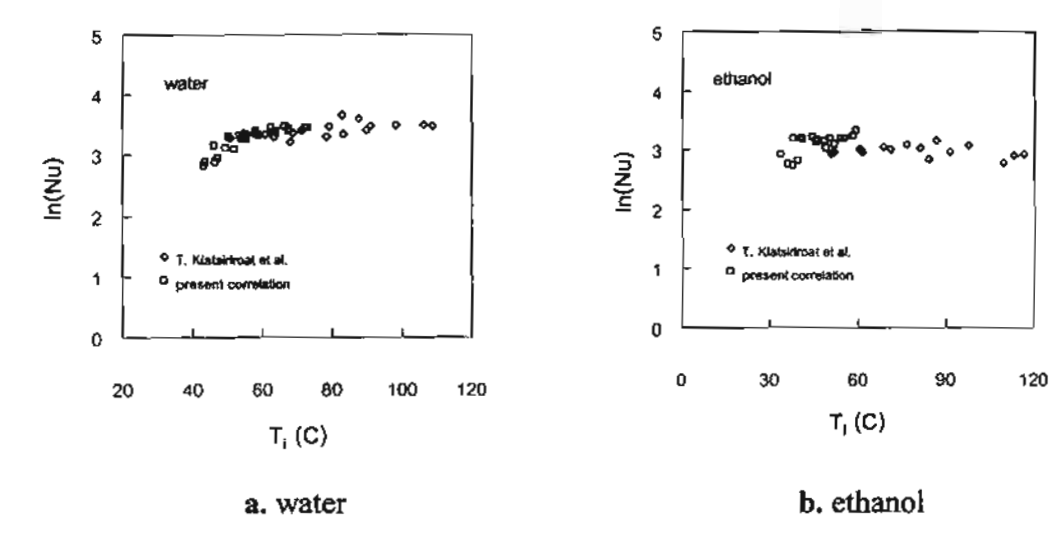


Figure 5 Comparison of Nusselt number of boiling of water and ethanol between present correlation and Kiatsiriroat et al. correlation.

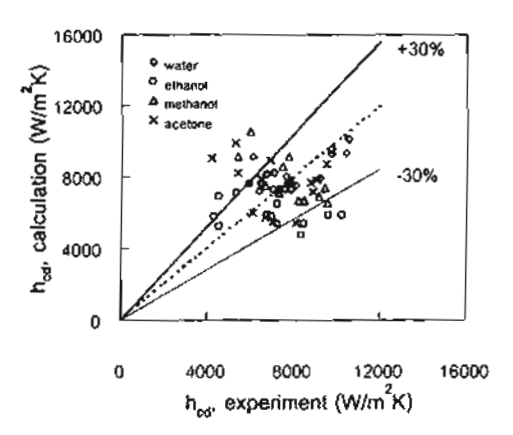


Figure 6 Comparison of condensation heat transfer coefficients inside the thermosyphon between the experimental and calculation data.

อดีพงศ์ นันทพันธุ์, จิรวรรณ เตียรถ์สุวรรณ และ ทนงเกียรติ เกียรติศิริโรจน์, การวิเกราะห์พฤติกรรมทางความ ร้อนของท่อความร้อนแบบเทอร์ โม ไซฟอนที่ใช้สารทำงานคู่ผสม, **สัมนาวิชาการวิศวกรรมเครื่องกลแห่งประเทศ** ไทยครั้งที่ 13, 2-3 ชันวาคม 2542, ชลบุรี.

สัมนาวิชาการวิศวกรรมเครื่องกลแห่งประเทศไทยครั้งที่ 13 2-3 ชันวาคม 2542 โรงแรม รอยัลคลิฟป์ชรีสอร์ท พัทยาใต้ ชลบุรี

การวิเคราะห์พฤติกรรมทางความร้อนของท่อความร้อนแบบเทอร์โมไซฟอน ที่ใช้สารทำงานคู่ผสม

Thermal Behavior Analysis of Thermosyphon Heat Pipe Using Binary Working Fluids

อดีพงศ์ นันทพันธุ์, จิรวรรณ เตียรก์สุวรรณ คณะพลังงานและวัสดุ มหาวิทยาลัยเทคโนโลยีพระจอมเกล้าธนบุรี กรุงเทพมหานคร 10140 ทนงเกียรติ เกียรติศิริโรจน์ ภาควิชาวิศวกรรมเกรื่องกล มหาวิทยาลัยเชียงใหม่ เชียงใหม่ 50200

Atipoang Nuntaphan, Jirawan Tiansuwan
School of Energy and Materials King Mongkut's University of Technology Thonburi Bangkok 10140
Tanongkiat Kiatsiriroat

Department of Mechanical Engineering Chlang Mai University Chiang Mai 50200

บทลัดบ่อ

งานวิจัยนี้ ศึกษาพฤติกรรมทางความร้อนของท่อความร้อนแบบ เทอร์โมไซฟอนที่ใช้สารทำงานคู่ผสม เอธานอล-น้ำ และไตรเอธิลืน ไกคอล-น้ำ โดยทำการศึกษาผลของพารามิเตอร์ต่างๆ ที่เกี่ยวข้อง กล่าวคือ อัตราส่วนผสมของสารทำงาน อัตราส่วน (อัตราส่วนความยาว ของส่วนระเทยต่อขนาดเส้นผ่านศูนย์กลางของท่อความร้อน : Le/d) ของท่อความร้อน และช่วงอุณหภูมิการทำงาน

จากการทดลองพบว่า อัตราการถ่ายเหลวามร้อนของท่อลวามร้อน ที่ใช้ เอธานอล-น้ำเป็นสารทำงาน ในกรณีที่อุณหภูมิแตกต่างเชิงล็อก ระหว่างน้ำมันร้อนและน้ำที่มาถ่ายเทลวามร้อนมีค่ำต่ำ(ไม่เกิน 100°C) อัตราการถ่ายเทลวามร้อนที่ใต้จะมีค่าสูงกว่าท่อลวามร้อนที่ใช้น้ำเป็น สารทำงาน และมีค่าใกล้เลียงกับอัตราการถ่ายเทลวามร้อนที่ใช้น้ำเป็น ความร้อนที่ใช้เอธานอลเป็นสารทำงาน และในกรณีอุณหภูมิแตกต่าง เชิงล็อกสูง(สูงกว่า 100°C) อัตราการถ่ายเทลวามร้อนของท่อลวาม ร้อนที่ใช้น้ำเป็นสารทำงานจะมีค่าสูงกว่าในกรณีที่ใช้สารทำงานคู่ผสม เอธานอล-น้ำ

ในกรณีของท่อความร้อนที่มีค่าอัตราส่วนสนทรรศน์สูง และช่วง อุณหภูมิการทำงานสูง พบว่ามักจะเกิดการท่วม(flooding)ของสาร ทำงานขึ้นภายในท่อความร้อน การผสมไตรเอธิลีนไกลคอลในน้ำ ประมาณ 25% จะช่วยลดภาวะวิกฤติดังกล่าวได้ในขณะที่อัตราการถ่าย เทความร้อนมีค่าลดลงเล็กน้อย

Abstract

Thermal behavior of a thermosyphon heat pipe using binary working fluids, ethanol-water and triethyleneglycol(TEG)-water,

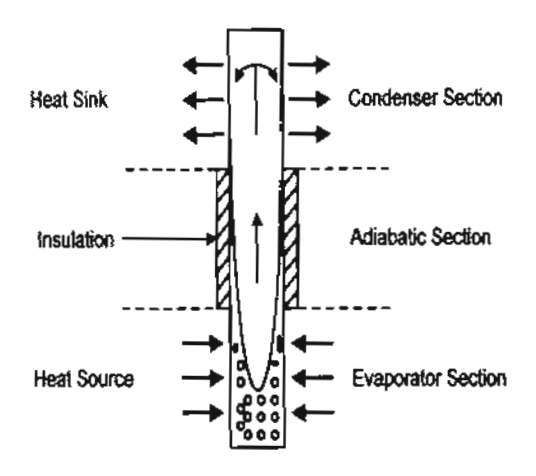
and the affecting parameters such as the mixtures content, the aspect ratio of pipe and the working temperature had been studied in this research work.

From the experimental, at low log mean temperature difference (lower than 100°C) of the hot oil and cold fluid stream, it is found that the thermosyphon using ethanol-water as a working fluid has higher heat transfer rate than that of pure water and close to pure ethanol. But at high log mean temperature difference (more than 100°C), the heat transfer rate of water is the heat.

In case of high aspect ratio of the pipe and high working temperature, the working fluid inside the pipe is always flooded. Low concentration of TEG in water (around 25%) can decrease this critical phenomenon, while the heat transfer rate is slightly reduced.

1. บทน้ำ

ท่อความร้อนแบบเทอร์โมไซฟอน (Thermosyphon Heat Pipe) เป็นอุปกรณ์ในการส่งถ่ายความร้อนจากแหล่งความร้อนสูงไปยังแหล่ง ความร้อนต่ำ โดยอาศัยหลักการเดือดและการควบแน่นของสารทำงาน ในท่อความร้อน หลักการทำงานของท่อความร้อนแบบเทอร์โมไซพ่อน แสดงดังรูปที่ 1



รูปที่ 1 หลักภารทำงานของท่อความร้อนแบบเทอร์โมใชฟอน

ท่อกวามร้อนแบบเทอร์โมไซฟอนตามารถแบ่งออกเป็น 3 ส่วนก็อ ส่วนระเทย (Evaporator Section) ส่วนที่ไม่มีการถ่ายเทความร้อน (Adiabatic Section) และส่วนควบแน่น (Condenser Section) โดยที่ แต่ละส่วนมีหน้าที่ดังต่อไปนี้

ส่วนระเทย จะมีหน้าที่คึงเอากวามร้อนออกจากแหล่งกวามร้อนสูง (Heat Source) โดยสารทำงานที่อยู่ภายใน เมื่อใต้รับความร้อนจะเกิด การเดือดเป็นไอและใหลขึ้นด้านยนไปยังส่วนควบแน่น โดยส่วนระเหย นี้ในท้อกวามร้อนแบบเทอร์โมไซฟอน จะเป็นส่วนที่อยู่ค่ำที่สุด

ส่วนที่ไม่มีการถ่ายเทความร้อน ส่วนนี้จะมีหน้าที่ในการส่งผ่าน ของใหลระหว่างส่วนระเหยและส่วนควบแน่น โดยทั่วใปแล้วส่วนนี้จะมี การหุ้มฉนาน เพื่อป้องกันความร้อนถ่ายเทออกนอกท่อความร้อน ใน บางครั้งส่วนนี้อาจจะไม่มีก็ได้ ส่วนมากแล้วส่วนนี้จะมีในท่อความร้อนที่ ส่งผ่านความร้อนระยะทางไกล ๆ

ส่วนถวบแน่น จะอยู่ปลายด้านบนสุดในท่อกวามร้อนแบบเทอร์โม ใชฟอน โดยมีหน้าที่ถ่ายเทความร้อนออกจากท่อกวามร้อนให้กับของ ใหล่ที่มารับความร้อน (Heat Sink) โดยการควบแน่น และสารทำงานที่ กวบแน่นแล้วจะใหล่ลงผู้ด้านล่างเพื่อรับเอาความร้อนจากส่วนระเหย และเกิดการใหล่เวียนเป็นวัฏจักรค่อไป

ท่อความร้อนแบบเทอร์โมไซฟอน โดยทั่วไปแล้วจะใช้สารทำงาน เดี๋ยวเช่น น้ำ, เอธานอล, สารทำความเย็นต่าง ๆ เป็นตัน ซึ่งในการเลือก ใช้สารดังกล่าวต้องให้เหมาะสมกับช่วงอุณหภูมิใช้งานของท่อความร้อน นั้น ๆ ท่อความร้อนที่ใช้ในการดึงความร้อนทิ้งกลับมาใช้ประโยชน์ จาก กระบวนการทางอุตสาหกรรมต่าง ๆ นิยมใช้น้ำเป็นสารทำงาน เนื่อง จากว่าน้ำมีค่าความร้อนแฝงของการกลายเป็นไอสูงและ สามารถใช้งาน ใด้ในช่วงอุณหภูมิของแหล่งความร้อนที่กว้าง (60-250°C) แต่อย่างไรก็ ตามถ้านำสารคู่ผสม(Binary Mixture) มาใช้ในท่อความร้อนเช่น เอธา นอล-น้ำ เมื่อให้ความร้อนแก่ส่วนระเหยของท่อความร้อน พบว่าสาร ระเหยง่ายซึ่งในที่นี้คือเอธานอล จะเกิดการเดือดกลายเป็นไอก่อนน้ำ ส่วนน้ำจะเดือดตามมาเมื่ออุณหภูมิเพิ่มสูงขึ้นจนถึงจุดเตือดของมัน ทำ ให้ที่ช่วงอุณหภูมิการทำงานคุ่ผสมเอธานอล-น้ำ มีค่าสูงกว่าในกรณีที่ใช้น้ำ เป็นสารเดี๋ยวในการทำงาน และในช่วงอุณหภูมิสูงที่สัดส่วนผสมบางคำ

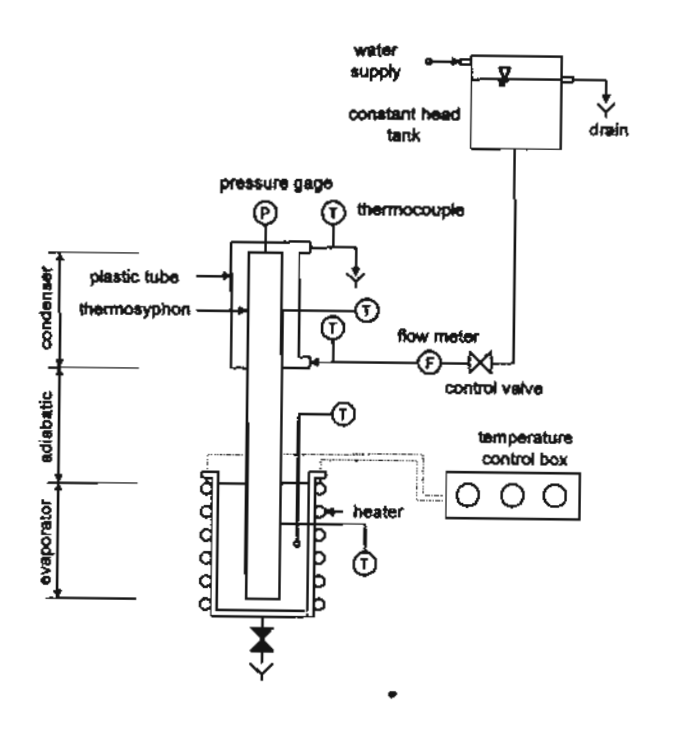
สมรรถนะในการถ่ายเพความร้อนไม่แตกต่างมากนักเมื่อเทียบกับการ ใช้น้ำเพียงอย่างเดียว

จากแนวก็ตดังกล่าวข้างต้นเป็นที่มาของงานวิจัยนี้ ซึ่งการใช้สารคู่ ผสมในท่อกวามร้อนแบบเทอร์โมไซฟอน จะช่วยทำให้สมรรถนะของ ท่อกวามร้อนดังกล่าวมีค่าสูงขึ้น เนื่องมาจากเหตุผลดังที่กล่าวมาข้าง ต้น ในโครงการวิจัยนี้ จะศึกษาถึงพฤติกรรมทางความร้อนของท่อ กวามร้อนแบบเทอร์โมไซฟอนที่ใช้สารคู่ผสมโดยจะศึกษาตัวอย่างของ สารคู่ผสม คือเอฮานอล-น้ำ ซึ่งเอธานอลมีจุดเดือดค่ำกว่าน้ำ (ประมาณ 20°C) และ ไตรเอธิลีนไกลคอล-น้ำ โดย ไตรเอธิลีนไกลคอล มีจุดเดือดสูงกว่าน้ำมาก (ประมาณ 170°C)

2. อุปกรณ์และวิธีการดำเนินการวิจัย

2.1 อุปกรณ์ในการวิจัย

งานวิจัยนี้จะทำการศึกษาการถ่ายเทความร้อนของท่อความร้อน แบบเทอร์โมไซฟอน ที่ใช้สารทำงานผสม โดยถ่ายเทความร้อนจาก แหล่งอุณหภูมิสูง ซึ่งในที่นี้คือ อ่างน้ำมันร้อน ไปยังแหล่งอุณหภูมิต่ำ ซึ่งก็คือ น้ำหล่อเย็น ลักษณะของอุปกรณ์ในการวิจัยแสดงดังรูปที่ 2 ซึ่ง มีส่วนประกอบที่สำคัญประกอบด้วย ท่อความร้อน, อ่างน้ำมันร้อน, ระบบน้ำหล่อเย็น และ อุปกรณ์การวัดและควบคุมอื่น ๆ



รูปที่ 2 อุปกรณ์ในการวิจัย

ท่อความร้อนแบบเทอร์โมไซฟอน ทำจากท่อสแดนเลส 304 ขนาด เส้นผ่านศูนย์กลาง 25.4 และ 12.7 mm. หนา 2.0 mm. ความยาวรวม 100 cm. โดยส่วนระเหยยาว 40 cm. ส่วนควบแน่นยาว 40 cm. ส่ว นอะเดียบาติกยาว 20 cm.

อ่างน้ำมันร้อน ประกอบด้วยขดถวดกวามร้อนขนาด 3000 W กวบกุมตัวยชุดปรับอุณหภูมิทางไฟฟ้า ติดตั้งเข้ากับภาชนะทรง กระบอกขนาดเส้นผ่านศูนย์กลาง 7 cm. ยาว 50 cm. และบรรจุด้วยน้ำ มันพาราฟิน ซึ่งทำหน้าที่เป็นตัวกลางในการถ่ายเทความร้อนระหว่าง ขดลวดความร้อนและส่วนระเทยของท่อความร้อน อุณหภูมิของน้ำมัน ร้อนสามารถปรับคำใต้อยู่ระหว่าง 50-225 °C

ระบบน้ำหล่อเอ็นของส่วนควบแน่น จะประกอบด้วยท่อโลหะทรง
กระบอกขนาดเส้นผ่านศูนย์กลาง 5.08 cm. ยาว 40 cm. สวมทับส่วน
กวบแน่นของท่อความร้อน และหุ้มฉนานภายนอกเพื่อป้องกันความ
ร้อนถ่ายเทสู่สิ่งแวดล้อม น้ำหล่อเย็นจะถูกควบคุมอัตราการไหลโดย
การใช้ลังน้ำที่มีความสูงคงที่

อุปกรณ์การวัดอุณหภูมิ จะประกอบด้วยเทอร์โมดับเปิลชนิด K โดยทำการวัดอุณหภูมิที่ตำแหน่งต่าง ๆ คือ วัดอุณหภูมิผิวท่อความร้อน ที่ระยะ 5,20,35,50,65,80 และ 95 cm. จากปลายของส่วนระเหย วัด อุณหภูมิน้ำมันพาราฟิน วัดอุณหภูมิน้ำหล่อเย็นขาเข้าและขาออกจาก ส่วนกวบแน่นของท่อกวามร้อน

อุปกรณ์การวัดความคัน จะใช้เกจความคัน วัดความคันภายในท่อ ความร้อนที่ด้านปลายของส่วนควบแน่น

2.2 วิธีการวิจัย

ทศสอบการถ่ายเทความร้อนของท่อกวามร้อนเมื่อใช้สารทำงานได้
แก่ น้ำ, เอชานอล และ ไดรเอชิลีนใกลกอล ที่อัตราส่วนการเดิม 50%
ของส่วนระเทย และสารผสมใต้แก่ เอชานอล-น้ำ และ ไตรเอชิลีนใกล
กอล-น้ำ ที่อัตราส่วนผสมของ เอชานอล และใตรเอชิลีนใกลกอล 25,
50, 75% โดยปริมาตร ที่อัตราส่วนการเดิม 50% โดยปริมาตรของส่วน
ระเทยโดยล่าอุณหภูมิของน้ำมันพาราฟินจะอยู่ ระหว่าง 50-225°C
และควบคุมอัตราการใหลของน้ำหล่อเย็นที่อุณหภูมิห้องให้คงที่ที่ 8.5
g/s

คำกวามดันและอุณหภูมิที่จุดต่างๆ จะบันทึกที่สภาวะคงตัว เพื่อ ทำการศึกษาพฤติกรรมทางความร้อนของท่อความร้อน

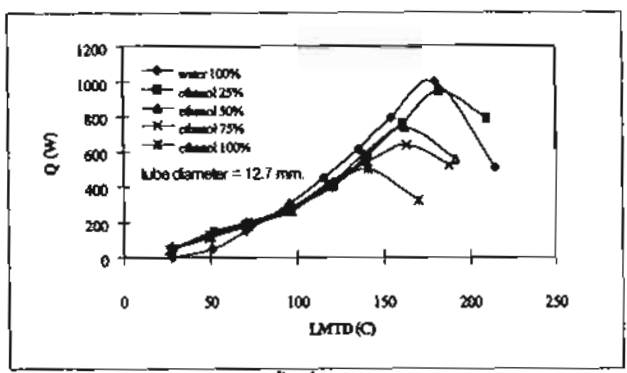
3. ผลการทดสอบและการวิเคราะห์

3.1 อัตราการถ่ายเทความร้อนของท่อความร้อน

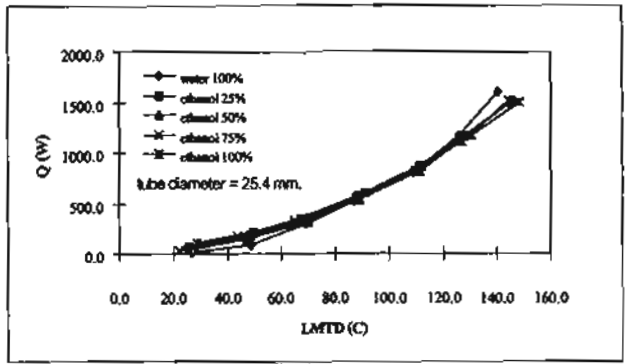
ความสัมพันธ์ระหว่าง อัตราส่วนการถ่ายเทความร้อนของท่อ ความร้อน กับอุณหภูมิแตกต่างเชิงล็อกระหว่างอุณหภูมิน้ำมันแล้ะน้ำที่ มารับความร้อน ของท่อความร้อนแบบเทอร์โมไซฟอนที่ใช้ น้ำ เอธา นอล โตรเอธิลีนไกลคอล เอธานอล-น้ำ และ ไตรเอธิลีนไกลคอล-น้ำ เป็นสารทำงานแสดงดังรูปที่ 3 ก.ข.ค.ง โดยที่นิยามของค่าอุณหภูมิ แตกต่างเชิงล็อก ในงานวิจัยนี้ ได้นิยามไว้ดังต่อไปนี้

$$\Delta T_{\text{lattd}} = \frac{(T_{wo} - T_{wi})}{\ln \left(\frac{T_{oil} - T_{wi}}{T_{oil} - T_{wo}} \right)}$$
(1)

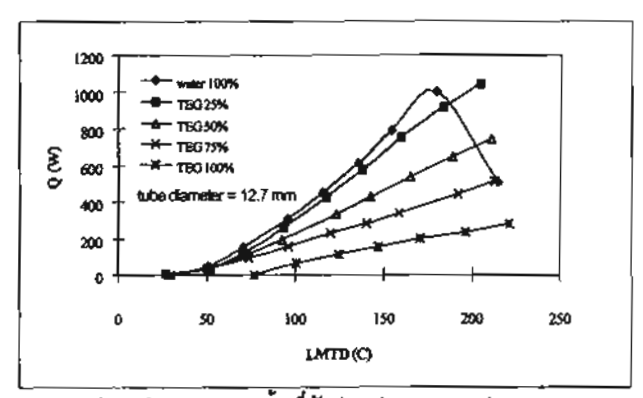
T_m และ T_m คืออุณหภูมิของน้ำหล่อเย็นเข้าและออกที่มารับความ ร้อนที่คอนเดนเซอร์ และ T_m คืออุณหภูมิน้ำมันที่ส่วนระเหยของท่อ ความร้อน



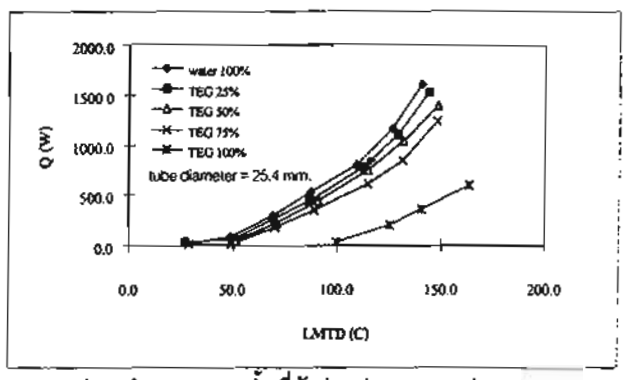
3ก. คู่สารทำงาน เอธานอล-น้ำ ที่สัดส่วนต่างๆ ขนาดท่อ 12.7 mm.



3บ. คู่สารทำงาน เอชานอล-น้ำ ที่สัดส่วนค่าง ๆ ขนาคห่อ 25.4 mm.



3ค. คู่สารทำงาน TEG.-น้ำ ที่สัดส่วนต่างๆ ขนาดท่อ 12.7 mm.



3ง. กู่สารทำงาน TEG.-น้ำ ที่สัดส่วนต่างๆ บนาตท่อ 25.4 mm.

รูปที่ 3 ความสัมพันธ์ของค่าอัตราการถ่ายเทความร้อน และคำความ แตกต่างอุณหภูมิเชิงล็อกต่าง ๆ ของท่อความร้อน จากการทดสอบพบว่า ในกรณีของท่อความร้อนที่ใช้สารทำงานคู่
ผสม เอชานอล-น้ำ ในช่วงอุณหภูมิการทำงานค่ำ อัตราการถ่ายเท
กวามร้อนที่ได้จะมีค่าสูงกว่า ท่อความร้อนที่ใช้น้ำเป็นสารทำงาน และมี
ค่าใกล้เกียงกับท่อความร้อนที่ใช้เอชานอลเป็นสารทำงาน ในขณะที่ใน
ช่วงอุณหภูมิการทำงานลูง อัตราการถ่ายเทความร้อนของท่อความร้อน
ที่ใช้น้ำเป็นสารทำงานจะมีค่าสูงกว่ากรณีที่ใช้สารทำงานคู่ผสม ดังรูปที่
ก และ ข ปรากฏการณ์ดังกล่าวเกิดขึ้นเนื่องจากการที่อุณหภูมิจุด
เดือดของเอชานอลมีค่าค่ากว่าน้ำทำให้ในช่วงอุณหภูมิการทำงานค่ำ
เอชานอลในสารทำงานคู่ผสมสามารถเดือต และส่งผ่านกวามร้อนได้ ใน
ขณะที่น้ำยังไม่เริ่มเดือด ในกรณีช่วงอุณหภูมิการทำงานลูง น้ำสามารถ
เดือดและส่งผ่านกวามร้อนได้ดีกว่ากรณีใช้สารทำงานคู่ผสม หรือ
เอชานอล ทั้งนี้เนื่องจากว่า ค่าความร้อนแฝงของการกลายเป็นไอของ
น้ำมีค่าสูงกว่า เอชานอล

นอกจากนี้ยังพบว่า ในกรณีท่อความร้อนขนาดเส้นผ่านศูนย์กลาง
12.7 mm. ที่ช่วงอุณหภูมิการทำงานสูงจะเกิดภาวะวิกฤติเนื่องจากการ
ท่วม (Flooding) ขึ้นภายในท่อความร้อน โดยอัตราการถ่ายเทความ
ร้อนสูงสุดจะแปรผกผันกับปริบาณเอธานอลในสารทำงานคู่ผสม ภาวะ
วิกฤติดังกล่าวเกิดขึ้นเนื่องจากอัตราล่วนสนทรรศน์ (อัตราล่วนความ
ยาวของส่วนระเหยต่อขนาดเส้นผ่านสูนย์กลางของท่อความร้อน: Lo/d
) ไม่เหมาะสม

ในกรณีการใช้สารทำงานคู่ผสม ใตรเอธิลีนไกลคอล-น้ำ ในท่อ กวามร้อน จากรูปที่ 3 ค และ ง พบว่าการส่งผ่านความร้อนของท่อ ความร้อนจะแปรผกผันกับปริมาณของไตรเอธิลีนไกลคอล และยังพบ ว่า ภาวะวิกฤติเนื่องจากการท่วมภายในท่อความร้อนขนาดเส้นผ่าน ศูนย์กลาง 12.7 mm. จะไม่เกิดขึ้น

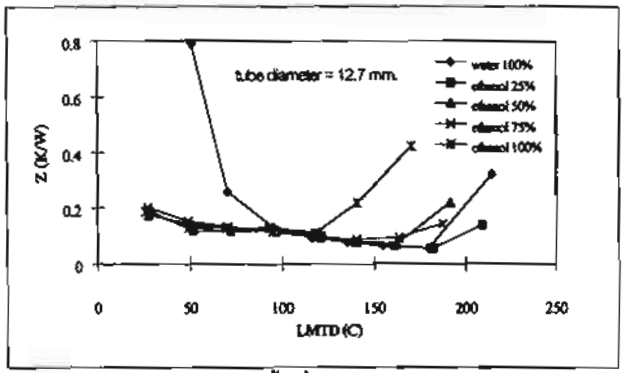
3.2 ความตัวนทานการถ่ายเทความร้อนภายในท่อความร้อน

ความสัมพันธ์ระหว่างความต้านทานการถ่ายเทความร้อนภายใน ท่อความร้อน และคำอุณหภูมิแตกต่างเชิงล็อก แสดงดังรูปหึ่ 4 ก.ข.ค และ ง โดยความต้านทานการถ่ายเทความร้อนภายในท่อความร้อน นิยามดังสมการดังนี้

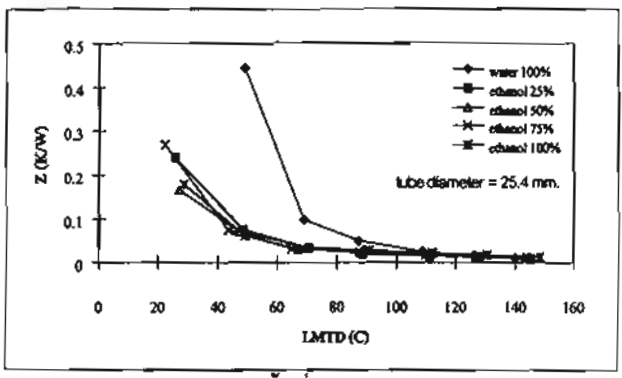
$$Z = \frac{T_{e,ave} - T_{c,ave}}{Q}$$

(2)

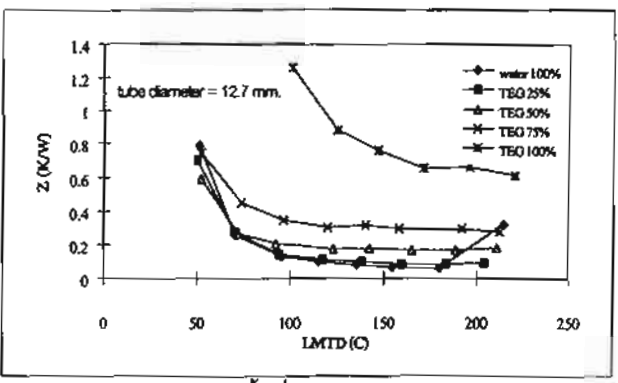
โดยที่สมการที่ 2 จะตั้งสมมุติฐานว่า การถ่ายเทความร้อนตาม แนวแกนของท่อความร้อนมีค่าน้อยมากเมื่อเทียบกับการถ่ายเทความ ร้อนภายในท่อความร้อน



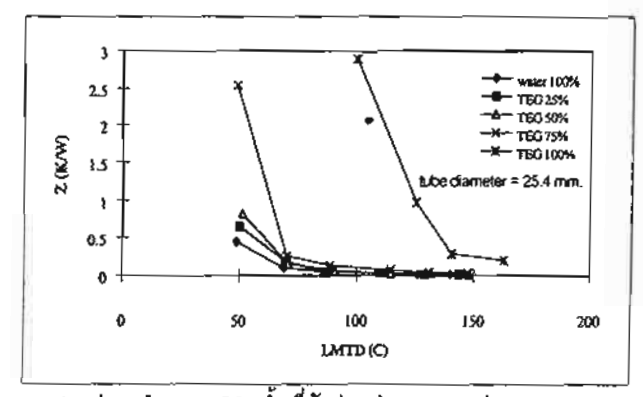
4n. คู่สารทำงานเอฮานอล-น้ำ ที่สัดส่วนต่าง ๆ ชนาดท่อ 12.7 mm.



4ข. คู่สารทำงาน เอชานอล-น้ำ ที่สัดส่วนต่าง ๆ ขนาดท่อ 25.4 mm.



4ค. คู่สารทำงาน TEG.-น้ำ ที่สัคส่วนต่างๆ ขนาดท่อ 12.7 mm.



4ง. กู่สารทำงาน TEG.-น้ำ ที่สัดส่วนต่างๆ ขนาดท่อ 25.4 mm.

รูปที่ 4 ความสัมพันธ์ระหว่างความต้านทานการถ่ายเทความร้อนภาย ในท่อความร้อนและอุณหภูมิแตกต่างเชิงล็อก

จากการทดลองพบว่า ความสัมพันธ์ของความต้านทานการถ่ายเท ความร้อนและอุณหภูมิแตกต่างเชิงล็อกสอดคล้องกับกรณีของความ สัมพันธ์ระหว่างอัดราการถ่ายเทกวามร้อนและอุณหภูมิแตกต่างเชิง ล็อก และมีแนวใน้มที่จะลู่เข้าสู่ถ่าคงที่เมื่ออุณหภูมิแตกต่างเชิงล็อกมีค่า สูงขึ้น และกลับมีค่าสูงขึ้นอีกเมื่อเกิดการท่วมขึ้นภายในท่อความร้อน

จากรูปที่ 4 ก และ ข จะพบว่าในกรณีช่วงอุณหภูมิแตกต่างเชิงล็ อกต่ำ ค่าความด้านทานการถ่ายเทความร้อนของน้ำจะมีค่าสูงกว่าของ สารทำงานคู่ผสม เอชานอล-น้ำ และเอชานอลบริสุทธิ์ อย่างเห็นได้ชัด ทั้งนี้เนื่องมาจากช่วงอุณหภูมิดังกล่าวน้ำยังไม่เริ่มเดือด ในขณะที่เอชา นอลสามารถเดือดและส่งผ่านความร้อนใต้แล้ว ในกรณีที่อุณหภูมิแตก ต่างเชิงล็อกมีค่าสูงขึ้น พบว่าค่าความต้านทานของการถ่ายเทความร้อนของท่อความร้อนขนาดเส้นผ่านศูนย์กลาง 25.4 mm. มีค่าใกล้เคียง กัน ในขณะที่ค่าความต้านทานของการถ่ายเทความร้อนขนาด 12.7 mm. มีค่าเพิ่มขึ้นอีกครั้งหนึ่ง ทั้งนี้เนื่องจากเกิดการ ท่วมขึ้นภายในท่อความร้อน

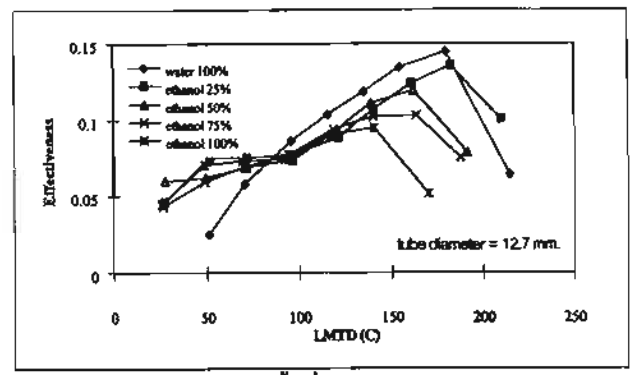
รูปที่ 4 ค และ ง เป็นกรณีของความต้านทานการถ่ายเทความ ร้อนของท่อความร้อนที่ใช้สารทำงานคู่ผสม ใตรเอธิสินใกลคอล-น้ำ จากรูปดังกล่าวพบว่า ความตัวนทานการถ่านเทความร้อนจะแปรผกผัน กับปริมาณใตรเอธิสินใกลคอล ในสารทำงานคู่ผสม และยังพบว่าภาวะ วิกฤติเนื่องจากการท่วมของสารทำงานภายในท่อความร้อนของท่อ ความร้อนขนาดเส้นผ่านศูนย์กลาง 12.7 mm. จะไม่เกิดขึ้น แต่กรณีของน้ำเพียงอย่างเดียวคำความด้านทานจะเพิ่มขึ้นอีก เมื่อเกิดการท่วม

3.3 ค่าประสิทธิผลของการถ่ายเทความร้อน

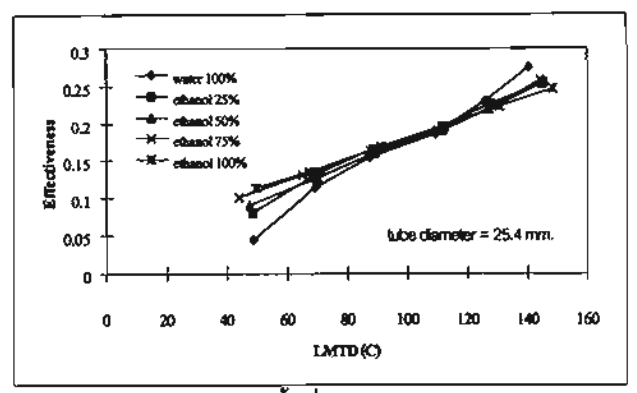
คำประสิทธิผลของการถ่ายเทความร้อนของท์อความร้อนสามารถ นิยามใต้ดังสมการต่อไปนี้

$$Effectiveness = \frac{T_{wo} - T_{wi}}{T_{oil} - T_{wi}}$$
 (3)

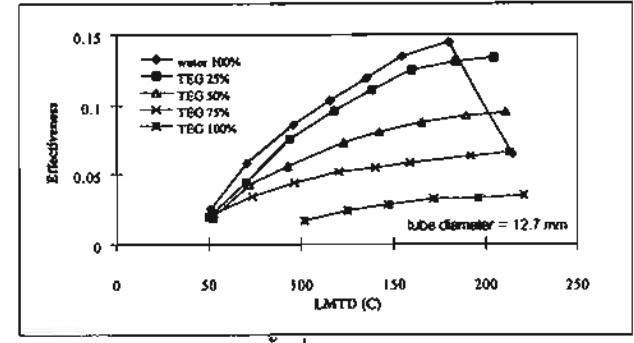
ความสัมพันธ์ระหว่างค่าประสิทธิผลและอุณหภูมิแตกต่างเชิงล็อก แสดงดังรูปที่ 5 ภ,ข,ก และ ง ซึ่งความสัมพันธ์ดังกล่าว สอดกล้องกับ ความสัมพันธ์ระหว่างอัตราการถ่ายเทความร้อนกับอุณหภูมิแตกต่าง เชิงล็อก (รูปที่ 3) และความความสัมพันธ์ระหว่างความต้านทานการ ถ่ายเทความร้อน กับอุณหภูมิแตกต่างเชิงล็อก (รูปที่ 4)



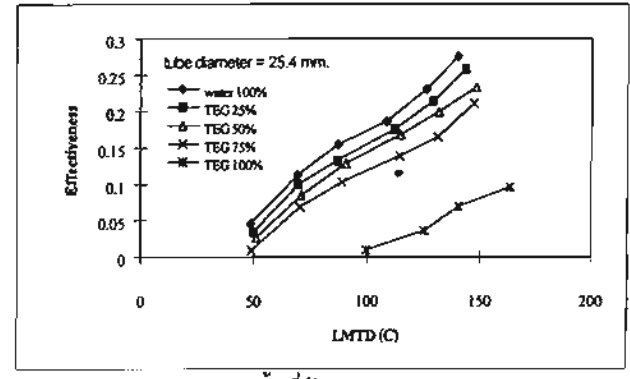
4ก, คู่สารทำงานเอธานอล-น้ำ ที่สัดส่วนต่างๆ ขนาดท่อ 12.7 mm.



4ช. คู่สารทำงาน เอธานอล-น้ำ ที่สัดส่วนค่าง ๆ ขนาคท่อ 25.4 mm.



4ค. กู้สารทำงาน TEG.-น้ำ ที่สัดส่วนต่างๆ ขนาดท่อ 12.7 mm.



4ง. กู่สารทำงาน TEG.-น้ำ ที่สัดส่วนต่าง ๆ ขนาดท่อ 25.4 mm.

รูปที่ 5 ความสัมพันธ์ของคำประสิทธิผลของการถ่ายเทความร้อนและ คำอุณหภูมิแตกต่างเชิงล็อก

3.4 การประยุกต์ท่อความร้อนแบบเทอร์โมไซพ่อนที่ใช้สารทำงาน คู่ผสมกับเครื่องแลกเปลี่ยนความร้อนแบบท่อความร้อน

1. กรณีใช้สารทำงานคู่ผสมเอชานอล-น้ำ

ในกรณีเครื่องแลกเปลี่ยนความร้อนที่ใช้งานในช่วงอุณหภูมิไม่สูง มากนัก (อุณหภูมิแตกต่างเชิงล็อกไม่เกิน 100°C) การใช้สารทำงานคู่ ผสมเอธานอล-น้าจะทำให้สมรรถนะของเครื่องแลกเปลี่ยนความร้อนสูง กว่าในกรณีที่ใช้น้ำเป็นสารทำงานเพียงอย่างเตียว ทั้งนี้เนื่องจากในช่วง ที่อุณหภูมิของกระแสร้อนมีค่าลดลง (ต่ำกว่า 100 °C) อัตราการถ่ายเท ความร้อนของท่อความร้อนที่ใช้สารทำงานคู่ผสมจะมีค่าสูงกว่าท่อกวาม ร้อนที่ใช้น้ำเป็นสารทำงาน ทำให้สมรรถนะในการถ่ายเทความร้อนรวม ของเครื่องแลกเบ่ลี่ยนความร้อนมีค่าสูงขึ้น

2. กรณีใช้สารทำงานคู่ผสมใตรเอธิลืนใกลคอล-น้ำ

ในบางกรณีที่อความร้อนที่ต้องการใช้มีขนาดยาวมากๆ เช่นท่อ กวามร้อนที่ใช้ดึงกวามร้อนจากใต้ดิน ขนาดของอัตราส่วน Lold จะไม่ เหมาะสม ในกรณีที่อุณหภูมิการทำงานมีคำสูง มักจะทำให้เกิดภาวะ วิกฤติเนื่องจากการท่วมได้ ภารผสม ใดรเอชิลีนใกลดอลลงไปในน้ำ เพียงเล็กน้อย (ประมาณ 25%) จะช่วยลดภาวะวิกฤติเนื่องจากการท่วม ลงได้ ในขณะที่อัตราการถ่วยเทกวามร้อนมีค่าลดลงเพียงเล็กน้อยเท่า

4. บทสรุป

ท่อความร้อนแบบเทอร์โมไซฟอนที่ใช้สารทำงานคู่ผสมมีศักยภาพ ในการพัฒนาขึ้นมาใช้บระโยชน์ ทั้งนี้เนื่องจากว่าในการเลือกอัตราส่วน และสารคู่ผสมที่เหมาะสม ในสภาวะการทำงานบางอย่าง ท่อความร้อน ดังกล่าวสามาถให้สมรรถนะที่สูงกว่าในกรณีของท่อความร้อนที่ใช้สาร เคียวเป็นสารทำงาน ทั้งนี้ขึ้นอยู่กับสภาวะการทำงานของท่อความร้อน ดังกล่าวค้วย ดังเช่นในการวิจัยนี้พบว่าในกรณีช่วงอุณหภูมิการทำงาน ต่ำท่อความร้อนที่ใช้สารทำงานคู่ผสมเอชานอล-น้ำ จะมีอัตราการถ่าย เทความร้อนที่สูงกว่าท่อความร้อนที่ใช้น้ำเป็นสารทำงาน และนอกจาก นี้ยังพบว่าการเติมไตรเอธิลินไกลคอลลงไปในน้ำเพียงเล็กน้อย (ประมาณ 25%) จะช่วยลดภาวะวิกฤติเนื่องจากการท่วมขึ้นภายในท่อ ความร้อนที่มีอัตราส่วน Le/d ไม่เหมาะสมลงได้

กิตติกรรมประกาศ

คณะผู้วิจัยขอขอบพระคุณสำนักงานกองทุนสนับสนุนการวิจัยที่ให้ ทุนสนับสนุนในการวิจัยครั้งนี้

รายการสัญลักษณ์

d = เส้นผ่านศูนย์กลางท่อความร้อน (m)

k = คำการนำความร้อนของท่อ (W/mK)

L = ความยาว (m)

Q = อัตราการถ่ายเทความร้อนของท่อความร้อน (W)

ะ = รัศมี (m²)

T = อุณหภูมิ(K)

∆T_{lmts} = อุณหภูมิแตกต่างเชิงล็อก (°C)

Z = ความตัวนทานทางความร้อน (KW)

Subscripts

ave = คำเฉลี่ย

c = ส่วนควบแน่น

e = ส่วนระเทย

i = ขาเข้า.ด้านใน

1 = ของเหลว

o = ขาออก, ด้านนอก

v = ไอ

w = ผนัง.น้ำ

บรรณานุกรม

- Shiralshi M., Kikuchi K. and Yamanishi T., (1981), "Investigation of Heat Transfer Characteristics of a Twophase Closed Thermosyphon", Heat Recovery Systems, Vol.1, pp.287-297, Pergamon Press
- Amornkitbamrung M., Wangnippanto S. and Klatsirlroat T., (1995), "Performance Studies on Evaporation and Condensation of a Thermosyphon Heat Pipe", 6th ASEAN Conf. on Energy Technology, Bangkok
- Engineering Sciences Data Unit, (1981), "Heat Pipes-Performance of Two-Phase Closed Thermosyphons" No. 81038
- Lide D.R. and Kehlaian H.V., (1994), "CRC Handbook of Thermophysical and Thermochemical Data", CRC Press

อติพงศ์ นันทพันธุ์, จิรวรรณ เตียรถ์สุวรรณ และ ทนงเกียรติ เกียรติศิริ โรจน์, การคำนวณสมรรถนะของเครื่องอุ่น อากาศแบบเทอร์ โมไซฟอน โดยที่ก่าสัมประสิทธิ์การถ่ายเทความร้อนไม่คงที่, การประชุมวิชาการเครือข่าย วิศวกรรมเครื่องกณแห่งประเทศไทยครั้งที่ 14, 2-3 พฤศจิกายน 2543, เชียงใหม่.

การประชุมวิชาการเครือข่ายวิศวกรรมเครื่องกลแห่งประเทศไทยครั้งที่ 14 2-3 พฤศจิกายน 2543 โรงแรมโนโวเทล เชียงใหม่

การคำนวณสมรรถนะของเครื่องอุ่นอากาศแบบเทอร์โมไซฟอนโดยที่ ค่าสัมประสิทธิ์การถ่ายเทความร้อนไม่คงที่ Performance Analysis of Thermosyphon Air Preheater With Variable Heat Transfer Coefficient

อติพงศ์ นันทพันธุ์ และ จิรวรรณ เตียรถ์สุวรรณ คณะพลังงานและวัสคุ มหาวิทยาลัยเทคโนโลยีพระจอมเกล้าธนบุรี กรุงเทพมหานคร 10140

> ทนงเกียรติ เกียรติศิริโรจน์ ภาควิชาวิศวกรรมเครื่องกล มหาวิทยาลัยเชียงใหม่ เชียงใหม่ 50200

Atipoang Nuntaphan and Jirawan Tiansuwan

School of Energy and Materials King Mongkut's University of Technology Thonburi Bangkok 10140

Tanongkiat Kiatsiriroat

Department of Mechanical Engineering Chiang Mai University Chiang Mai 50200

บทลัดย่อ

งานวิจัยนี้ ได้เสนอวิธีการในการคำนวณสมรรถนะของ เครื่องอุ่นอากาศแบบเทอร์โมไซพ่อน ซึ่งโดยทั่วไปจะตั้ง สมมุติฐานว่าอัตราการถ่ายเทความร้อนของท่อความร้อนแต่ ละท่อในเครื่องอ่นอากาศมีคำคงที่ โดยในงานวิจัยนี้ได้ทำ การเปรียบเทียบวิธีการคำนวณดังกล่าวกับวิธีการที่กำหนด ให้อัตราการถ่ายเทความร้อนของท่อความร้อนในเครื่องอุ่น อากาศแบรเปลี่ยนไปตามสภาวะของอุณหภูมิอากาศที่มา แลกเปลี่ยนความร้อนกัน โดยทำการสร้างโปรแกรมจำลอง สถานการณ์เพื่อคำนวณสมรรถนะของเครื่องอุ่นอากาศ โดย อาศัยหลักการทั้งสองแบบเบรียบเทียบกัน จำลองสถานการณ์พบว่า การตั้งสมมุติฐานว่าอัตราการถ่าย เทความร้อนของท่อความร้อนมีค่าคงที่ จะใช้ได้ดีกับกรณีของ เครื่องอุ่นอากาศแบบไหลสวนทางกันที่มีอัตราการไหลของ อากาศร้อนและเย็นเท่ากัน ส่วนในกรณีของอัตราการใหลของ อากาศร้อนและเย็นไม่เท่ากันและกรณีของเครื่องอุ่นอากาศ แบบไหลดามกัน พบว่าสมมุติฐานดังกล่าว ให้การคำนวณ สมรรถนะของเครื่องอุ่นอากาศคลาดเคลื่อน

Abstract

This research work presents an approach to calculate performance of the thermosyphon air preheater. Normally, the heat transfer rate of the thermosyphon in the air preheater is assumed constant. In this work, the heat transfer rate depends on the working conditions of the air in the thermosyphon heat exchanger. The simulated results had been compared with those of the conventional approach. It is found that both approaches had the same result for counter current flow with equal mass flow rates of hot and cold streams. For unbalance counter current flow and parallel flow, the conventional are showed oversized value.

1. บทน้ำ

เครื่องอุ่นอากาศแบบเทอร์โมไซฟอน เป็นอุปกรณ์แลก เปลี่ยนความร้อนชนิดหนึ่งที่นิยมใช้ในการดึงความร้อนทิ้ง จากไอเสียที่เกิดจากการเผาไหม้ของหม้อไอน้ำ มาใช้ในการ อุ่นอากาศก่อนเข้าห้องสันดาป ซึ่งเป็นการเพิ่มสมรรถนะของ หม้อไอน้ำให้สูงขึ้น และนอกจากนี้เครื่องอุ่นอากาศแบบเทอร์ โมไซฟอน ยังสามารถนำมาประยุกต์ใช้ในกระบวนการทาง อุตสาหกรรมต่าง ๆ ได้มากมาย ทั้งนี้เนื่องจากอุปกรณ์ดัง กล่าวมีข้อดีหลายประการ อาทีเช่น ให้อัตราการถ่ายเทความ ร้อนสูง ความดันตกคล่อมน้อย ราคาถูก และสามารถติดตั้ง ได้งำย

ในการออกแบบเครื่องอุ่นอากาศแบบเทอร์โมไซฟอน โดยปกติแล้วจะตั้งสมมุติฐานให้อัตราการถ่ายเทความร้อน ของท่อความร้อนแต่ละท่อมีค่าคงที่เท่ากัน [1] แต่ในทาง ปฏิบัติแล้ว อัตราการถ่ายเทความร้อนของท่อความร้อนในแต่ ละตำแหน่งในเครื่องอุ่นอากาศจะมีค่าไม่เท่ากัน อุณหภูมิของอากาศที่มาแลกเปลี่ยนความร้อนกัน ดังนั้นการ ใช้สมมูติฐานข้างต้นอาจจะไม่ถูกต้องนัก ทำให้การคำนวณ ออกแบบขนาดของเครื่องอุ่นอากาศเกิดความผิดพลาด นั้น ในงานวิจัยนี้ จะทำการทดสอบสมมูคิฐานดังกล่าวว่า สามารถใช้ได้ในลักษณะใดบ้าง โดยจะทำการออกแบบ โปรแกรมคอมพิวเตอร์เพื่อใช้ในการคำนวณสมรรถนะของ เครื่องอุ่นอากาศ ทั้งในกรณีของการใช้สมมูติฐานอัตราการ ถ่ายเทความร้อนของท่อความร้อนมีค่าคงที่ และในกรณีของ อัตราการถ่ายเทความร้อนของท่อความร้อนแปรเปลี่ยนไป ตามสภาวะของอุณหภูมิอากาศที่มาแลกเปลี่ยนความร้อนกัน เพื่อศึกษาถึงความเหมาะสมในการนำเอาสมมุติฐานอัตราการ ถ่ายเทความร้อนคงที่ มาใช้ในการออกแบบเครื่องอุ่นอากาศ แบบเทอร์โมใชฟอน

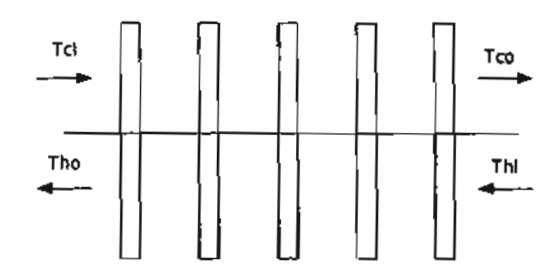
2 ทฤษฎีที่เกี่ยวข้องกับงานวิจัย

การคำนวณการถ่ายเทความร้อนของเครื่องอุ่นอากาศ แบบเทอร์โมไซฟอน สามารถพิจารณาได้ดังรูปที่ 1 ซึ่งมีราย ละเอียดดังต่อไปนี้

อัตราการถ่ายเทความร้อนรวมของเครื่องอุ่นอากาศแบบ เทอร์โมไซฟอนสามารถคำนวณได้จากสมการดังนี้

$$Q = (UA)_t \Delta T_{lmtd}$$
 [1]

โดยที่ Q คืออัตราการถ่ายเทความร้อนรวม (UA), คือค่า สัมประสิทธิ์การถ่ายเทความร้อนรวมพื้นที่ ของเครื่องอุ่น อากาศ ΔT_{imid} คือ อุณหภูมิแตกต่างเชิงล็อก



รูปที่ 1 การถ่ายเทความร้อนของเครื่องอุ่นอากาศแบบ เทอร์โมไซพ่อน

ค่าสัมประสิทธิ์การถ่ายเทความร้อนรวมพื้นที่ ของเครื่อง อุ่นอากาศแบบเทอร์โมใชฟอนสามารถคำนวณใค้ดังนี้

$$\frac{1}{(UA)_{t}} = \frac{1}{h_{ev,o}A_{ev,ot}} + \frac{1}{h_{cd,o}A_{cd,ot}} + \frac{1}{h_{ev,i}A_{ev,it}} + \frac{1}{h_{cd,i}A_{cd,it}} + \frac{\ln(r_{o}/r_{i})}{2\pi k_{m}L_{ev,t}} + \frac{\ln(r_{o}/r_{i})}{2\pi k_{m}L_{cd,t}}$$
[2}

Klatsiriroat et.al. [2] ได้ทำการศึกษาถึงค่าสัมประสิทธิ์ การถ่ายเทความร้อนของการเดือดในท่อเทอร์โมไซพ่อน ที่ใช้ น้ำเป็นสารทำงาน และได้สร้างสมการคำนวณค่าสัมประสิทธิ์ การถ่ายเทความร้อนของการเดือด โดยตัดแปลงสมการของ Roshenow ดังนี้

$$h_{ev,i} = \frac{18.688}{\Delta T_{ev} C_1} \left[\left(\frac{\Delta T_{ev}}{C_2} \right)^3 \right]^{0.3572}$$

$$C_1 = \frac{1}{\mu_{wl} \lambda_w} \sqrt{\frac{g_c \sigma_w}{g(\rho_{wl} - \rho_{wv})}}$$

$$C_2 = \frac{\lambda_w Pr_{wl}}{Cp_{wl}}$$
[3]

โดยที่ ∆T_{av} คืออุณหภูมิแตกต่างระหว่างผิวและสาร ทำงานที่ส่วนระเทยของท่อความร้อน

นอกจากนี้ยังได้ทำการสร้างสมการเอมไพริกัลเพื่อ คำนวณค่าสัมประสิทธิ์การถ่ายเทความร้อนของการควบแน่น ภายในท่อความร้อนแบบเทอร์โมไซฟอนที่ใช้น้ำเป็นสาร ทำงาน โดยดัดแปลงมาจากสมการของ Nusselt ดังนี้

$$h_{cd,i} = 0.943 \left(\frac{\rho_{wl}^2 g \lambda_w k_{wi}^3}{\mu_{wl} L_{cd} \Delta T_{cd}} \right)^{0.233}$$
 [4]

โดยที่ ∆T_∞ คืออุณหภูมิแตกต่างระหว่างผิวและสาร ทำงานที่ส่วนควบแน่นของท่อความร้อน

ESDU [3] ได้เสนอสมการในการกำนวณค่าสัมประสิทธิ์ การถ่ายเหลวามร้อนของอากาศร้อนที่ไหลผ่านกลุ่มท่อติด ครีบแบบไหลตามขวาง (cross flow) ดังนี้

$$h = \frac{\overline{Nu} \, k_a}{D_a}$$
 [5]

$$\overline{Nu} = 0.242 \, \text{Re}^{0.658} \! \left(\frac{f_s}{f_h} \right)^{0.297} \! \left(\frac{S_t}{S_I} \right)^{-0.091} \text{Pr}^{0.333}$$

3. โปรแกรมการจำลองสถานการณ์

โปรแกรมการจำลองสถานการณ์ที่ใช้ในการคำนวณ สมรรถนะของเครื่องอุ่นอากาศแบบเทอร์โมไซฟอนในงาน วิจัยนี้ สามารถแบ่งออกเป็น 2 ส่วนคือ โปรแกรมที่สร้างขึ้น จากสมมุติฐานอัตราการถ่ายเทความร้อนของท่อกวามร้อนคง ที่ และไม่คงที่ (ขึ้นกับสภาวะของอากาศที่มาแลกเปลี่ยน ความร้อน) โดยลักษณะของเครื่องอุ่นอากาศที่ใช้ในการ คำนวณมีรายละเอียดดังต่อไปนี้

จำนวนท่อความร้อน	49	ท่อ
จำนวนแถวของท่อความร้อน	7	แถว
การจัดเรียง	แบบเห	ลื่อมกัน
S ₁	0.053	m
S _I	0.046	m
S_d	0.053	m
ขนาดท่อกวามร้อน	0.027	m
ความยาวของส่วนระเหย	0.4	m
ความยาวของส่วนควบแน่น	0.4	m

สารทำงาน	น้ำ	
ลักษณะของครีบ	แบบว	งกลม
ความหนาแน่น	10 คร	ร้าบ/inch
ความสูงครีบ	0.01	m
วัสดุ (ท่อและคร ี บ)	stainle	ss 304
อุณหภูมิขาเข้าของอากาศร้อน	200	°C
อุณหภูมิชาเช้าของอากาศเย็น	30	°c

Flow-charts ของโปรแกรมในการคำนวณสมรรถนะของ เครื่องอุ่นอากาศแบบเทอร์โมไซฟอน ในกรณีของการใช้ สมมุติฐานอัตราการถ่ายเทความร้อนเท่ากัน และสมมุติฐานที่ อัตราการถ่ายเทความร้อนไม่เท่ากันในกรณีของการไหลสวน ทางและไหลตามกัน แสดงในรูปที่ A1-A3 ในภาคผนวกตาม สำคับ โดยในงานวิจัยนี้ จะใช้โปรแกรม Turbo Pascal for Windows 1.5 ในการคำนวณสมรรถนะของระบบ

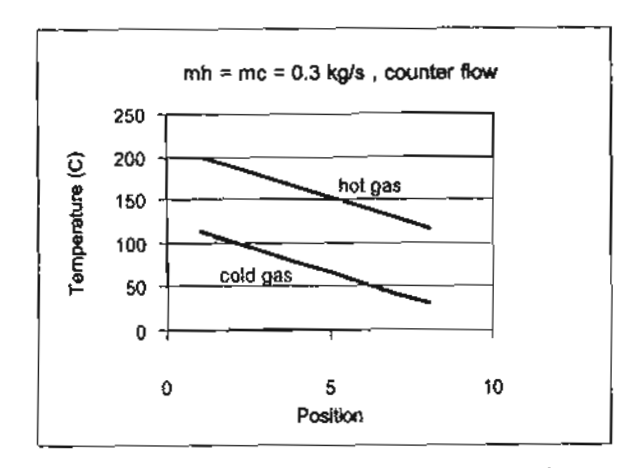
รูป กา ซึ่งแสดง Flow-chart ในการดำนวณสมรรถนะ ของเครื่องอุ่นอากาศแบบใหลสวนทางหรือแบบใหลตามกัน โดยกำหนดให้ค่าอัตราการถ่ายเทความร้อนมีค่าเท่ากันทุก ท่อ ซึ่งเป็นการดำนวณแบบวนลูป เพื่อหาคำอัตราการถ่ายเท ความร้อนรวมและอุณหภูมิขาออกของอากาศร้อนและเย็น

รูป ก2-3 เป็นการคำนวณอัตราการถ่ายเทความร้อนของ ท่อความร้อนในเครื่องอุ่นอากาศที่ละแถว เพื่อหาคำอุณหภูมิ ของอากาศด้านเข้าและออกจากท่อความร้อนตลอดจนอัตรา การถ่ายเทความร้อนในแต่ละแถว

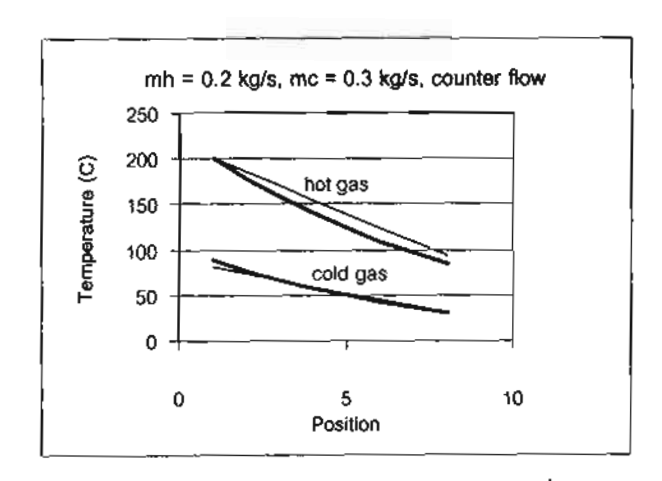
4. ผลการจำลองสถานการณ์และการวิเคราะห์

รูปที่ 2 ก-ง แสดงการเปรียบเทียบอุณหภูมิของอากาศ ร้อนและเย็นที่ได้จากผลการจำลองสถานการณ์ในกรณีของ การใช้สมมุติฐานอัตราการถ่ายเทความร้อนคงที่และไม่คงที่ ในกรณีของเครื่องอุ่นอากาศแบบไหลสวนทางกัน ที่มีอัตราการใหลของอากาศร้อนและเย็นเท่ากัน จากรูปจะพบว่า อุณหภูมิของอากาศร้อนและเย็นที่ได้จากการคำนวณทั้งสอง แบบมีค่าเท่ากัน ซึ่งหมายถึงในกรณีนี้การใช้สมมุติฐานแบบเดิมให้การคำนวณที่ถูกต้องแม่นยำ

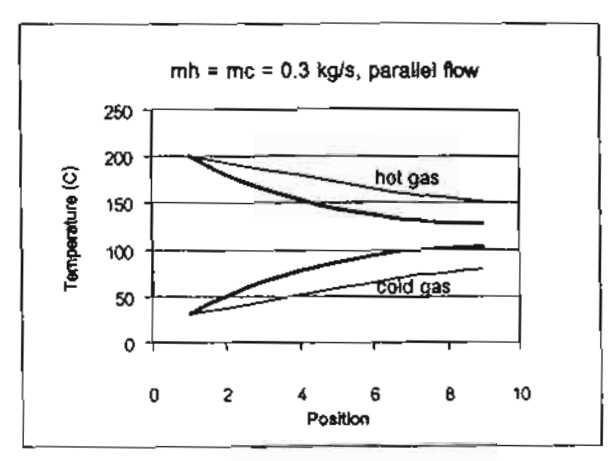
รูปที่ 2ข-ง เป็นกรณีของอุณหภูมิของอากาศร้อนและเย็น ในกรณีของเครื่องอุ่นอากาศแบบไหลสวนทางกันโดยอัตรา การไหลของอากาศร้อนและเย็นไม่เท่ากัน และในกรณีของ เครื่องอุ่นอากาศแบบไหลตามกัน ทั้งในกรณีของอัตราการ ไหลของอากาศแบบเท่ากันและไม่เท่ากันตามลำดับ ในกรณี ตั้งกล่าวนี้จะพบว่าการใช้สมมุติฐานที่ว่าอัตราการถ่ายเท ความร้อนคงที่จะให้ความคลาดเคลื่อนในการคำนวณ
อุณหภูมิของอากาศสูง โดยเฉพาะอย่างยิ่งในกรณีของเครื่อง
อุ่นอากาศแบบไหลตามกัน ซึ่งส่งผลให้การคำนวณอุณหภูมิ
ขาออกของอากาศร้อนและเย็นที่ได้สูงและค่ำกว่าความเป็น
จริง ซึ่งถ้านำไปใช้ในการออกแบบเครื่องอุ่นอากาศจะทำให้
ได้เครื่องอุ่นอากาศที่มีขนาดใหญ่เกินความจำเป็น



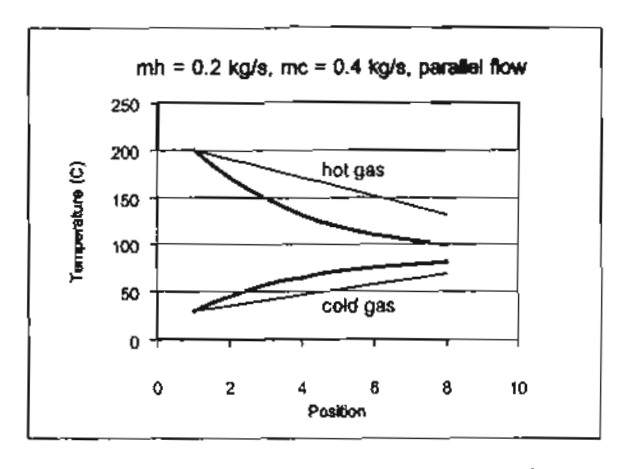
 ก. อุณหภูมิของอากาศร้อนและเย็นในกรณีของเครื่องอุ่น อากาศแบบไหลสวนทางกัน โดยมีอัตราการไหลของ อากาศร้อนและเย็นเท่ากัน



 อุณหภูมิของอากาศร้อนและเย็นในกรณีของเครื่องอุ่น อากาศแบบไหลสวนทางกัน โดยมีอัตราการไหลของ อากาศร้อนและเย็นไม่เท่ากัน



 ค. อุณหภูมิของอากาศร้อนและเย็นในกรณีของเครื่องอุ่น อากาศแบบไหลตามกัน โดยมีอัตราการใหลของ อากาศร้อนและเย็นเท่ากัน

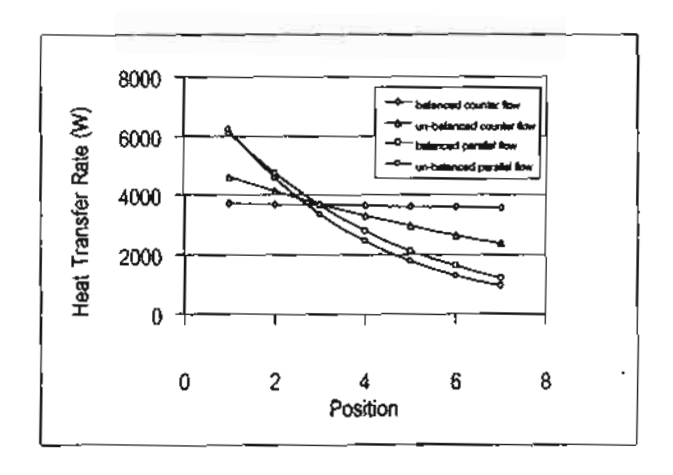


 ง. อุณหภูมิของอากาศร้อนและเย็นในกรณีของเครื่องอุ่น อากาศแบบไหลตามกัน โดยมีอัตราการไหลของ อากาศร้อนและเย็นไม่เท่ากัน

รูปที่ 2 อุณหภูมิของอากาศร้อนและเย็นของเครื่องอุ่นอากาศ แบบค่างๆ ที่ได้จากการคำนวณโดยใช้สมมุติฐานทั้ง สองแบบ

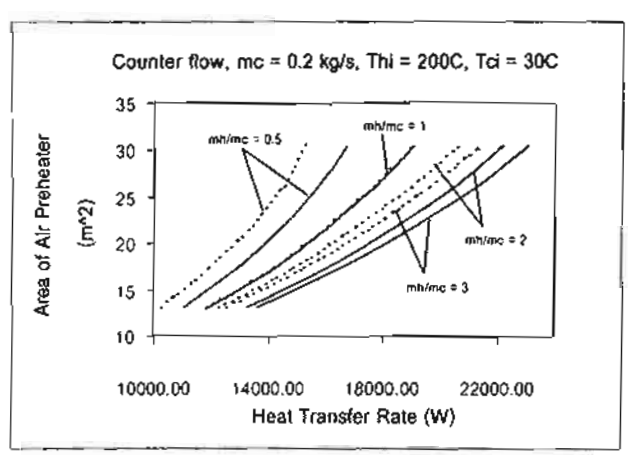
note: _____ อัตราการถ่ายเทความร้อนคงที่ _____ อัตราการถ่ายเทความร้อนไม่คงที่

รูปที่ 3 แสดงอัตราการถ่ายเทความร้อนของเครื่องอุ่น อากาศแบบไหลสวนทางและไหลตามกันทั้งในกรณีอัตราการ ใหลของอากาศเท่ากันและไม่เท่ากัน จากรูปพบว่า ในกรณี ของเครื่องอุ่นอากาศแบบไหลสวนทางกันที่มีอัตราการไหล ของอากาศร้อนและเย็นเท่ากัน จะมีค่าอัตราการถ่ายเทความ ร้อนในแต่ละแถวของท่อความร้อนคงที่ ซึ่งส่งผลให้ผลต่าง ของอุณหภูมิอากาศร้อนและเย็นที่ตำแหน่งต่างๆ ในเครื่องอุ่น อากาศประเภทนี้มีคำคงที่ สำหรับในกรณีอื่นๆ พบว่าอัตรา การถ่ายเทความร้อนมีค่าไม่คงที่ ดังนั้นการใช้สมมุติฐาน อัตราการถ่ายเทความร้อนคงที่สำหรับในกรณีนี้เป็นสิ่งที่ไม่ ถูกต้อง



รูปที่ 3 อัตราการถ่ายเทความร้อนของท่อความร้อนใน แต่ละแถวของเครื่องอุ่นอากาศแบบต่างๆ

รูปที่ 4 แสดงพื้นที่ในการแลกเปลี่ยนความร้อนของ เครื่องอุ่นอากาศแบบเทอร์โมไซฟอนแบบไหลสวนทางกัน ที่ ได้จากการคำนวณทั้งสองแบบ จากรูปพบว่า ในกรณีของ อัตราการใหลของอากาศร้อนและเย็นไม่เท่ากัน การใช้สมมุติ ฐานอัตราการถ่ายเทความร้อนคงที่ จะทำให้พื้นที่ ที่ได้จาก การคำนวณมีค่าสูงเกินความจำเป็น สำหรับในกรณีอัตราการ ไหลเท่ากัน พบว่าพื้นที่ที่ได้จากการคำนวณทั้งสองแบบมีค่า เท่ากัน



รูปที่ 4 พื้นที่ผิวของเครื่องอุ่นอากาศที่ได้จากการคำนวณ ทั้งสองแบบ

Q constant Q un-constant

5. สรุปผลการวิจัย

การออกแบบเครื่องอุ่นอากาศแบบไหลสวนทางกันโดยมี อัตราการไหลของอากาศร้อนและเย็นคงที่ สามารถใช้สมมุติ ฐานอัตราการถ่ายเทความร้อนคงที่ได้ แต่ในกรณีของอัตรา การไหลของอากาศร้อนและเย็นไม่เท่ากัน หรือในกรณีของ เครื่องอุ่นอากาศแบบไหลสวนทางกัน การใช้สมมุติฐานดัง กล่าวจะมีความคลาดเคลื่อนในการคำนวณสูง

6. กิดติกรรมประกาศ

คณะผู้จัดทำขอขอบพระคุณสำนักงานกองทุนสนับสนุน การวิจัยที่ให้ทุนอุดหนุนในการทำวิจัยครั้งนี้

เอกสารถ้างอิง

- Engineering Science Data Unit, "Heat Pipe Performance of Two Phase Closed Thermosyphons", Item No. 81038, UK., 1981
- Kiatsiriroat T., Nuntaphan A. and Tiansuwan J., "Thermal Performance Enhancement of Thermosyphon Heat Pipe with Binary Working Fluids" Experimental Heat Transfer, Vol 13, No 2, 2000
- Hewitt G.F., Shires G.L. and Bott T.R., "Process Heat Transfer", CRC Press., 1994

รายการสัญลักษณ์

 $A = Area (m^2)$

Cp = Heat capacity (J/kgK)

D = Diameter of pipe (m)

 f_h = Fin height (m)

 $f_s = Gap between fins (m)$

g = Gravitational acceleration (9.81 m/s2)

g_c = Constant (1kgm/Ns²)

h = heat transfer coefficient (W/m2K)

k = Thermal conductivity (W/mK)

L = Length (m)

m = mass flow rate (kg/s)

Nu = Nusselt number

Pr = Prandtl number

Q = Heat transfer rate (W)

Re = Renold number

 S_{α} = Pitch of tubes on the diagonal plane (m)

S_i = Pitch of tubes in direction of flow (m)

 S_t = Pitch of tubes in plane perpendicular to flow

(m)

T = Temperature (°C)

 ΔT_{instd} = Log mean temperature difference ($^{\circ}$ C)

Greek Letters

μ = Viscosity (kg/ms)

 ρ = Density (kg/m³)

 λ = Latent heat of vaporization (J/kg)

σ = Surface Tension (N/m)

subscript

a = air

c = cold air

cd = condenser

ev = evaporator

h = hot air

i = inlet, inside

1 = liquid phase

m = metal

o = outlet, outside

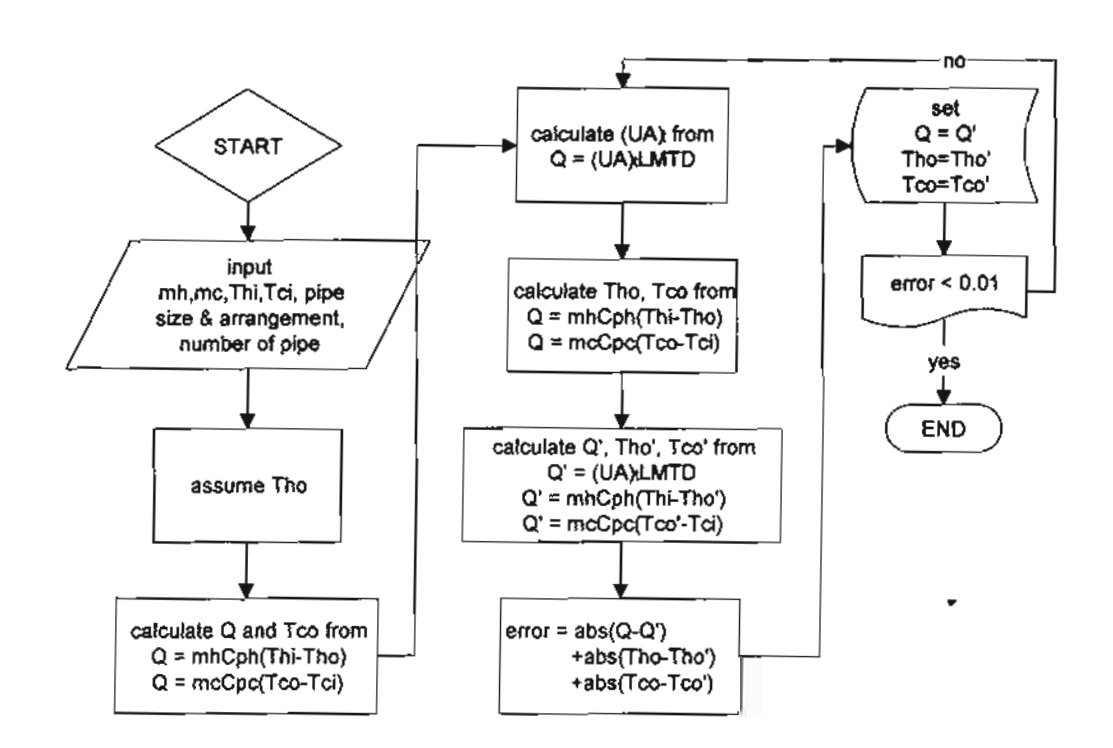
s = surface

t = total

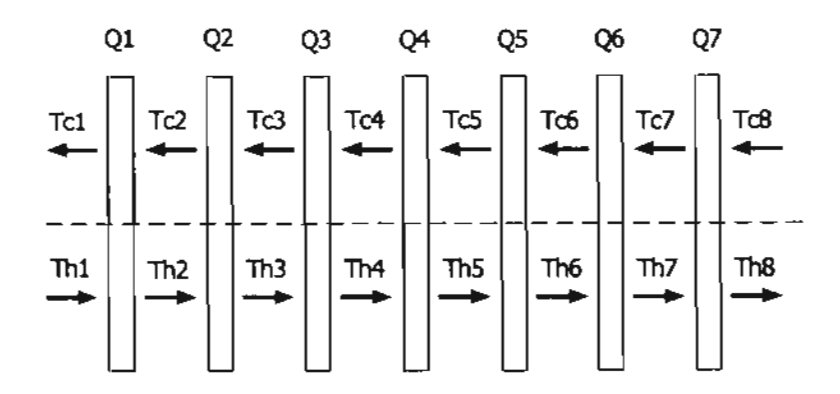
v = vapor phase

w = water

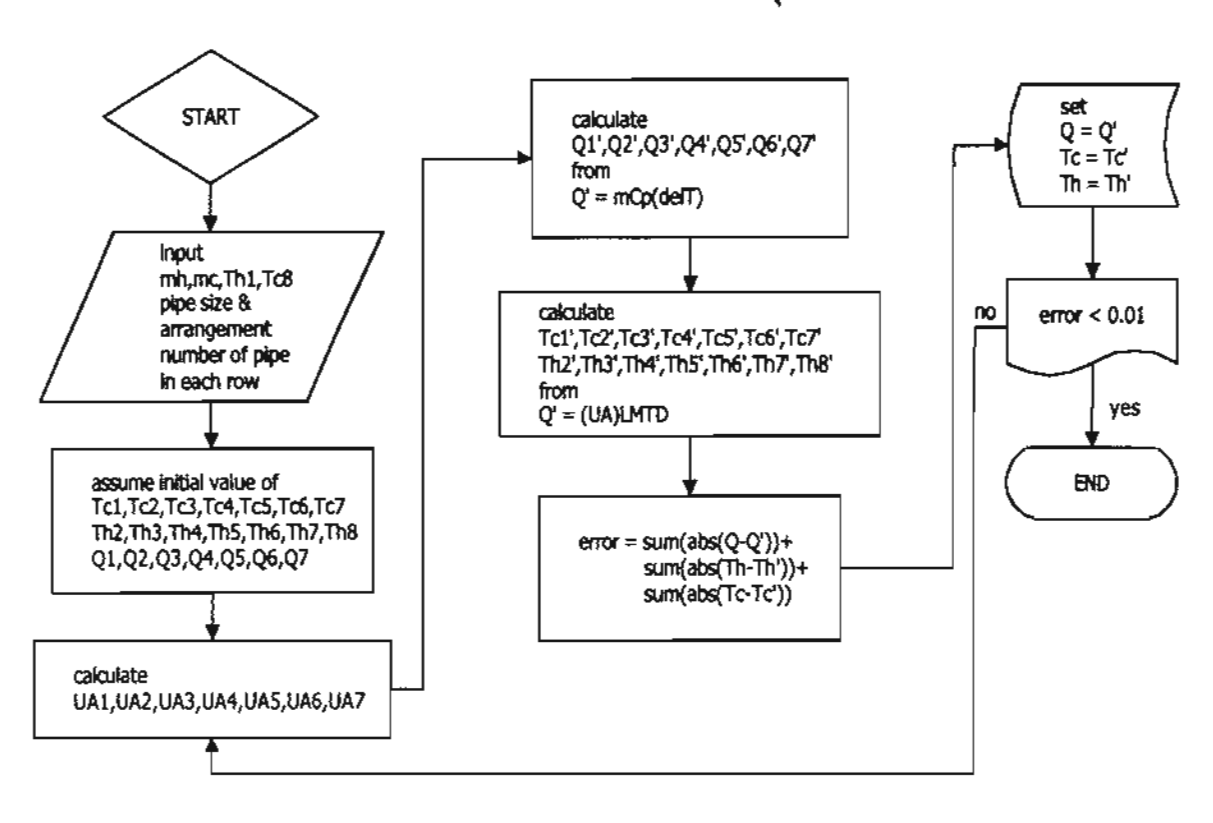
ภาคผนวก



รูปที่ กร แผนภาพในการคำนวณสมรรถนะของเครื่องอุ่นอากาศแบบเทอร์โมไซฟอน ในกรณีของอัตราการถ่ายเทความร้อนคงที่

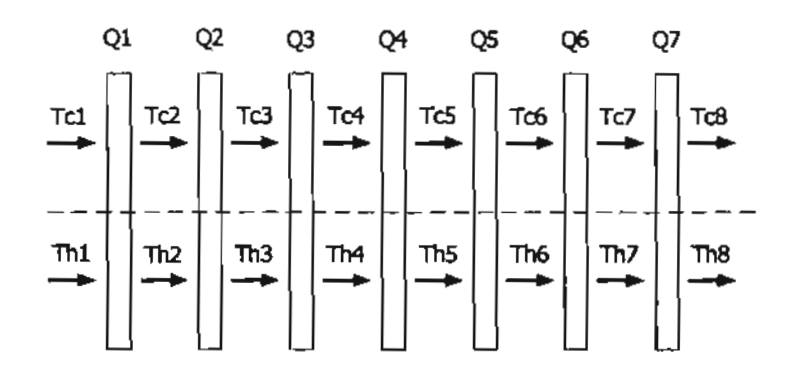


ก. ทิศทางการใหลของกระแสร้อนและเย็นในเครื่องอุ่นอากาศแบบใหลสวนทางกัน

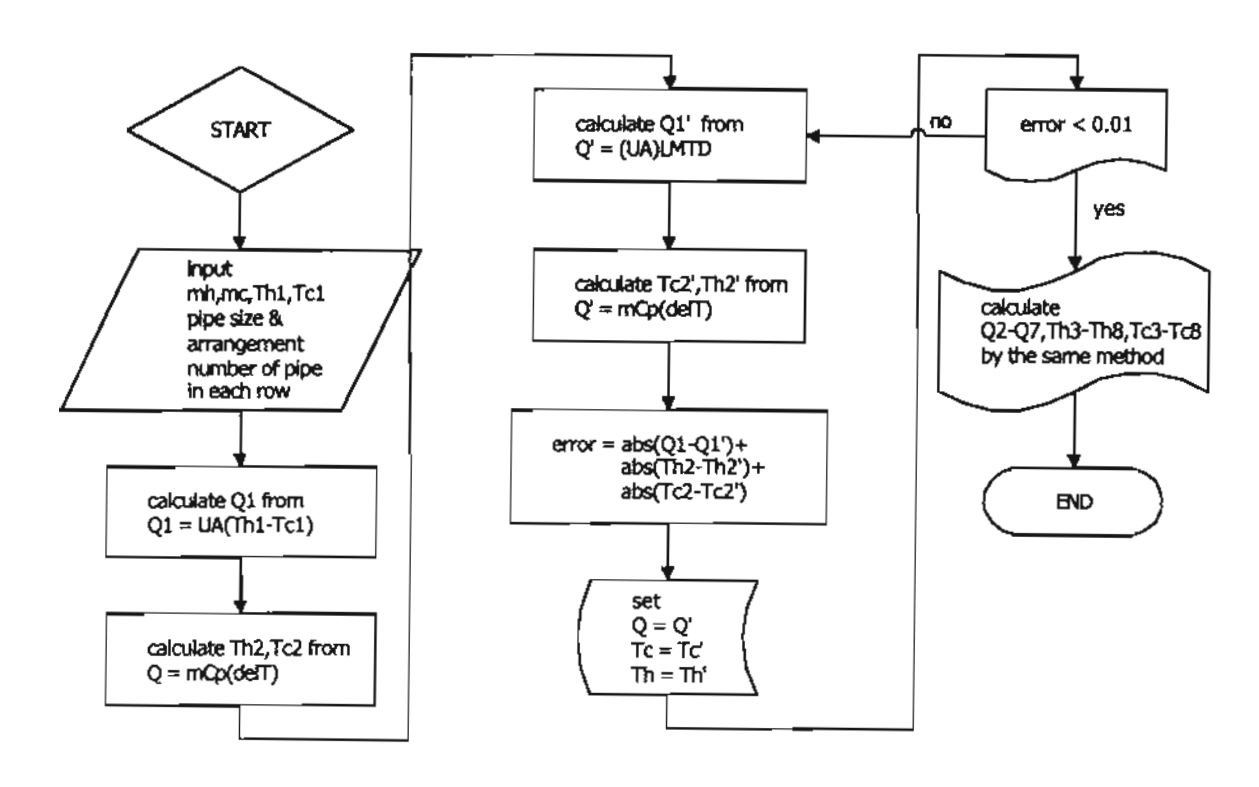


ข. แผนภาพในการคำนวณสมรรถนะของเครื่องอุ่นอากาศแบบไหลสวนทางกัน

รูปที่ n2 แผนภาพในภารคำนวณสมรรถนะของเครื่องอุ่นอากาศแบบเทอร์โมไซฟอนแบบไหลสวนทางกัน ในกรณีของอัตราการถ่ายเทความร้อนไม่คงที่คงที่



ก. ทิศทางการใหลของกระแสร้อนและเย็นในเครื่องอุ่นอากาศแบบใหลตามกัน



ข. แผนภาพในการคำนวณสมรรถนะของเครื่องอุ่นอากาศแบบไหลตามกัน

รูปที่ ก3 แผนภาพในการคำนวณสมรรถนะของเครื่องอุ่นอากาศแบบเทอร์โมไซพ่อนแบบไหลตามกัน ในกรณีของอัตราการถ่ายเทความร้อนไม่คงที่